THE UNIVERSITY *of* EDINBURGH

DIGITAL CORRELATION TECHNIQUES FOR IDENTIFYING DYNAMIC SYSTEMS

by

Brian William Finnie

Thesis presented for the Degree of Doctor of Philosophy of the University of Edinburgh in the Faculty of Science

May, 1966

ACKNOWLEDGEMENTS

The research described in this thesis was carried out at the University of Edinburgh from October 1963 to November 1965. I am grateful to Professor W.E.J. Farvis for the facilities available in the Department of Electrical Engineering.

I would also like to thank Dr. G.T. Roberts for his guidance and encouragement throughout the work, and Mr. A. McParland for his efforts towards realising the hardware involved.

The work on quantisation formed part of a study carried out for the Dounreay Experimental Reactor Establishment. Mr. F.D. Boardman and Mr. D.C. Menzies of the United Kingdom Atomic Energy Authority contributed to several illuminating discussions.

Finally, I wish to acknowledge the comments and suggestions of staff and colleagues in the Electrical Engineering Department.

CONTENTS

8. APPENDICES (continued)

1. THE IDENTIFICATION PROBLEM

A frequent problem in physics and engineering is that of determining a mathematical model for the dynamic performance of a system. It is particularly useful to be able to make measurements which enable such a model to follow changes in the system dynamics in the course of normal operation.

Linear control theory, although now being replaced by a more general approach, can still form the basis for such system analysis. Cross correlating signals from a linear process can give a great deal of information about the process dynamics without injecting any test disturbances, or, when test signals are possible, cross correlation can be used to recover dynamic information in the presence of considerable background noise. The use of specially constructed test signals can make cross correlation a powerful technique in the identification of dynamic systems.

Correlation Analysis. The autocorrelation function of a signal x(t) is defined by (1.1)

$$R_{xx}(\tau) = \lim_{T\to\infty} \frac{1}{T}\int_0^T x(t)\,x(t-\tau)\,dt \qquad (1.1)$$

A similar expression defines the cross correlation function for two signals x (t), y(t)

$$R_{xy}(\tau) = \lim_{T\to\infty} \frac{1}{T}\int_0^T y(t)\,x(t-\tau)\,dt \qquad (1.2)$$

where the parameter τ is a time delay introduced between the two components of the integral.

The power spectrum $G(\omega)$ of the signal x(t) is theFourier transform of $R_{xx}(\tau)$, as defined in (1.3) and (1.4)

$$G_x(\omega) = \frac{2}{\pi}\int_0^\infty R_{xx}(\tau)\cos\omega\tau\, d\tau \qquad (1.3)$$

$$R_{xx}(\tau) = \int_0^\infty G_x(\omega)\cos\omega\tau\, d\omega \qquad (1.4)$$

The cross power spectrum for x(t) and y(t) can also be obtained by transforming $R_{xy}(\tau)$. This is a complex function, since $R_{xy}(\tau)$ is not, in general, symmetrical, and can be used to determine the frequency response of the system connecting x(t) and y(t).

The usefulness of the correlation technique for identification, however, lies in the ability to determine the impulse response of the system without the need to artificially disturb it far from its normal operating condition. Under favourable conditions the actual normal operating signals can be used, or a low amplitude test signal may be injected instead.

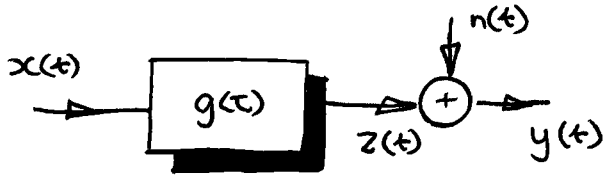

Figure 1.1 A system

The system in figure 1.1 has two observable signals x(t) and y(t), and a disturbance n(t) which contaminates the true response z(t) of the system. It is shown in appendix (1.1) that,

$$R_{xy}(\tau) = \int_0^\infty g(\tau)\, R_{xx}(\tau-u)\, du + R_{xn}(\tau) \qquad (1.5)$$

If the disturbance n(t) is uncorrelated with x(t) then

$$R_{xn}(\tau) = 0 \tag{1.6}$$

for all τ, and

$$R_{xy}(\tau) = \int_0^\infty g(\tau)\, R_{xx}(\tau - u)\, du \tag{1.7}$$

(1.7) shows that the cross correlation function $R_{xy}(\tau)$ is the same as the response of the system to an input signal $R_{xx}(\tau)$, if the disturbance signal n(t) is uncorrelated with x(t). Further, if $R_{xx}(\tau)$ is a delta function then the convolution is eliminated and

$$R_{xy}(\tau) = g(\tau) \tag{1.8}$$

(1.8) demonstrates that the impulse response $g(\tau)$ may be obtained directly from the cross correlation function if $R_{xx}(\tau)$ is a delta function. For this to be true signal x(t) must contain power over the entire frequency range. This may well be the case in many situations. If x(t) is not sufficiently wide band, however, (1.7) may be used to obtain g(t) with the application of some further computing effort. An alternative approach is to introduce a wide band test signal of low amplitude, which is uncorrelated with the signals already present. This becomes signal x(t) in figure 1.1 and the operating signals are 'disturbances' on the measurement.

Finite averaging time. The previous section is strictly true only when (1.2) is mechanised exactly. In practice the infinite limit is not possible, and the statistics of the signals will cause some uncertainty in the result.

The effect of the statistical properties of both the wanted and unwanted

signals on the estimate of the correlation function has been treated in many text books [1, 2, 3]. However, an inconsistency in terminology and symbols makes it desirable to restate the basic results here.

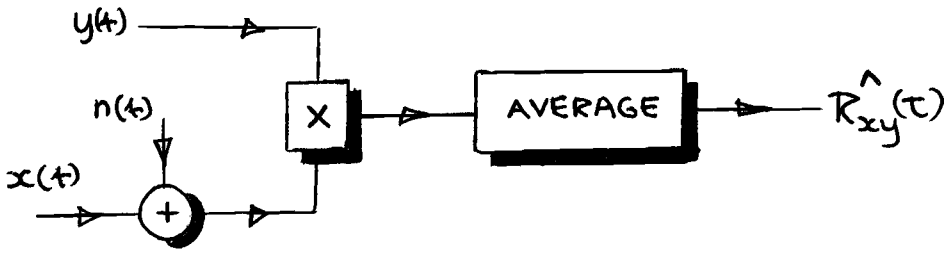

Figure 1.2 Correlation in presence of noise

In figure 1.2 the two desired signals x(t) and y(t) are contaminated by disturbances, lumped together as n(t). The estimate $\hat{R}_{xy}(\tau)$ of the cross correlation function will have a variance due to the statistical properties of x(t), y(t) and n(t), and finite averaging time T. Since n(t) is assumed uncorrelated with x(t) or y(t), the variance of $\hat{R}_{xy}(\tau)$ may be written

$$V^2 = V_R^2 + V_N^2 \tag{1.9}$$

where V^2 is the total variance of the estimate, V_R^2 is that part of the variance due entirely to x(t) and y(t), V_N^2 is the additional variance introduced by the disturbance n(t). V_R^2 and V_N^2 are given approximately by (1.10) and (1.11).

$$\left.\begin{aligned} V_R^2 &\simeq \frac{\pi}{T}\sigma_x^2 G_y(0) \\ \text{or} \quad V_R^2 &\simeq \frac{\pi}{T}\sigma_y^2 G_x(0) \end{aligned}\right\} \tag{1.10}$$

$$V_N^2 \simeq \frac{\pi}{T}\sigma_x^2 G_n(0) \tag{1.11}$$

where σ_x^2 is the total power in x(t),

σ_y^2 is the total power in y(t),

$G(0)$ is the low frequency power per unit bandwidth.

A brief justification of these expressions is given in appendix (1.2).

Some practical disadvantages of correlation Measurement of a correlation function will usually be required for several values of delay, and if results are required on-line these points on the curve must be computed simultaneously. The multichannel correlator in figure (1.3) shows the difficulties which will be present.

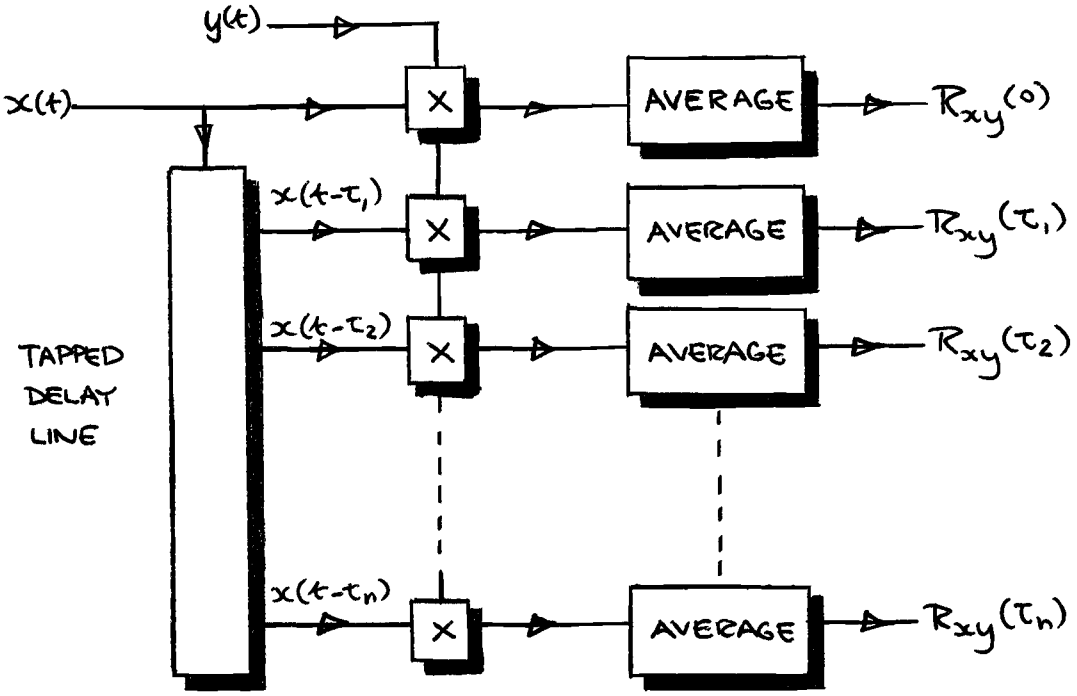

Figure 1.3. Multichannel correlator

The three basic requirements of a correlator - delay, multiplication, and integration (or filtering) represent individually considerable computing capacity either in digital or analog form. Simultaneous operation of up to fifty channels or more is unrealistic using analog equipment, and takes up a large proportion of the capacity of a general purpose digital computer. Because of this correlation analysis has been restricted in the main to off-line computation using recorded data [4, 5]. Appendix (1.3) gives an estimate of computing capacity required to realise the correlator of figure 1.3 by conventional means.

The use of digital computers in on-line measurement of system performance is now enhanced by the increasing availability of small, high speed, scientific and data processing computers. However, there have existed two factors which discourage the use of correlation analysis on such a computer. These are

1) The large number of time consuming multiplication operations

2) The amount of storage required for delaying the signal

These two factors do not make correlation analysis impossible on a digital computer, but consume so much time and storage as to make time sharing with other operations impossible. These other operations would typically be those required to make use of the computed correlation function, so there is some interest in finding ways around these difficulties.

Outline of work The present work is aimed at evaluating and improving some recently suggested techniques which simplify the calculation of correlation functions. The next chapter examines the technique of coarse quantisation of data, suggested by Watts [6, 7], which can be used to eliminate multiplication and some of the storage requirements from a correlator.

Chapter 3 describes a new technique, which does away with a great deal of storage in an on-line correlator, and is based on a well known result on sampling.

The use of specially constructed binary sequences as test signals is discussed in Chapter 4 [8, 9, 10]. These sequences have advantages not only for simplifying the correlation procedure, but also in situations where recovering the test signal from background noise is a problem. Some attention is paid in Chapter 5 to the application of binary sequences to multivariable identification

and some useful results are presented.

The techniques outlined are shown to be useable in practical situations, and will enable greater use to be made of correlation analysis in system identification.

2. CORRELATION USING QUANTISED SIGNALS

A correlator has been proposed by Watts [6, 7] which has several practical advantages. In this correlator, figure 2.1, the signal to be delayed is first coarsely quantised, that is, its value at any time is rounded off to the nearest of a few discrete levels. This is illustrated in figure 2.2.

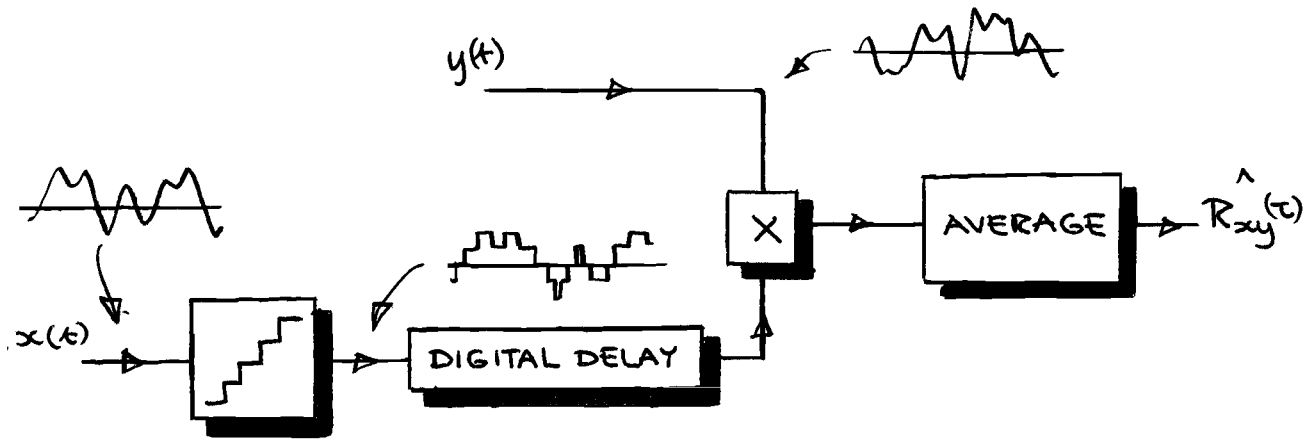

Figure 2.1 Quantising the delayed signal of a correlator

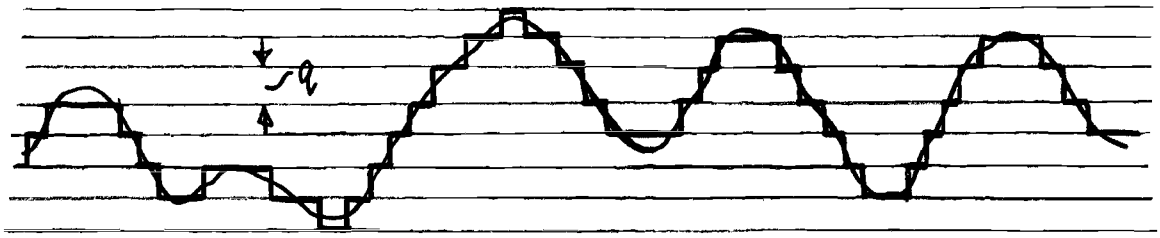

Figure 2.2 Quantisation of a signal

The important feature of this correlator is that the interval q between quantum levels need not be small compared to the excursion of the signal. For a signal with a Gaussian amplitude probability distribution Watts has shown that a quantum interval of as much as twice the r.m.s. value of the signal, that is

$$q/\sigma \leq 2 \qquad (2.1)$$

can give results which are accurate to within 2%. This leads to the possibility that a Gaussian signal may be described by only three equal zones as shown in figure 2.3. This contrasts with the resolution of 1% or better which is usually aimed for, when digitising data.

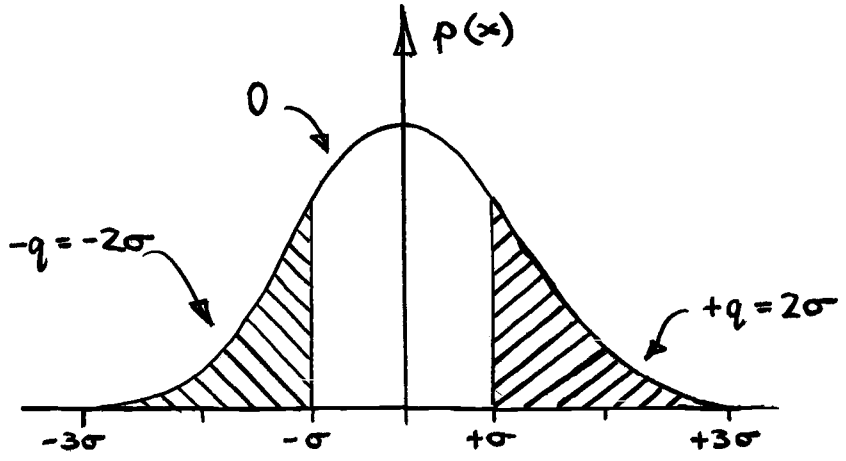

Figure 2.3 Three level quantisation

The correlator in figure 2.1 now takes on an extremely simple form. The delay need only accept and store two bit binary information, and multiplication becomes gated addition or subtraction.

When the choice of interval q, and the number of levels has been made, however, there is a restriction on the magnitude of the input signal. In the suggested three level case, if the r.m.s. value of the signal falls below q/2 then the requirement of (2.1) is not met. If the r.m.s. value is greater than q/2, then the quantiser cannot accommodate the extreme excursions of the signal and saturation is introduced. Also, a d.c. component in the input to this quantiser may have a considerable effect. The characteristic function method used by Watts to analyse the effects of quantisation does not conveniently lend itself to a quantiser with a restricted number of levels. The following

sections prove the validity of (2.1) using a different approach which also allows the effects of overload, and of the dc component in the signal to be readily evaluated.

In Watts' work no attempt is made to evaluate quantitatively the effect of finite averaging time. However, by extending a result derived by Watts it is possible to assess the effect of practical averaging times on an estimate of the correlation function.

The equivalent gain technique The approach used to analyse figure (2.1) uses the equivalent gain technique for non-linearities, familiar to control engineers [11]. It has been shown that a single valued non-linearity which is subject to a random input can be replaced by an equivalent gain K, and an additional distortion signal n (t), Both K and n (t) are dependent on the r.m.s. and mean values of the input signal x(t). The process is illustrated in figure 2.4.

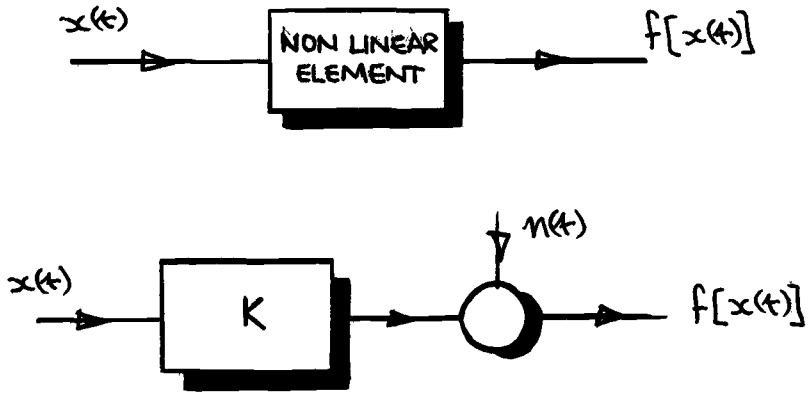

Figure 2.4 Equivalent gain of a non-linear element

It is shown in appendix (2.1) that if K is chosen so as to minimise the mean square value of n(t), then n(t) is itself uncorrelated in the statistical sense with

x(t). Figure 2.4 now allows the effect of a non-linearity in a correlator to be analysed. If one channel contains some non-linearity it can be replaced by the appropriate K, and n(t), figure 2.5.

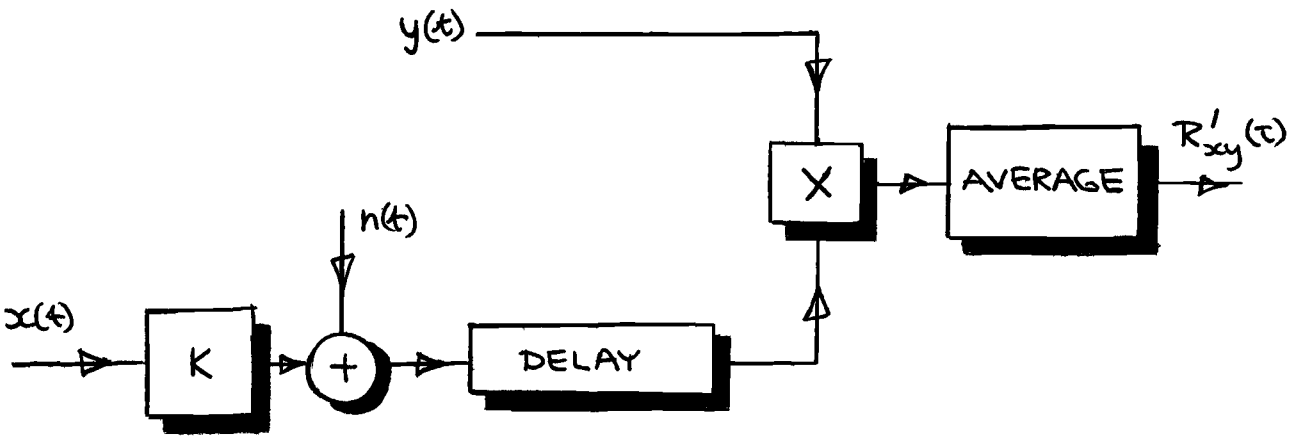

Figure 2 5 Replacing a non-linearity in a correlator by its equivalent gain, and distortion

The situation is immediately simplified to the problem of correlating y(t) with Kx(t) in the presence of uncorrelated disturbance n(t). With infinite averaging time the computed function $R'_{xy}(\tau)$ will be given by (2.2)

$$R'_{xy}(\tau) = K R_{xy}(\tau) \qquad (2.2)$$

when $R_{xy}(\tau)$ is the true cross correlation between x(t) and y(t). In practice in addition to the variance on the estimate due to the statistical properties of x(t) and y(t), there will be an additional variance introduced by n(t).

Since the quantiser can be represented by the non-linear characteristic of figure 2 6, it follows that its effect in a correlator can be determined from a knowledge of its equivalent gain K, and the properties of the quantisation noise

n(t). These topics will now be discussed.

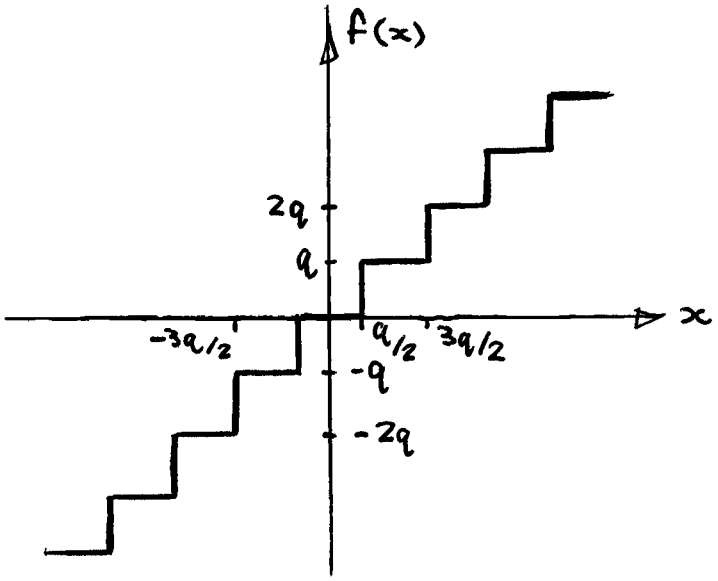

Figure 2.6 Quantiser as a non-linear characteristic

Equivalent gain of quantiser The equivalent gain K of the non-linear characteristic in figure 2.6 is evaluated in appendix 2.2 as a function of the r.m.s. value σ , and mean level x_0 of the input signal x(t). Figure 2.7 shows how K varies for a multilevel quantiser and a three level quantiser. Some conclusions are now obvious. For the multilevel quantiser with no saturation (the case analysed by Watts), if $\sigma/q \geq 1/2$, the quantiser may be replaced by unity gain with at most 2% inaccuracy for any input mean value. If only three levels are available the allowable range of σ is considerably reduced. Figure 2.7 can be used to make an operating decision in a particular case. Note that there is also some error introduced by ignoring the tails of the distribution, figure 2.3. This is shown up by the maximum value of K in the three level case only being 0.95. It can also be seen from figure 2.7 that the effect of d.c. on the three level quantiser is considerable, and is to be avoided.

In all cases, if the r.m.s. value of the signal can be measured separately,

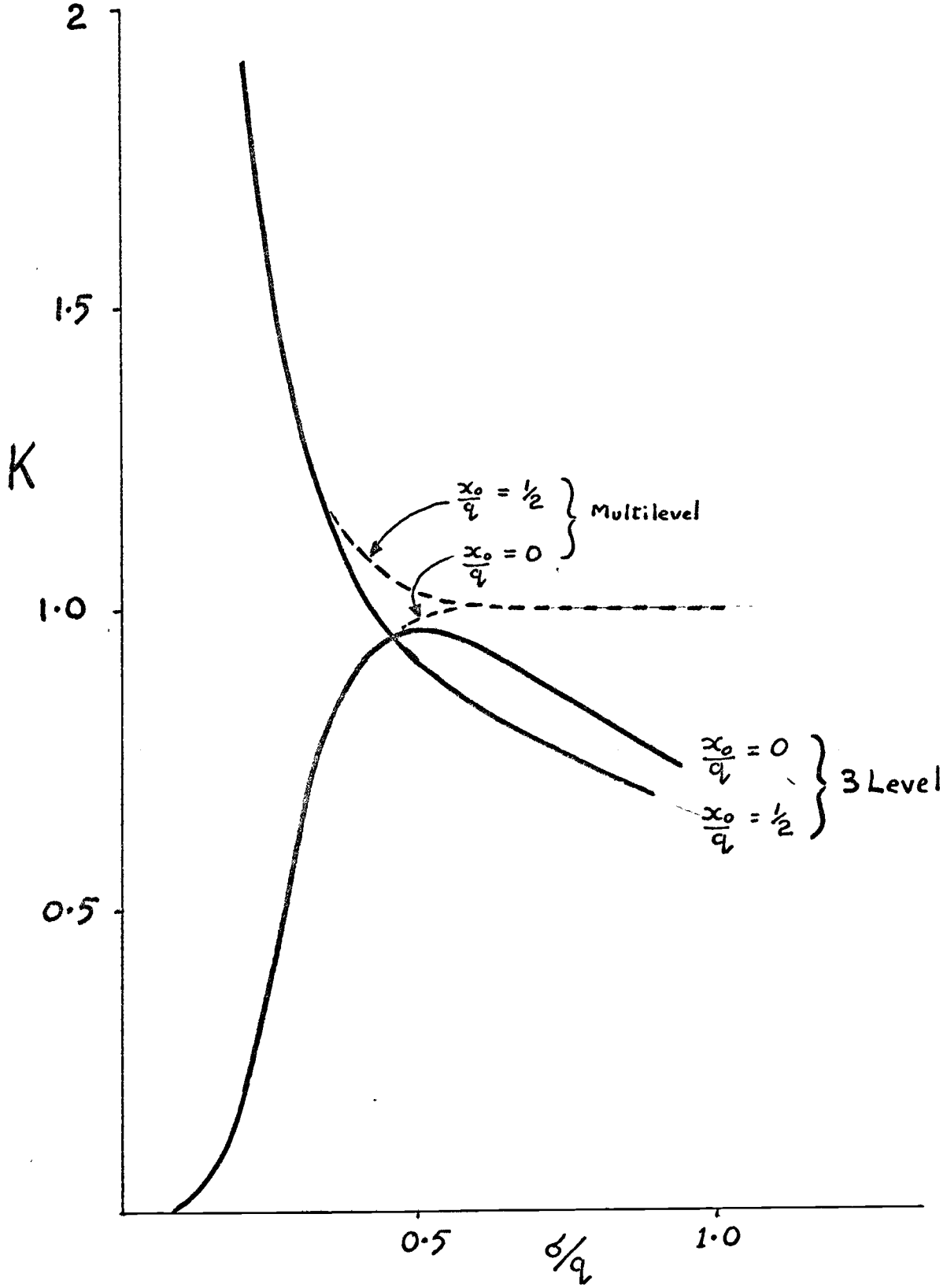

Figure 2.7 The equivalent gain K of a quantiser in the presence of a random Gaussian input with r.m.s. value σ and d.c. component x_0.

figure 2.7 allows the calculated correlation function to be scaled accordingly.

D.C. Characteristic of quantiser in presence of random input It is of some interest to study the response of the quantiser to the mean value of the input signal. If the mean value, x_o and the a.c. component x(t) of the input signal X(t) are regarded as separate, that is

$$X(t) = x(t) + x_o \qquad (2.3)$$

then the quantiser can be represented by the system in figure 2.8.

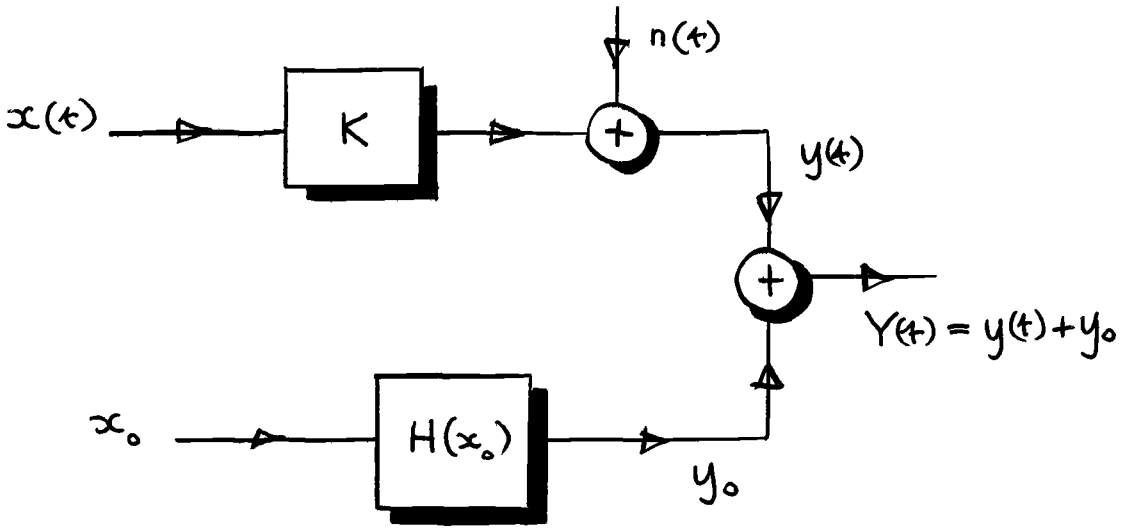

Figure 2.8 Equivalent circuit of a quantiser in the presence of a d.c. component

In figure 2.8 the mean value of the output is regarded as having been obtained from the mean value of the input through a d.c. characteristic, $H(x_o)$ which is also a function of the r.m.s. value of the a.c. component. This function is derived in detail in appendix 2.3 and figure 2.9 illustrates the form of the characteristic for various values of σ/q.

If there is no a.c. component ($\sigma=0$) then the characteristic is simply the original staircase non-linearity. However, as the input r.m.s. value increases

the d.c. characterictic becomes more linear until for $\sigma/q > 1/2$ it is indistinguishable within 1.2% from a straight line.

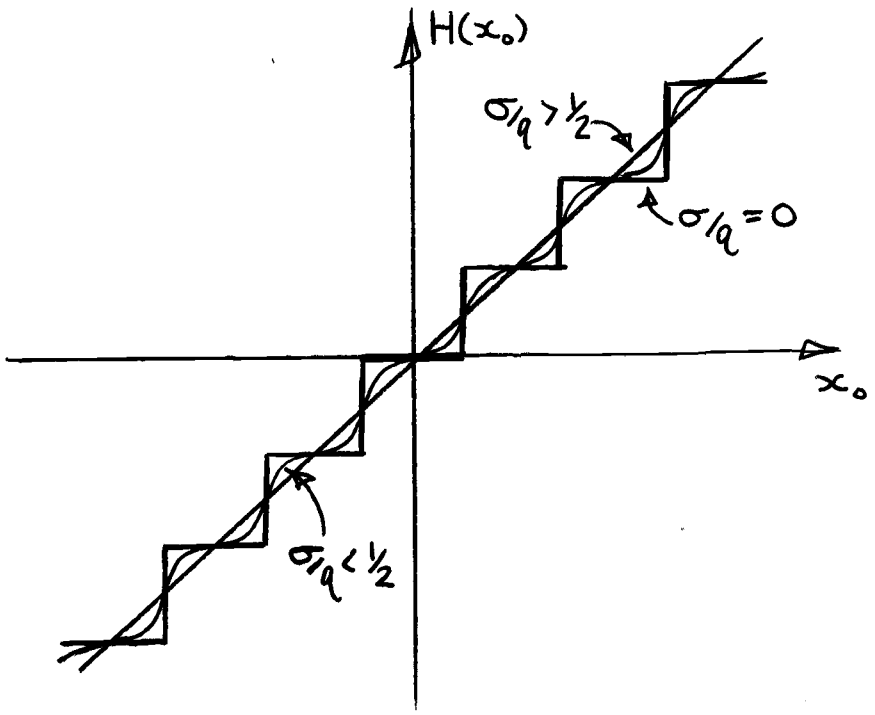

Figure 2.9 DC characteristic of quantiser

This is an example of the dither effect well known to control engineers and more particularly is an example of the behaviour of a non-linearity in the presence of more than one input. This topic is treated in detail by Somerville and Atherton [12, 13]. They show that the function $H(x_o)$ in figure 2.9 is also the non-linear characteristic seen by some other signal component in the input which may replace the mean value x_o. This is shown in figure 2.10 where the input signal is now

$$X(t) = x(t) + z(t) \qquad (2.4)$$

where x(t) is the gaussian random noise, but z(t) may be noise, or a deterministic signal such as a sine wave.

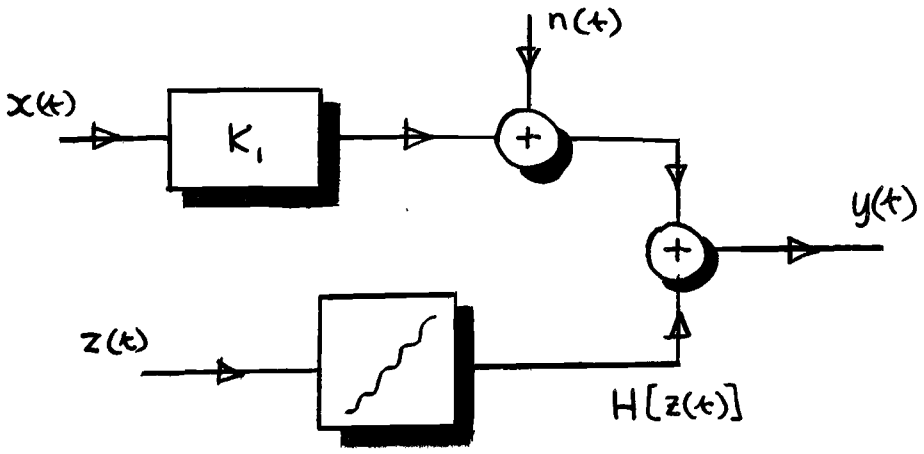

Figure 2.10 Quantiser subject to two inputs

The characteristic H(z) may now be replaced by an equivalent gain K_2, say. It can be seen from figure 2.9 that if the r.m.s. value of x(t) is sufficiently large, H(z) is a straight line and

$$K_2 = 1 \qquad 2.5$$

If X(t) in (2.4) is the input to a correlator containing a quantiser in one channel, it follows that a sinusoidal component z(t) can be recovered undistorted, if it is contaminated with sufficient noise to make (2.5) true. This is an interesting example of noise being essential to the recovery of the signal which it may be masking.

Effect of Finite Averaging Time. In a practical measurement the product of the correlator input signals can only be averaged over a finite time, or a finite number of samples. Because of the statistical nature of the input signals there will be some uncertainty in the estimate. The quantisation noise in figure 2.5 will introduce a further uncertainty on the measurement. The magnitude of this additional uncertainty, as measured by the increase in variance of the estimate, is an important quantity in evaluating the usefulness of the coarse quantisation technique.

It has been shown in appendix 1.2 that the additional variance of the estimate due to disturbing noise is related to the noise power contained within the bandwidth of the wanted signal. To find this, the power density spectrum of the noise must evaluated.

Power Series Method. The equivalent gain technique is an offshoot of a more general expression for the autocorrelation function of the output signal from a non-linearity [11, 14]. The full expression is given by (2.6) with reference to figure 2.11.

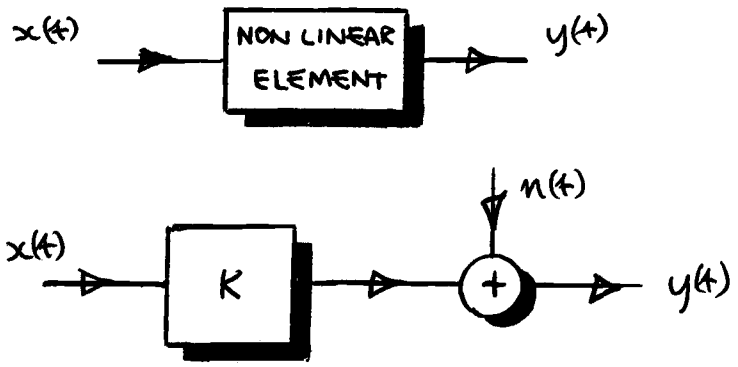

Figure 2.11 Non-linear element

$$R_{yy}(\tau) = \alpha_1^2 \rho_x(\tau) + \alpha_2^2 \rho_x^2(\tau) + \alpha_3^2 \rho_x^3(\tau) + \ldots \qquad (2.6)$$

where Ryy (τ) is the autocorrelation function of y(t)

and $$\rho_x(\tau) = R_{xx}(\tau)/\sigma_x^2$$

is the normalised autocorrelation function of the input.

The α's of (2.6) are coefficients determined from a knowledge of the non-linearity and the input probability density function. It can be shown that

$$\alpha_1 = K \qquad (2.7)$$

where K is the equivalent gain of the non-linearity.

In figure 2.11, since x(t) and n(t) are independent random variables

$$R_{yy}(\tau) = K^2 R_{xx}(\tau) + R_{nn}(\tau) \qquad (2.8)$$

Comparing (2.6) and (2.7) with (2.8) it follows that

$$R_{nn}(\tau) = \alpha_2^2 \rho^2(\tau) + \alpha_3^2 \rho^3(\tau) + \ldots . \qquad (2.9)$$

The autocorrelation function of the quantisation noise may be calculated from (2.9), and transformed to find the power spectrum. This approach is followed in appendix 2.4, but it is shown that the resulting power series solution is unwieldy and difficult to solve.

Alternative Approach. Watts also uses the concept of 'quantisation noise' but defines this as the difference between input and output of the quantiser. Thus Watts' noise only coincides with the distortion considered here when K = 1. In this case it will be appropriate to use Watts' expression for the autocorrelation function of quantisation noise, given by (2.10)

$$\frac{R_{nn}(\tau)}{q^2} = -\frac{1}{4\pi^2} \sum_{k\neq 0} \sum_{m\neq 0} \frac{(-1)^{k+m}}{km} \varepsilon^{-j2\pi(k+m)a} \varepsilon^{-2\pi^2\left(\frac{\sigma}{q}\right)^2 (k^2+m^2+2\rho km)} \qquad (2.10)$$

where $\rho = \rho(\tau)$ is the normalised autocorrelation function of the input.

In appendix 2.5, (2.10) is shown to simplify considerably, and it is possible to take the Fourier Transform. The power density spectrum can be evaluated in terms of σ/q, and the average number of zero crossings per second of the input signal. This allows the relevant parameters of the quantisation noise to be determined in any practical situation with very simple instrumentation. The full expression for the noise spectrum is given by (2.11) and figure 2.12 shows this function plotted against normalised frequency.

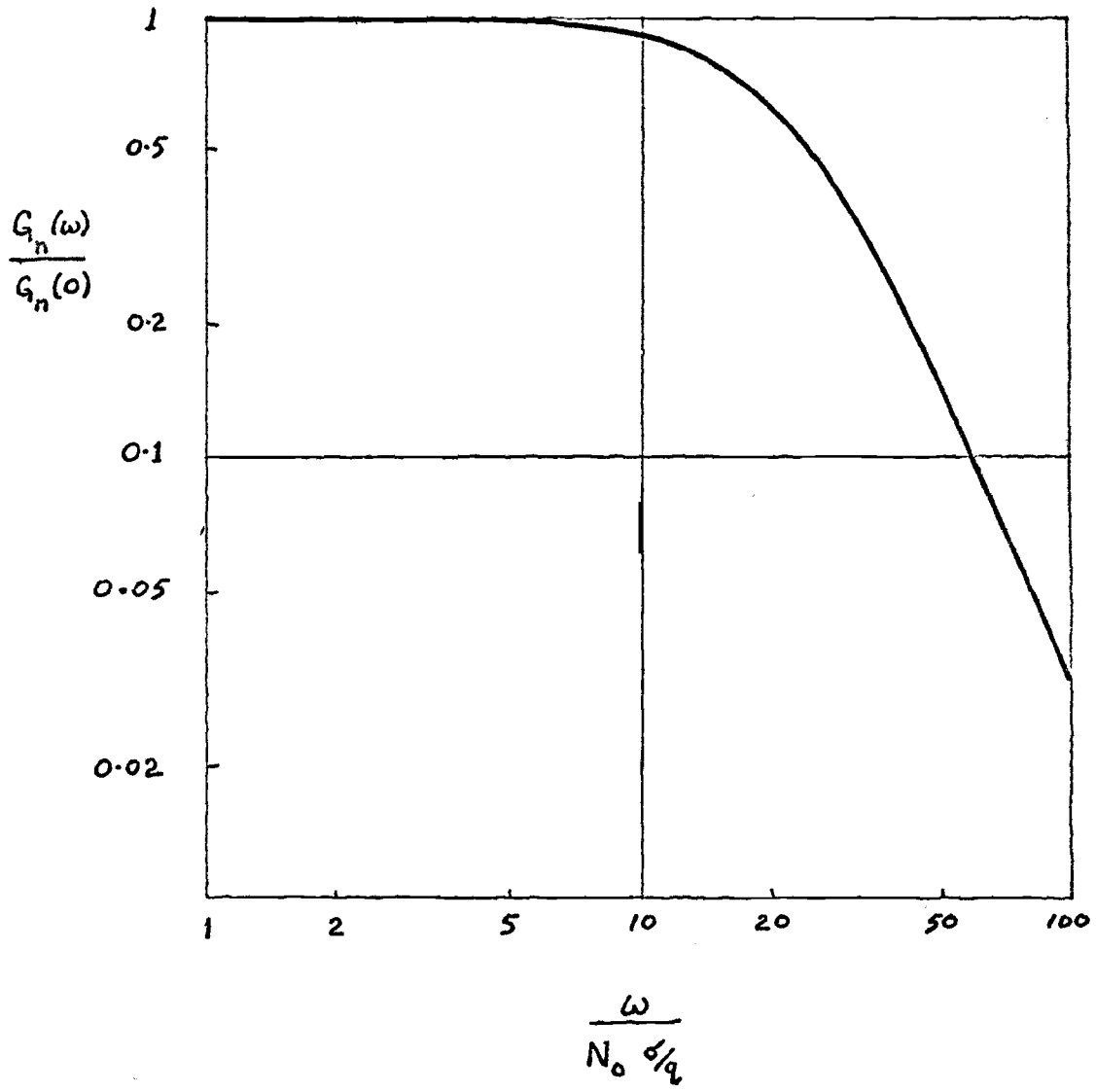

Figure 2.12 Power spectrum of quantiser noise

$$\frac{G(\omega)}{q^2} = \frac{1}{\pi^4} \frac{1}{2\sqrt{2\pi}\,(\sigma/q)N_0} \sum_{1}^{\infty} \frac{1}{k^3} \varepsilon^{\omega^2/k\omega_n^2} \qquad (2.11)$$

where $N_0 = \sqrt{-\rho''(0)}$

is the average number of zero crossings per second of input signal, and

$$\omega_n = 2\sqrt{2}\ \pi^2 \frac{\sigma}{q} N_0 \qquad (2.12)$$

Experimental verification of figure 2.12 has been obtained for several classes of input spectrum.

Two important observations can be made from figure 2.12.

a) The noise spectrum is flat from d.c. independent of input spectral characteristics.

b) The noise is wideband with respect to the input.

Cross correlation in the presence of wideband noise has already been mentioned in Chapter 1 and Appendix 1.2 and (1.10) and (1.11) allow an estimate to be made of the effect of quantisation in a particular case.

It is shown in Appendix 2.6 that if V_R^2 is the variance of the estimate due to the statistical properties of the input signals alone, and quantisation noise introduces some additional variance V_N^2, then

$$V_N^2/V_R^2 = A\left(q/\sigma\right)^3 \qquad (2.13)$$

where a typical value for A may be .006. This means that for $\sigma/q = 1/2$ quantisation introduces only about 5% additional variance on the estimate.

When a sampled system is used, this result will be degraded slightly if the sampling frequency is not higher than the noise bandwidth, since frequency folding will place more noise power within the signal bandwidth.

It has been demonstrated that quantising the delay channel of a correlator into only three levels is theoretically feasible, and confers many practical advantages. A disadvantage, however, is the sensitivity to variations in the signal level at the quantiser input, figure 2.7. If the system is being used on-line then such variations are likely to be encountered, so some way of avoiding the difficulty is desirable.

One solution is to use five level quantisation, using levels -2, -1, 0, 1, 2. The multiplication by two can still be realised digitally by a simple sideways shift operation before adding, so that computing effort is not greatly increased. The range of r.m.s. value accommodated may be taken from figure 2.13, which shows how the equivalent gain varies with σ/q for the five level quantiser.

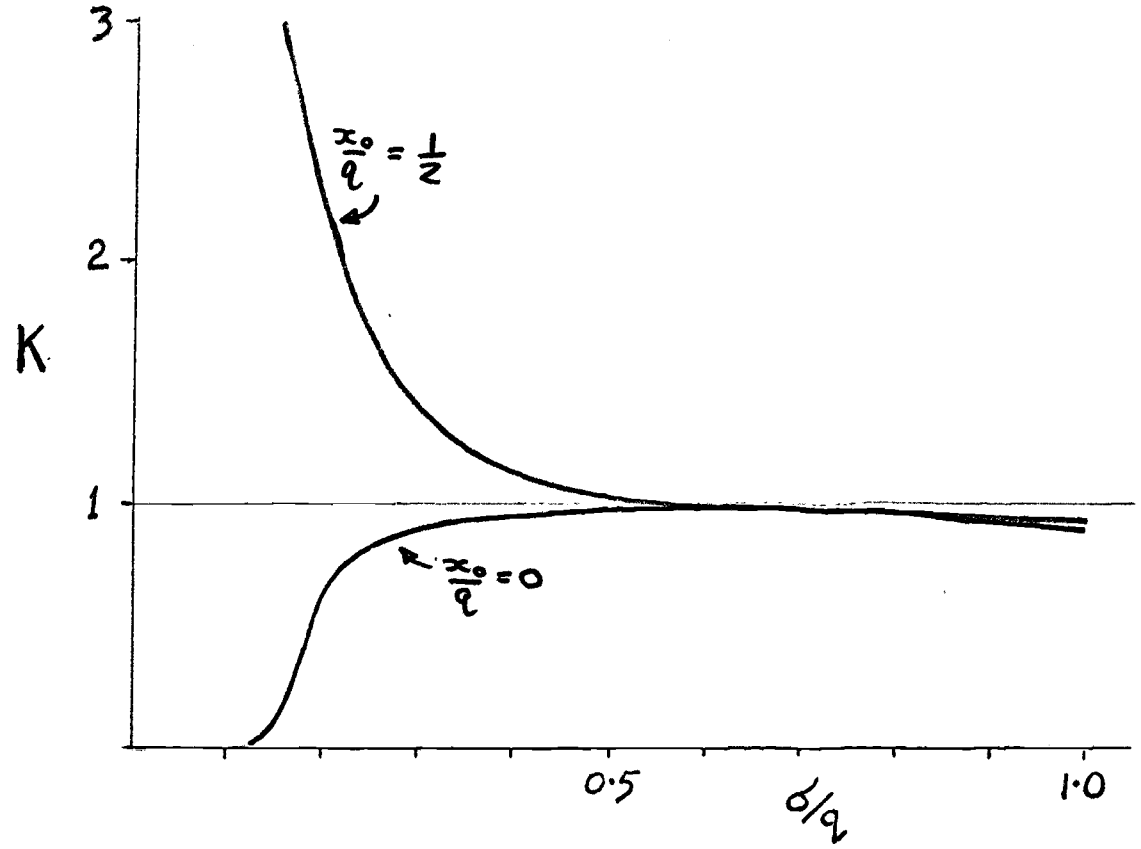

Figure 2.13 Equivalent gain for five level quantiser

Watts suggested a modification to the basic diagram of figure 2.1 to obtain greater dynamic range. The multilevel quantised signal is differentiated so that the input to the delay will still only be +q, 0, -q as in figure 2.14.

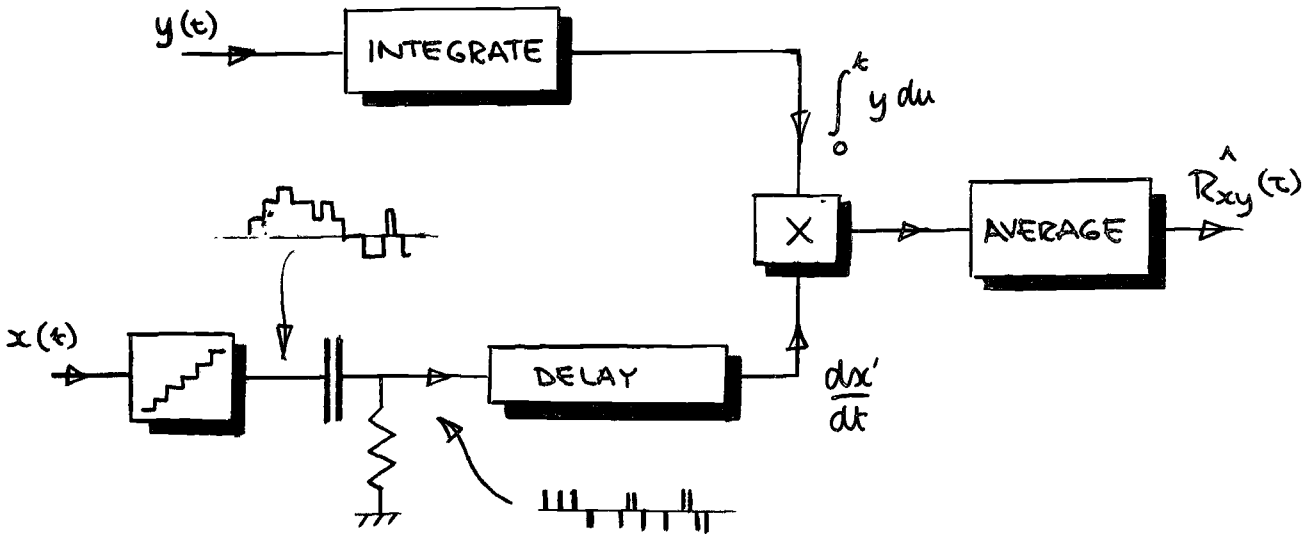

Figure 2.14 Correlation using integration by parts

An integrator is introduced to the other channel, and the system can be analysed by recognising the operations as those involved in integration by parts. The complete analysis is given in Appendix 2.7 where it is also shown that this method causes a further doubling of the variance on the estimate. This may be an allowable sacrifice in terms of the dynamic range achieved. However, in practical instrumentation the integrator in the direct channel could lead to considerable problems of drift and overload, unless the signal y(t) is first put through a suitable high pass filter.

Velocity Limiting Due To Sampling. The scheme of figure 2.14 has been treated as if the input signals were continuous in time. In a sampled system a further difficulty arises. If the sampling frequency is too low, then it is possible for the signal to change by more than one level between sampling

instants. The succeeding delay and gating circuit interpret such a change as only one unit. An exact analysis of the effect of this is difficult but by making some approximations it is possible to make an estimate of the appropriate sampling frequency to avoid such saturation.

The arrangement in the delay channel is repeated in figure 2.15

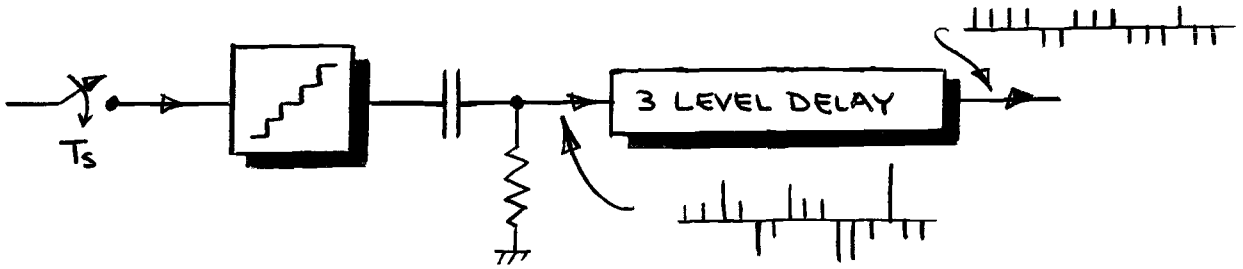

Figure 2.15 Differentiating in the delay channel

The input x(t) is sampled, and quantised. The 'differentiating' circuit in fact takes the difference of successive samples. Ideally these differences are delayed and used to multiply the second input signal of the correlator. In fact each difference is only interpreted as an indication that the signal has increased, decreased, or remained constant, since the previous sample and the magnitude of any change is always taken to be one quantum step q although when the signal velocity is high the actual difference will frequently be more than a single step.

This leads to the diagram of figure 2.16 where a limiting device is artifically introduced to represent the restriction on the size of successive differences.

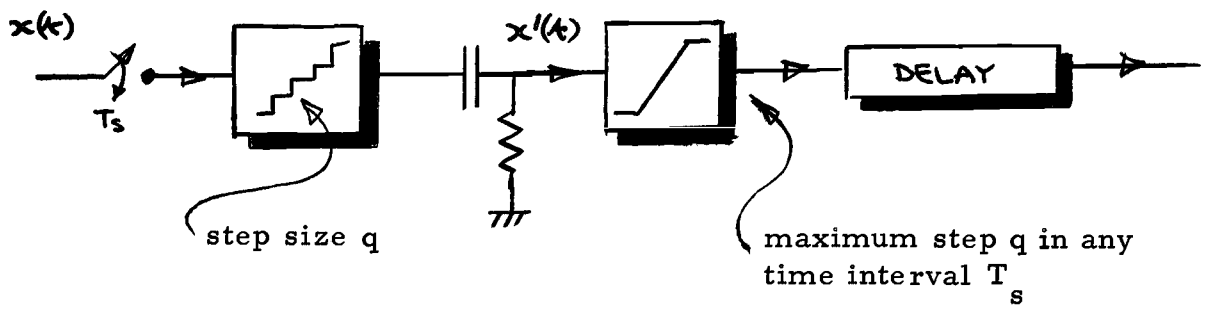

Figure 2.16 Limiting successive differences

If the quantum step q, and sampling time T_s are sufficiently small the signal $x'(t)$ in figure 2.16 will approximate closely to the derivative of $x(t)$. In this case figure 2.16 can be further simplified.

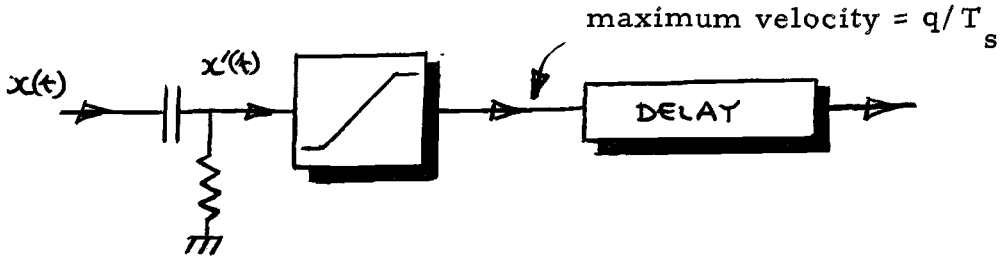

Figure 2.17 Velocity limiting

In figure 2.17 the whole system is reduced to the differentiater and the non-linearity, which now limits at a velocity q/T_s. This non-linearity can finally be replaced by its equivalent gain K_v to the velocity signal, and an appropriate noise signal $n_v(t)$. The limiter non-linearity has been analysed by several authors [40, 41, 42] and figure 2.18 shows how K_v and total noise power vary with input level. It is seen that saturation may be avoided if the r.m.s. velocity σ_v is such that

$$\sigma_v T_s/q < 0.4 \qquad (2.14)$$

and in this case the additional noise can be regarded as negligible. The overall effect on the correlator is illustrated in figure 2.19.

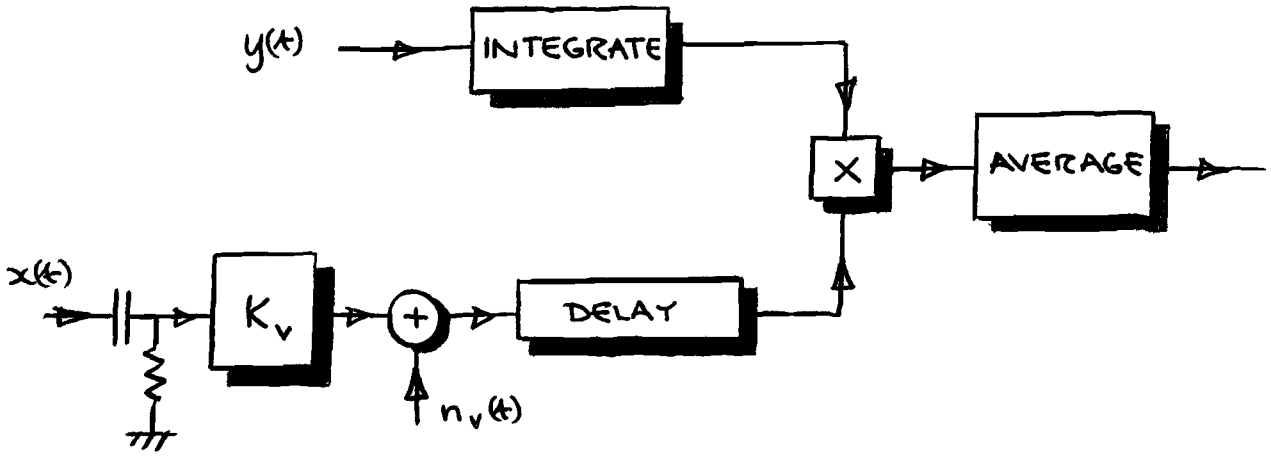

Figure 2.19 The effect of velocity limiting in the correlator

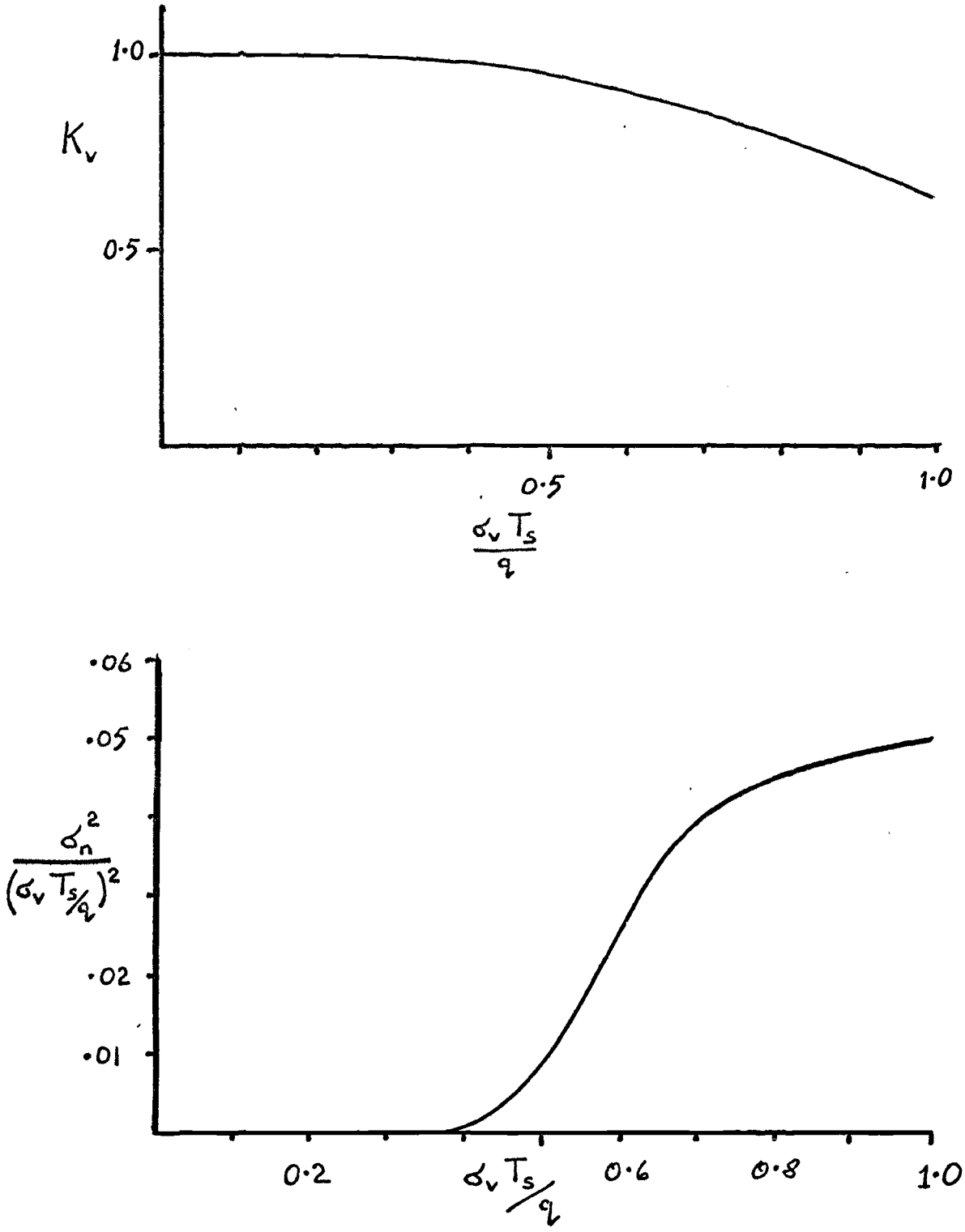

Figure 2.18 Equivalent gain and noise power due to velocity limiting.

The effect of velocity limiting can be neglected if (2.14) is true.

Applying (2.14) to a simple case shows that the sampling frequency for $\sigma/q \simeq 1/2$ should be about 6 times the cut off frequency of the signal spectrum. In practice this is realistic, since such a sampling frequency would be required to resolve the initial portion of the correlation function.

If the signal is coarsely quantised to, say three levels, the number of times that such a signal changes by more than one level between sampling instants will be considerably less than the time the true velocity exceeds q/T_s, and the approximations made in this section will suggest a far worse result than would be obtained in practice. However, it is considered that even this approximate analysis justifies the practical use of integration by parts in a quantised correlator.

Summary. The forms of quantised signal correlator proposed by Watts have been evaluated and found to be useable when the limitations imposed by such practical considerations as finite averaging time, and dynamic range, are taken into account. The equivalent gain method used to analyse overload situations has resulted in a very simple representation of the quantiser when used for correlation, and allows the observation that deterministic signals may still be recovered from noise by correlation, even after coarse quantisation.

Coarse quantisation can be used to simplify multiplication, and to reduce the word length of the individual samples to be delayed. An on-line digital correlator embodying the principles of this chapter has been constructed, and is described in appendix 10. Figure 2.20 shows a typical autocorrelation function

computed by this instrument, using both three level quantisation, and integration by parts.

The instrument accepts signals directly from the plant and processes them to produce a continuously up-dated estimate of the correlation function for 50 discrete values of delay parameter. The minimum increment in delay is 3 milliseconds and there is no limit to the maximum delay. In order to follow variations in the computed correlation function with time, the averaging process is realised by a low pass digital filter. The time constant of this filter can be varied over a wide range from a minimum of 300 milliseconds.

A continuous visual display of the computed correlation function is presented on a CRT screen, figure 2.20. The display is repeated at 3 millisecond intervals regardless of the actual time scale of the computation. In situations where the correlation function is changing with time, the display system is able to present a continuously moving picture. The rate at which this picture changes is determined by the chosen filter time constant, figure 2.21. Figure 2.22 illustrates the autocorrelation function of a sine wave in noise, computed using three level quantisation. Note the spike at zero delay, due to the contaminating wideband noise.

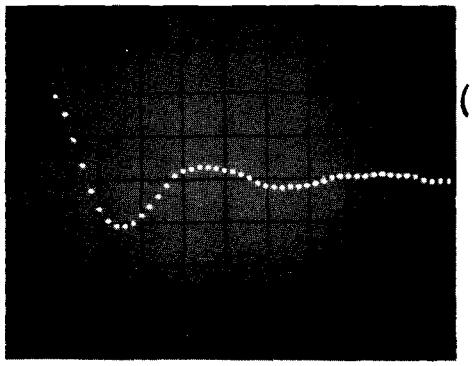

(a)

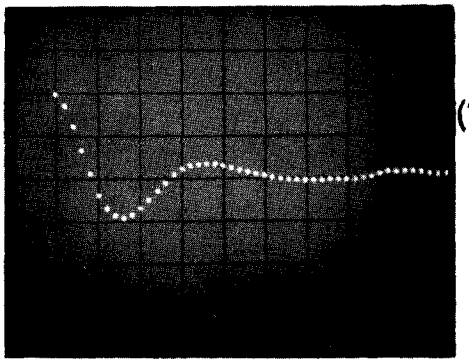

(b)

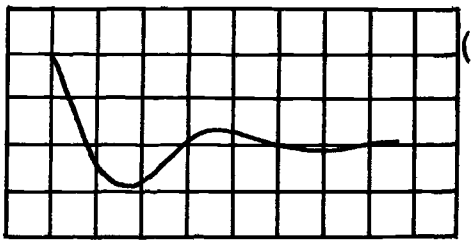

(c)

Figure 2.20

Autocorrelation function computed on-line. Horizontal scale 1 division = 50mS.

(a) using three level quantisation in one channel

(b) using integration by parts to obtain a three level signal

(c) theoretical autocorrelation function,

$R(\tau) = 1.047 \exp. (-0.945\tau) \cos (3.04\tau+0.3)$

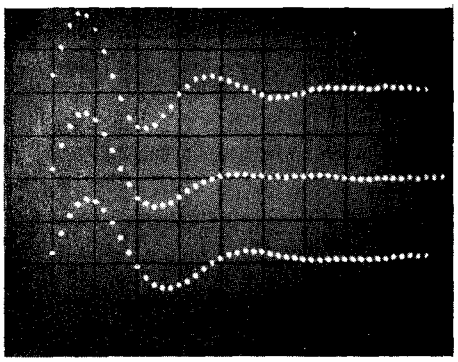

(a)

Figure 2.21

On line cross correlation using three level quantisation. Horizontal scale: 1 division = 50mS.

(a) Multiple exposure photograph showing correlation function when the system dynamics are changing with time. Averaging filter time constant is 20 seconds.
Upper trace. display before change
Centre trace. display 20 seconds after a step change in system dynamics
Lower trace. display after 60 seconds.

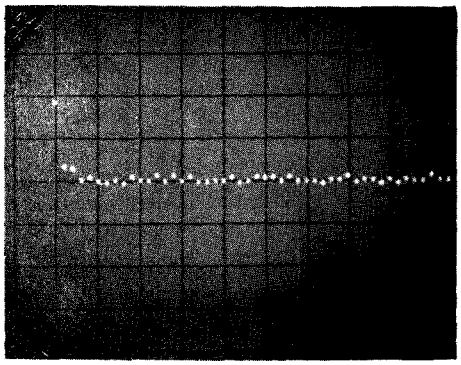

(b)

(b) Input noise autocorrelation function.

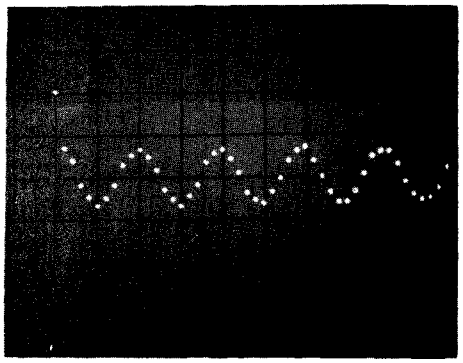

Figure 2.22

Autocorrelation function of 1 volt r.m.s., 10Hz, sine wave in approximately 2 volts r.m.s. wideband noise. Horizontal scale: 1 division = 50mS.

3. COARSE SAMPLING IN A MULTICHANNEL CORRELATOR

The previous chapter has shown how the usual operations in a correlator may be simplified by coarsely quantising the amplitude of one signal. In this chapter the possibility is considered of grading the sampling interval to reduce the storage requirements in a multichannel correlator.

A typical correlation function may have the form of figure 3.1, and could be adequately defined by points unevenly distributed along the delay axis as shown.

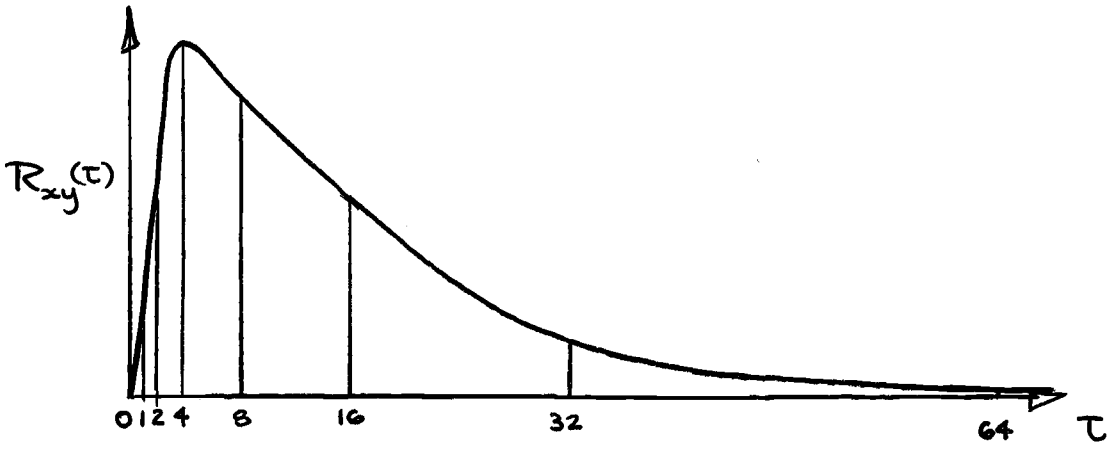

Figure 3.1. Uneven grading of sample points

To compute the correlation function function for all the points in figure 3.1 some form of tapped delay system is necessary. A common arrangement is illustrated in figure 3.2.

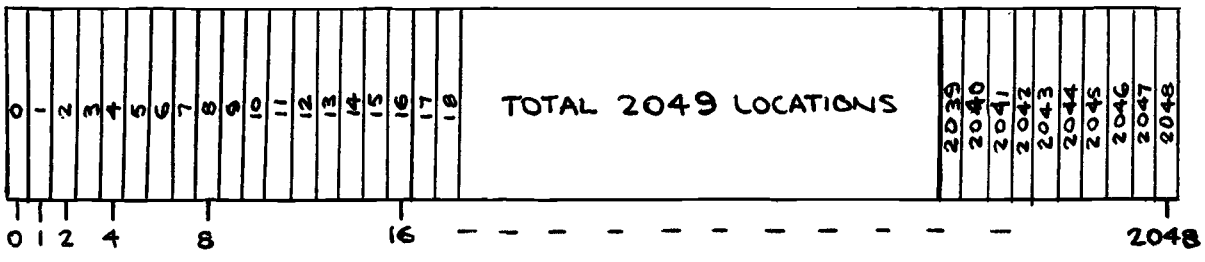

Figure 3.2 A tapped digital delay line for correlation

An undesirable feature of this arrangement is the considerable storage required for a relatively small number of computation points. An additional disadvantage arises when a single arithmetic unit is used serially for each tapping point, figure 3.3

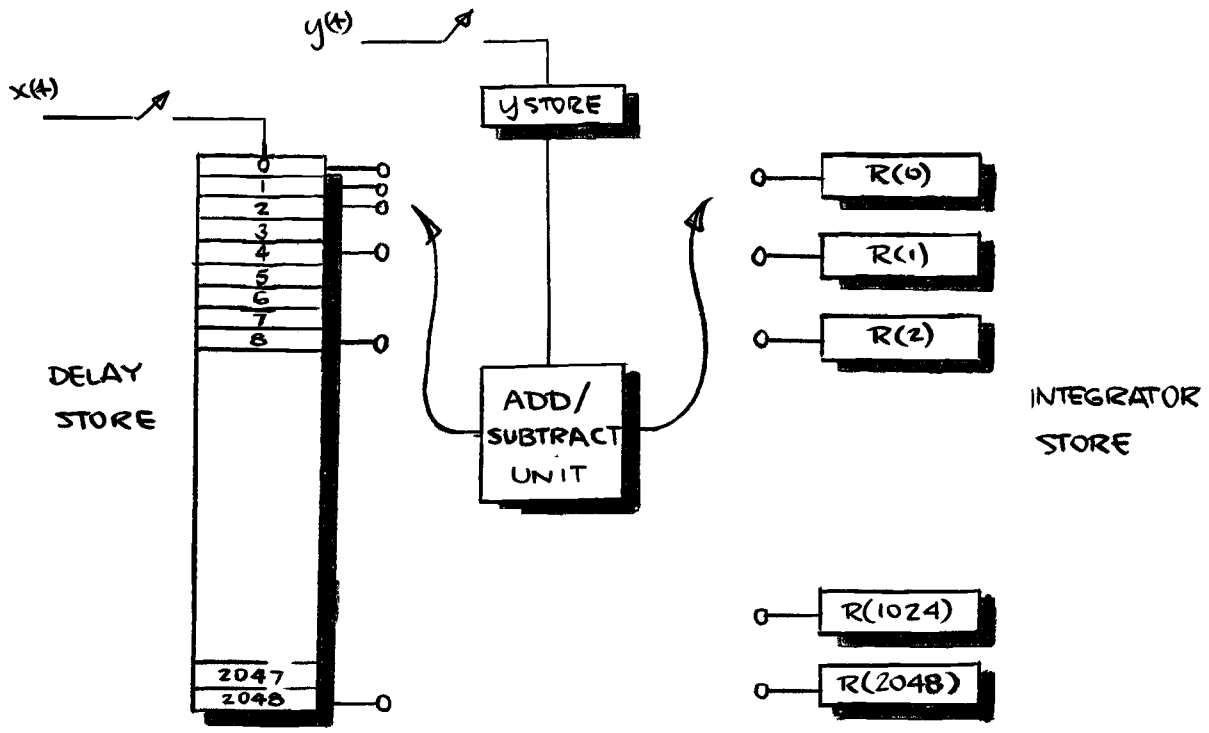

Figure 3.3 Time sharing the arithmetic unit

The maximum sample rate is determined by the resolution desired on the steep part of the correlation function. In the arrangement of figure 3.3 the arithmetic unit serves all tapping points in the time of one sampling interval, and continues scanning at this maximum sample rate. Thus the arithmetic unit is likely to be largely unavailable for any other processing required of it by the computer.

It will be established that, in general, the sampling interval for any tapping point may be conveniently chosen to suit the delay required. This is illustrated in figure 3.4.

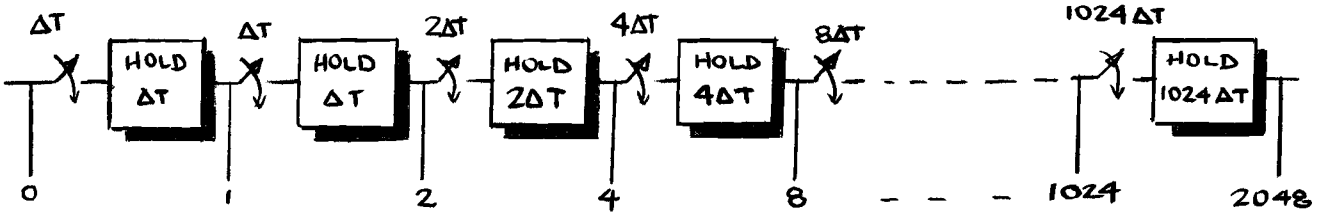

Figure 3.4 Grading the sample rate on a delay line

Using this arrangement, only one storage location is required for each delay tapping, and further, the sample rate, and hence the processing rate, is much reduced at long delays, allowing the possibility of making more efficient use of the arithmetic unit.

For this scheme to be possible it is necessary to establish that sampling at a lower rate than would be required to eliminate aliasing [15] still allows the correlation function to be calculated, and that the additional uncertainty introduced is within acceptable limits.

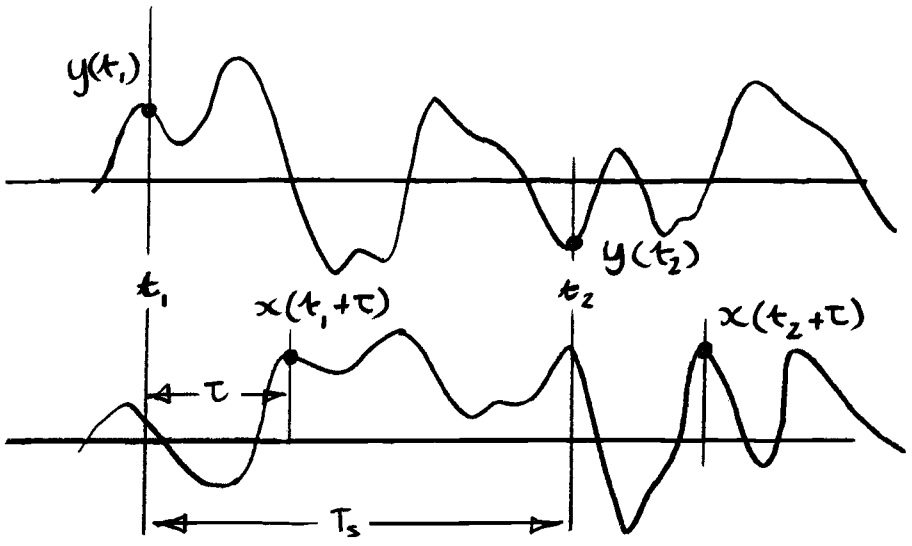

Figure 3.5 Illustrating the sampling process

Effect of coarse sampling. The problem is summarised in figure 3.5. The product of the samples $x(t_i)y(t_i+\tau)$ are to be averaged, when the sample pairs are taken T_s apart. This situation is treated by Lee [3] and it is demonstrated that unless x(t) or y(t) contain components synchronous with the sample rate, then the following identity is true.

$$\lim_{N\to\infty} \frac{1}{N} \sum_{i=1}^{N} y(t_i)\, x(t_i+\tau) \equiv R_{xy}(\tau) \qquad (3.1)$$

This means that a correlator using the graded delay scheme of figure 3.4 will give an accurate estimate of the correlation function when the infinite averaging time is realised.

Finite Averaging Time. The variance of an estimate using N statistically independent samples is well known [1, 3, 16]. In the present case individual samples will be independent if T_s is sufficiently large. As T_s is reduced, successive samples are no longer independent, and the variance of the estimate increases if the same number of samples is used. This is illustrated in figure 3.6.

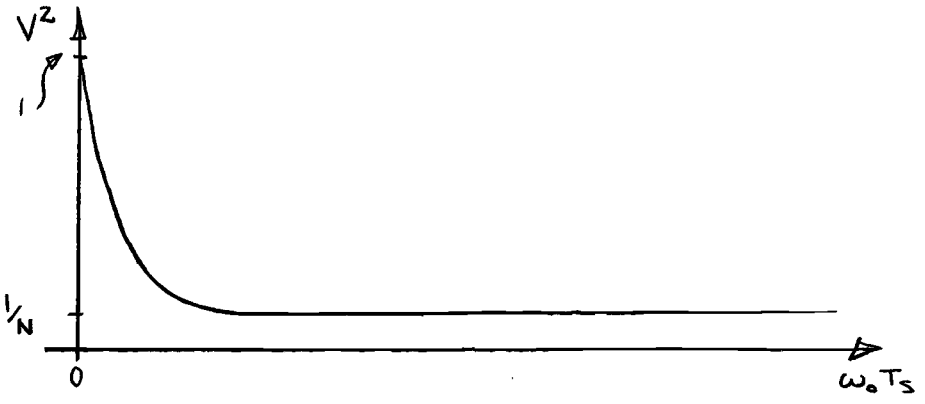

Figure 3.6 Effect of sampling interval on estimate made from a fixed number of samples of a signal whose bandwidth is ω_0

In an on-line correlator using different sample rates for different delays, the number of samples in an averaging time T will be fewer for long delays than

for short delays. Some difference in the variance of the estimate is expected over the full range of delay.

For the case of fixed averaging time T there will be $N = T/T_s$ samples. If T_s is large, samples will be independent, but few in number so that the variance will be large, and proportional to T_s . This is illustrated by the part of the curve beyond 'c' in figure 3.7.

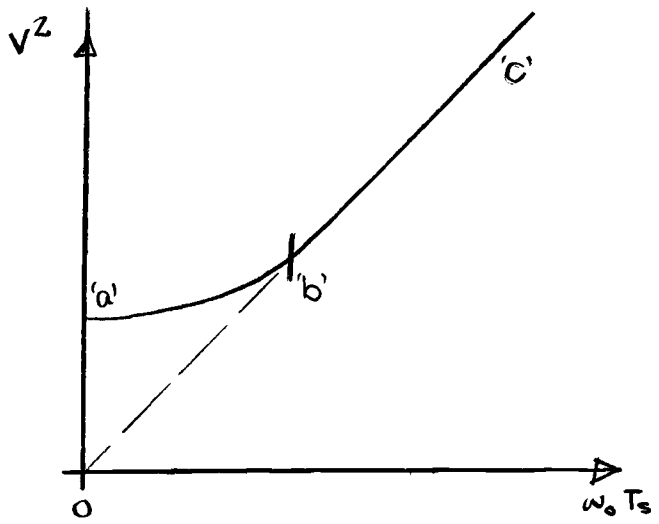

Figure 3.7 Effect of sampling interval on estimate made in fixed time T

As T_s reduces, the number of samples is increased and the variance becomes less, section 'c'-'b' in figure 3.7. Eventually, however, reduction of T_s does not lead to any further reduction in variance, since samples are no longer independent. The increase in variance caused by this, figure 3.6, offsets the increased number of samples used, section 'b'-'a', figure 3.7. The variance at 'a' on figure 3.6 is that obtained when the signals are continuous in time.

The results stated in this section, can be demonstrated using Lee's treatment of inter-sample dependence [3] .

This is done in appendix 3 1 where it is also shown that in a typical case, grading the delay line by coarse sampling causes the variance of the estimate to be approximately 30% greater on the tail of the correlation function than it is on the initial section

It is concluded that the concept of grading can be used to advantage in a correlator

4. IDENTIFICATION USING BINARY TEST SEQUENCES

Previous chapters have dealt with techniques which allow correlation analysis to be used when the signals from the process are Gaussian. If a test signal is permitted then these techniques could also be applied when the test disturbance is Gaussian white noise. However, the use of a specially constructed test signal can lead to the same savings in equipment, and give some additional advantages in terms of noise reduction.

Cross correlation using a wideband random test signal s(t) was shown in Chapter 1 to give an estimate of the impulse response of the system in figure 4.1 from (4.1).

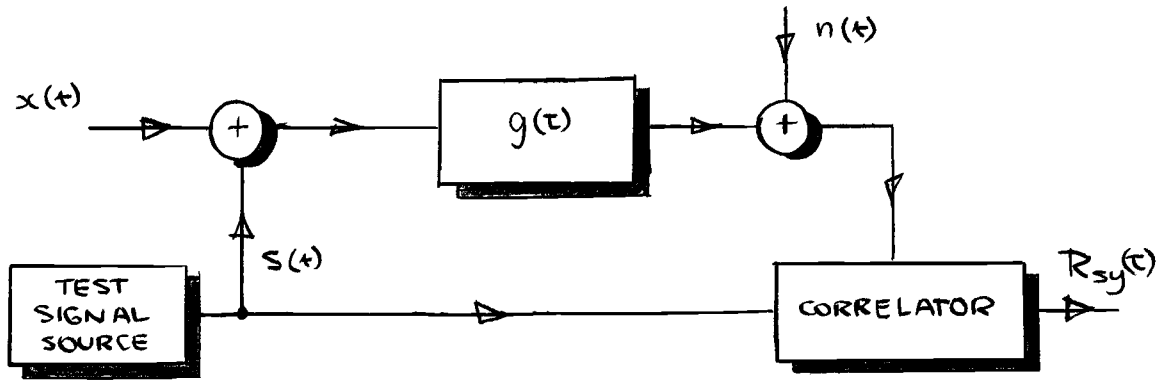

Figure 4.1 An identification system

$$g(\tau) \simeq R_{sy}(\tau) \tag{4.1}$$

This use of a random signal for s(t) has the disadvantage in that even with no additional disturbance there will be some uncertainty in the estimate [2, 3, 17, 18, 19]. For example figure 4.2 shows estimates of the impulse response of a first order filter using a random test signal with no other disturbance on the measurement. Even for long averaging times there is consider-

able scatter on the curve, due entirely to the random nature of the input signal. In practice there will also be additional uncertainty due to the disturbance n(t) in figure 4.1.

The scatter in the result due to the statistical nature of the test signal can be completely eliminated by using a periodic test signal, and averaging over an integral number of periods. The total number of periods used may be increased to reduce the scatter caused by the disturbance n(t). This is illustrated in figure 4.3.

Periodic binary sequences. A periodic binary signal can be constructed which is well suited to the scheme of figure 4.1. Such a signal and its autocorrelation function are illustrated in figure 4.4

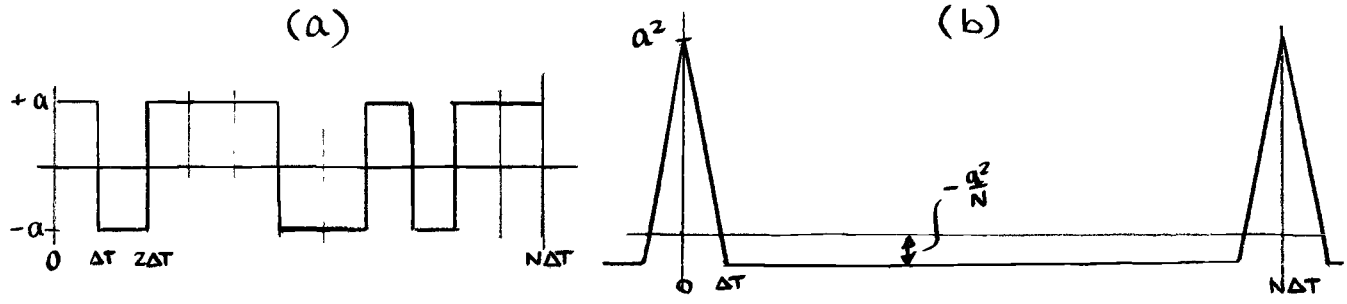

Figure 4.4 (a) Periodic binary sequence with changeovers at multiples of ΔT.

(b) Autocorrelation function of this sequence

The signal has only two levels, $\pm a$, so that the advantages outlined before for coarse quantisation are immediately obtained without further approximations. The autocorrelation function of the sequence approximates to a train of impulses $N\Delta T$ apart. The cross correlation function will be the response of the system to this impulse train, and $N\Delta T$ should be large enough for successive impulse responses not to overlap.

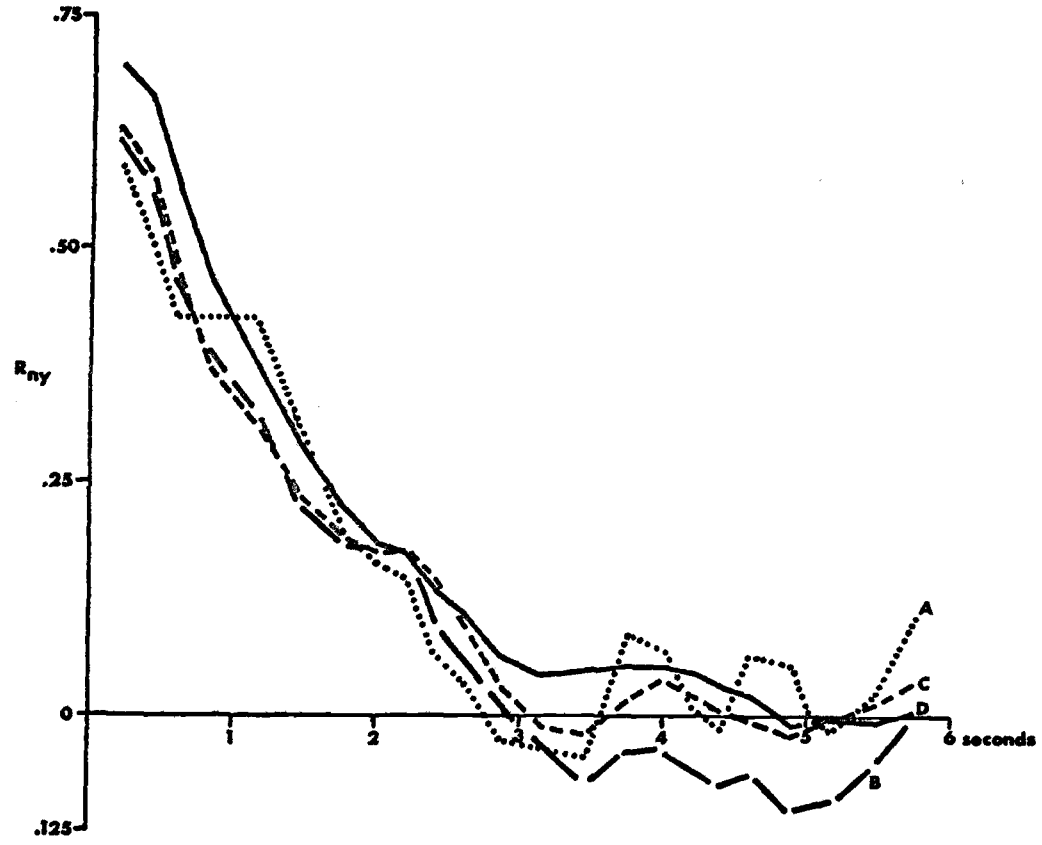

Figure 4.2 Cross correlation between a white noise input and the output from a first order system of one second time constant. The averaging times are (a) 20 sec (b) 40 sec (c) 100 sec (d) 200 sec.

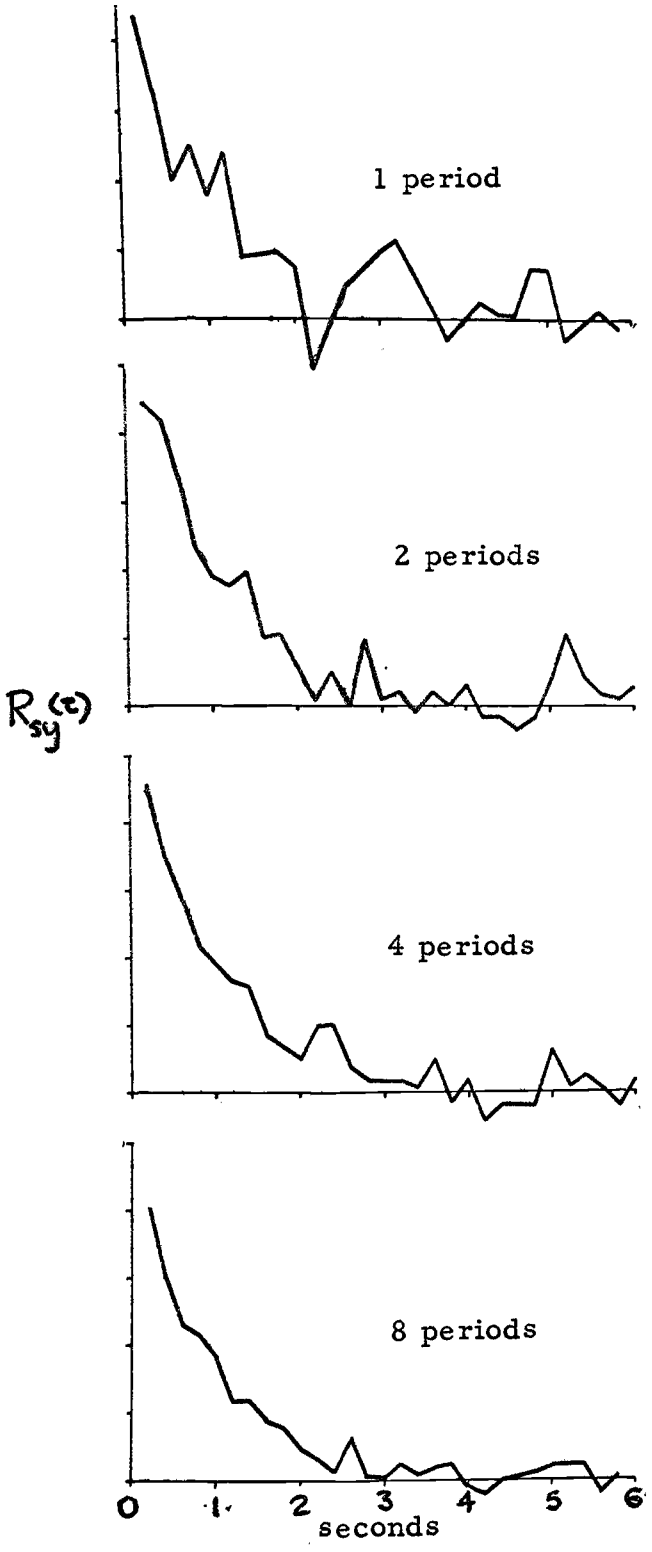

Figure 4.3

Effect of multiple period averaging. Test signal has. N=31, $\Delta T=0.2$, and total period = 6.2 seconds.

The finite width of the autocorrelation function peak will give rise to some error in the computed impulse response. The effect of this is shown in figure 4.5 where the computed $R_{sv}(\tau)$ is compared to the true g(t) for various ΔT.

It is possible to choose a ΔT which gives an acceptable error. A ratio of 0.4:1 between ΔT and the system time constant can give reasonable results in many circumstances.

Power spectrum of a periodic binary sequence. The effect of the parameters ΔT, and N on the sequence autocorrelation function have been pointed out. It is interesting to relate these parameters to the power spectrum of the sequence, since traditionally the frequency domain has been used to describe system dynamics. The power spectrum $G(\omega)$ of the sequence in figure 4.4(a) will have the form shown in figure 4.6

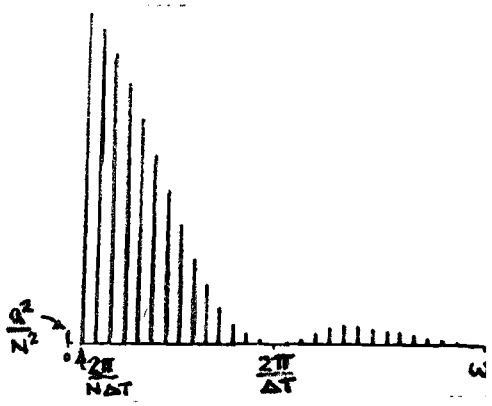

Figure 4.6 Power spectrum of a binary sequence with clock interval ΔT and period $N\Delta T$.

This is a line spectrum, containing harmonics ω_n of the fundamental frequency $2\pi/N\Delta T$. The envelope is given by (4.1)

$$G(\omega_n) = 2a^2 \frac{N+1}{N^2} \cdot \frac{\sin^2 \omega_n \Delta T/2}{(\omega_n \Delta T/2)^2} \qquad (4.1)$$

There is also a spike at zero frequency. This is because, in general, periodic sequences of the type under discussion spend one more clock interval at the '+a' level than at the '-a' level in one full period. The d.c. power is then a^2/N^2. It is this feature also which gives rise to the non-zero base line of the autocorrelation function, figure 4.4(b).

It can be seen from figure 4.6 that most of the signal power is contained below the clock frequency $2\pi/\Delta T$. This should therefore be arranged to cover the frequency band of interest.

Figure 4.7 shows how the choice of ΔT and N in the time domain is reflected in the frequency domain. Figure 4.7 (a) shows the cross correlation function for 1st and 2nd order systems using a sequence with $\Delta T = 0.2$ seconds and N = 31. This choice of ΔT gives good resolution on the initial part of the correlation function, and the total period $N \Delta T$ is long enough to contain one complete response. Figure 4.7(b) shows the power spectrum of the sequence in comparison with the frequency response functions (power gain) of the two systems. The first frequency component is in the region of the 3dB point on the first order response. This contrasts with the approach which might be made using sine wave test signals, where it is usual to start the analysis with frequencies on the flat part of the response.

Effect of background noise. In the presence of a background disturbance n(t), the variance of the estimate using a binary sequence can be reduced by the appropriate choice of N and ΔT. Typical results for a first order system are shown in figure 4.8.

The total averaging time $T = N\Delta T$ is the same in each case. There is a

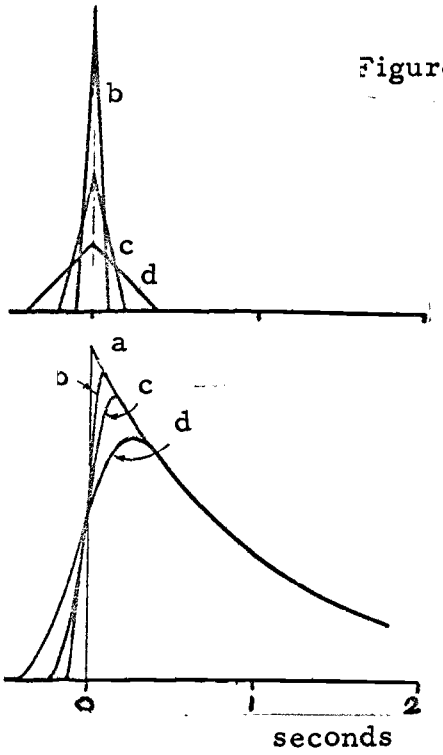

Figure 4.5 Effect of input autocorrelation function peak width on the computed cross-correlation function for first order system. Time constant = 1 sec.

(a) Expected result for perfect impulse autocorrelation function.
(b) Result for binary signal with $\Delta T = 0.1$ sec.
(c) Result for $\Delta T = 0.2$ sec.
(d) Result for $\Delta T = 0.4$ sec.

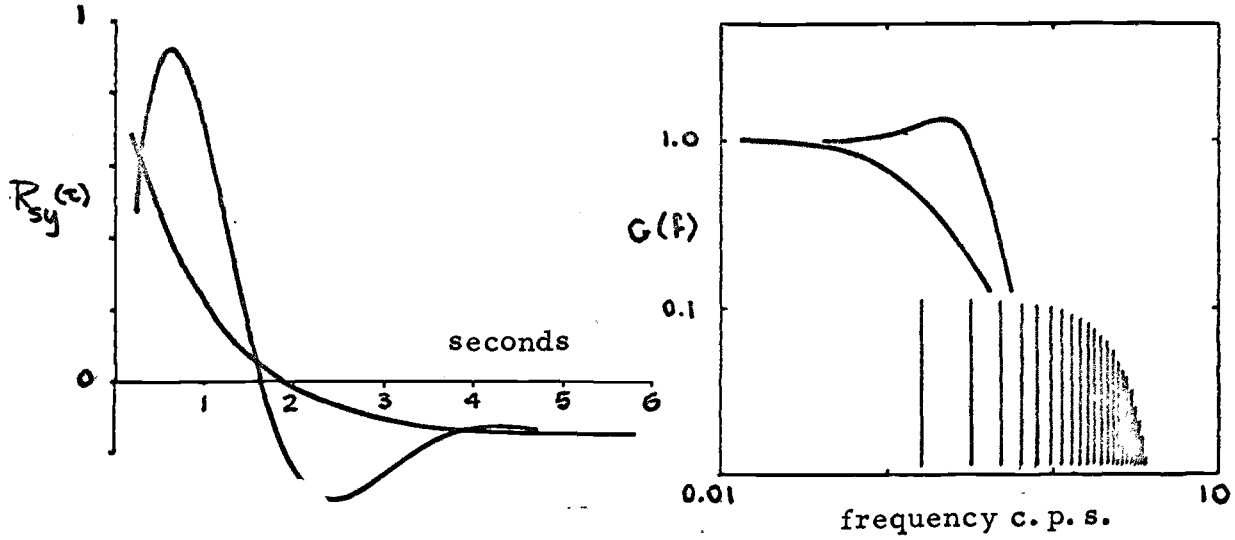

Figure 4.7 (a) Derived impulse response for first and second order systems.
(b) Transfer functions of the first and second order systems compared with the power spectrum of the test signal N=31, $\Delta T = 0.2$

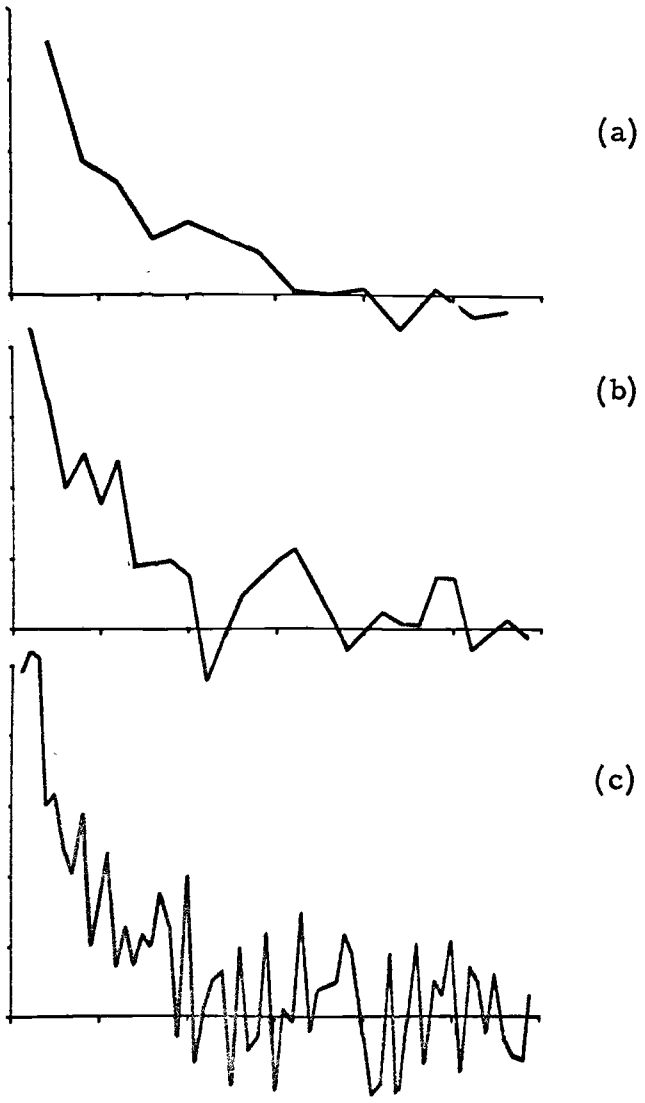

Figure 4.8 Effect of variation in the parameters N and ΔT. of the test signal with background noise present. Total period approximately constant at about 6 seconds. System time constant 1 second. Averaging time one complete period.

(a) $N = 15$, $\Delta T = 0.4$ sec.
(b) $N = 31$, $\Delta T = 0.2$ sec.
(c) $N = 63$, $\Delta T = 0.1$ sec.

significant improvement in the result as ΔT is increased and it can be shown that

$$V^2 \propto 1/(\Delta T)^2 \tag{4.2}$$

where V^2 is the variance of the estimate [20].

Figure 4.3 has already demonstrated that averaging over several periods also reduces the effect of the noise. In this case

$$V^2 \propto 1/KN\Delta T \tag{4.3}$$

where $KN\Delta T$ is the total averaging time [20].

Generating a periodic binary sequence. An important feature of the binary test signal described in the previous sections is that it is readily generated using simple digital circuitry. Although several mathematical techniques are available for finding sequences with the prescribed properties the most convenient practical approach uses a binary shift register. The basis for this is given in detail by various authors, notably Elspas [24], Birdsall and Ristenbatt [21], and Briggs [9]. An outline is given in appendix 4.1 and an example will serve to illustrate the method here.

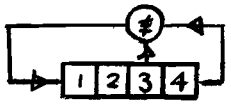

1 0 0 0
0 1 0 0
0 0 1 0
1 0 0 1
1 1 0 0
0 1 1 0
1 0 1 1
0 1 0 1
1 0 1 0
1 1 0 1
1 1 1 0
1 1 1 1
0 1 1 1
0 0 1 1
0 0 0 1
1 0 0 0

Figure 4.10 A shift register sequence generator

The four stage shift register in figure 4.10 has logical feedback from the final two stages to the input. The logic compares the two stages and generates '1' if they are different, 'O' if they are the same. This is then the new input to the shift register. The table in figure 4.10 shows how the content of the register changes with successive clock pulses. After 15 pulses the content returns to its original state, and the pattern repeats. This is an example of a general rule that, if the feedback is chosen correctly a maximal length sequence of length $N = 2^n - 1$ will result from an n--stage shift register generator. Such a sequence can be shown to possess the features shown in figure 4.4 if the 'O' level is interpreted as -1 and the '1' level as +1 [25].

Multivariable systems. The usefulness of the binary sequence for system identification is well established [8, 9, 28-34], and interest is now focussed on the possibility of using these sequences to identify several input - output characteristics simultaneously. Some aspects of this will be treated in the next chapter.

5. CROSS CORRELATION PROPERTIES OF SEQUENCES

A multi-input identification problem is illustrated in figure 5.1.

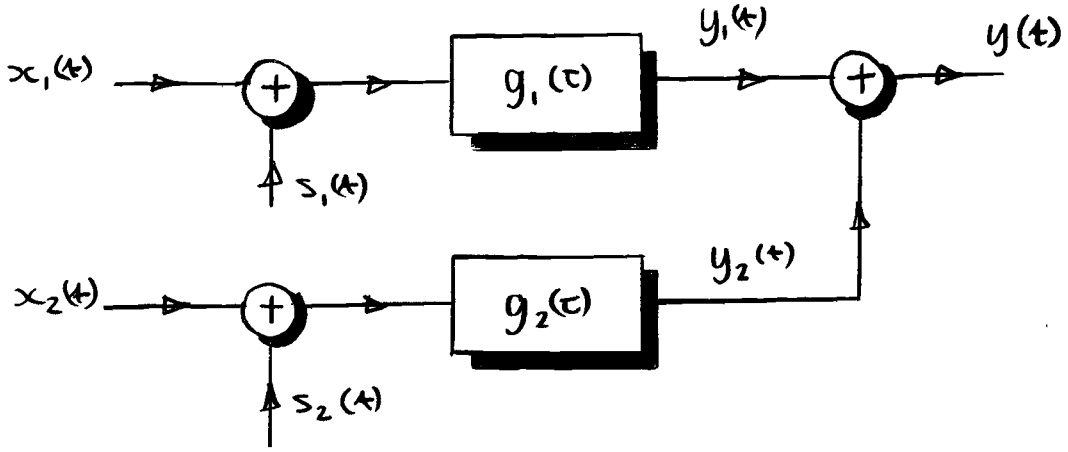

Figure 5.1 A two input identification problem

Here a single output is dependent on two inputs through two separable response functions $g_1(\tau)$ and $g_2(\tau)$. These could be identified by injecting an appropriate test signal first into $g_1(\tau)$ and then into $g_2(\tau)$, and cross correlating the output with each in turn as in figure 4.1. However, in any on-line system it is desirable to be able to monitor the two responses simultaneously.

Consider an ideal case in which $x_1(t) = x_2(t) = 0$.

Now the only disturbance on the measurement of $R_{s_1 y_1}(\tau)$ is $y_2(t)$.

$$R_{s,y}(\tau) = \int_0^\infty g_1(u) R_{s,s_1}(\tau - u)\, du \quad + R_{s,y_2}(\tau) \tag{5.1}$$

The second term in (5.1) will be an error on the measurement.

$$R_{s,y_2}(\tau) = \lim_{T\to\infty} \frac{1}{T} \int_0^T \int_0^\infty g_2(u)\, s_2(t-u)\, du \cdot s_1(t-\tau)\, dt$$

$$= \int_0^\infty g_2(u) \lim_{T\to\infty} \frac{1}{T} \int_0^T s_2(t-u)\, s_1(t-\tau)\, dt \cdot du$$

$$= \int_0^\infty g_2(u)\, R_{s_1 s_2}(\tau - u)\, du \tag{5.2}$$

From (5.1) and (5.2) it can be seen that unless

$$R_{s_1 s_2}(\tau) = 0 \tag{5.3}$$

for all τ, $g_1(u)$ cannot be recovered from (5.1).

In the case of sequences of equal length some bounds are available for the cross correlation between them. If two maximal length sequences have N bits then it can be shown [35] that the smallest peak M_c on the cross correlation between them will be limited by (5.4).

$$M_c > \sqrt{\frac{1}{N} - \frac{1}{N^2}} \tag{5.4}$$

The cross correlation between all shift register sequences of equal length, from N = 15 to N = 127 has been evaluated using a digital computer. Table 5.1 compares the observed smallest peak with the minimum prescribed by (5.4).

N	$\sqrt{\frac{1}{N} - \frac{1}{N^2}}$	M_c
15	0.25	0.47
31	0.177	0.29
63	0.125	0.24
127	0.089	0.13

Table 5.1 Minimum peak of cross correlation function

The results of the computer study are detailed in appendix 5.1, together with a summary of the properties observed. The principal conclusion to be drawn is that it is not possible to obtain two equal length sequences with zero, or even constant, cross correlation for all values of delay.

Modification of a periodic binary sequence. A technique for synthesising two sequences which have specified cross correlation properties has been suggested from various sources [25, 36, 37]. To generate two sequences which are mutually uncorrelated, a maximal length sequence length N is modified by inverting alternate bits in the sequence.

The new sequence will now have period 2N and is found to be uncorrelated with the original source sequence. The autocorrelation function of this new sequence is shown in figure 5.2.

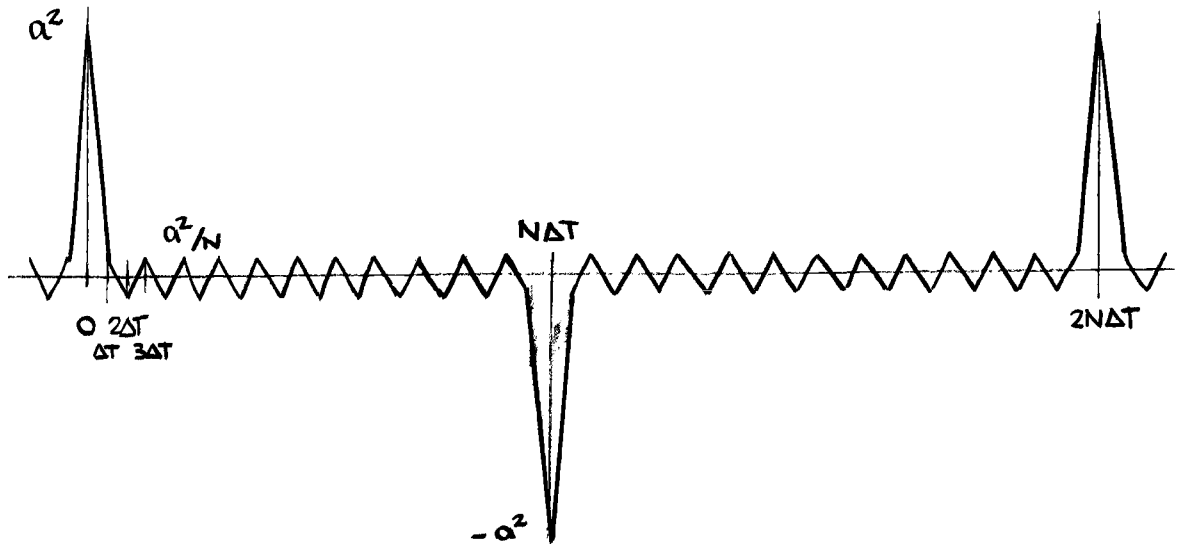

Figure 5.2 Autocorrelation function of modified binary sequence

This still exhibits the delta function like characteristic which is required for identification, but also has a ripple component. However, the frequency of this ripple will be above the pass band of the system if the coice of ΔT is consistent with the need to have a wide band signal. Figure 5.3 shows a pair of impulse responses $g_1(t)$ and $g_2(t)$ in figure 5.1 computed simultaneously using a shift register sequence for one system and the modified sequence for the other. The ripple component is hardly in evidence.

The procedure outlined above for modifying the shift register sequence amounts to multiplying that sequence by a subsequence -1, +1, -1, +1, etc. Can this approach be extended to obtain further uncorrelated sequences?

A table of 'orthogonal sequences' of length 8 has been published in connection with coding theory [38] and is repeated in table 5.2. This contains the sequence

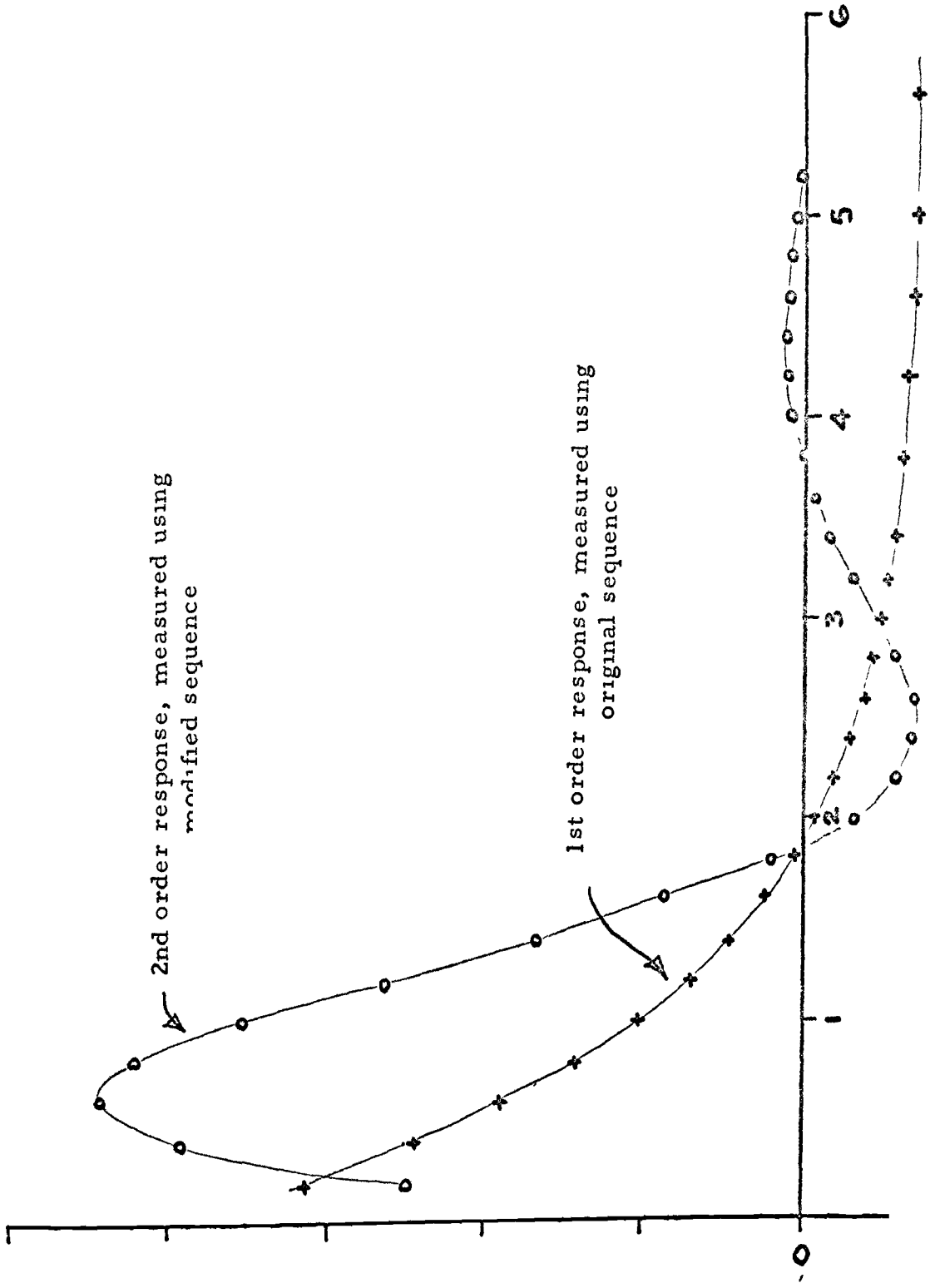

Figure 5 3 Simultaneous measurement of two impulse responses by using two uncorrelated sequences

-1, +1, -1, +1, already discussed. In addition three other separate cyclic sub-sequences are available which have been found to give new uncorrelated sequences in the same way. Descriptions of the resulting autocorrelation functions are given in Appendix 5.2.

1 0 1 0	1 0 1 0
1 1 0 0	1 1 0 0
1 1 1 1	0 0 0 0
1 0 1 0	0 1 0 1

Table 5.2 'Orthogonal' sequences which can be used to modify a shift register sequence to produce a set of uncorrelated sequences.

The concept of modified sequences leads to a solution of a difficulty which is likely to be encountered frequently in practice. Use of a periodic sequence of the type originally described relies on the system memory being less than a complete period. If the system contains an integrator, however, the periodic signal can not be used in its present form unless some correction is made to the result. Since many real systems contain an integrator in the form of a motor, it is felt that some other solution would be useful. In this connection a new form of modified sequence has an interesting property.

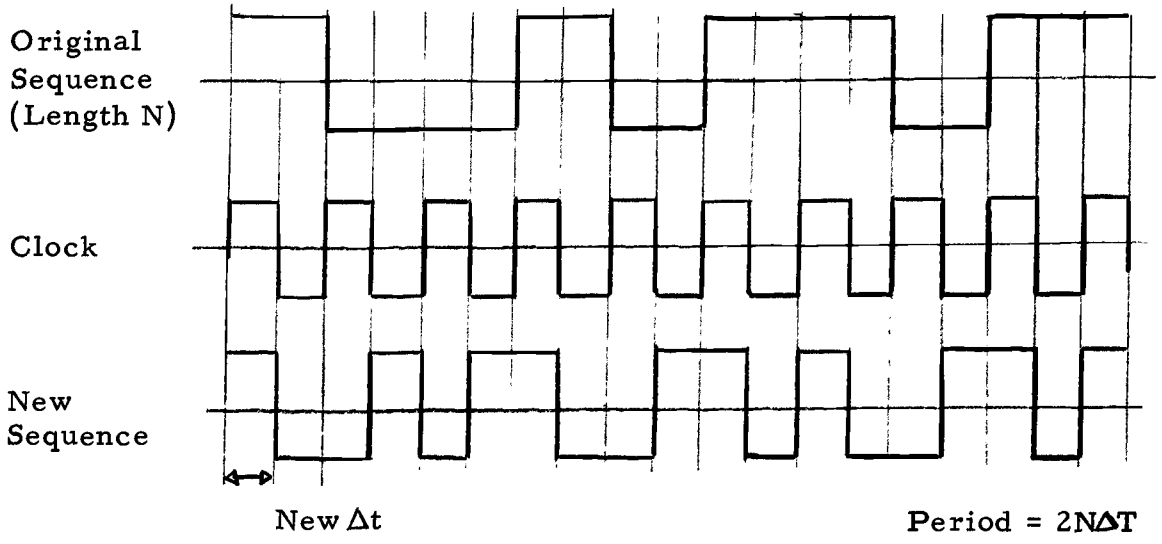

Figure 5.4 Modifying a shift register sequence with the clock

In figure 5.4 a shift register sequence is multiplied by the clock square wave, which has a period equal to one clock interval. The result of the operation is that each bit is multiplied by +1 for the first half of the interval and by -1 for the other half. It is apparent that the resulting modified sequence will exhibit a 'high pass' characteristic, since it cannot remain at any level for longer than two half periods. The autocorrelation function and the power spectrum of this sequence are derived in Appendix 5.3. The autocorrelation function is illustrated in figure 5.5.

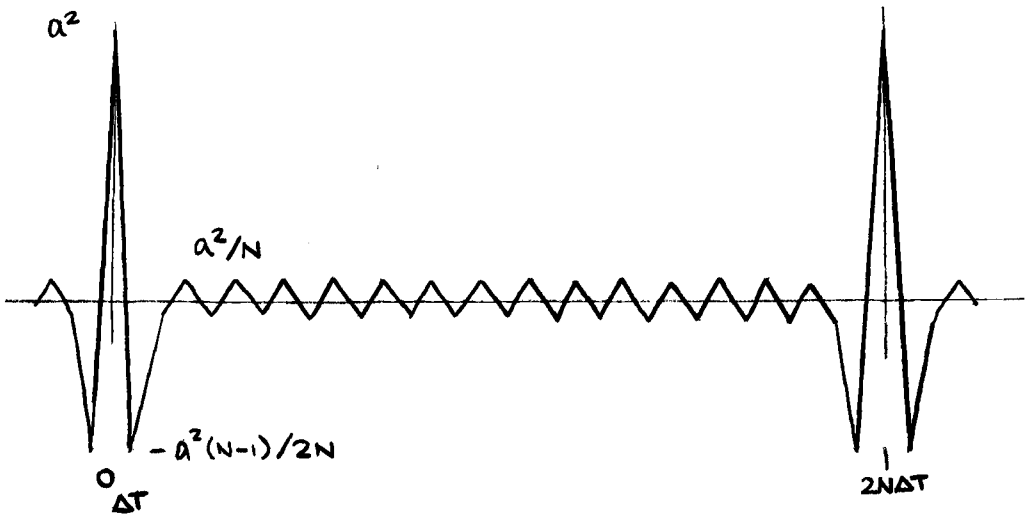

Figure 5.5 The autocorrelation function of a clock modified sequence

The use of this sequence is demonstrated in figure 5.6 where the integrator is separated from the rest of the system, and the response at various points to the modified sequence autocorrelation function is shown. It can be seen from this diagram that using a clock modified sequence in a system containing an integrator allows an approximation to be made to the derivative of the overall system impulse response.

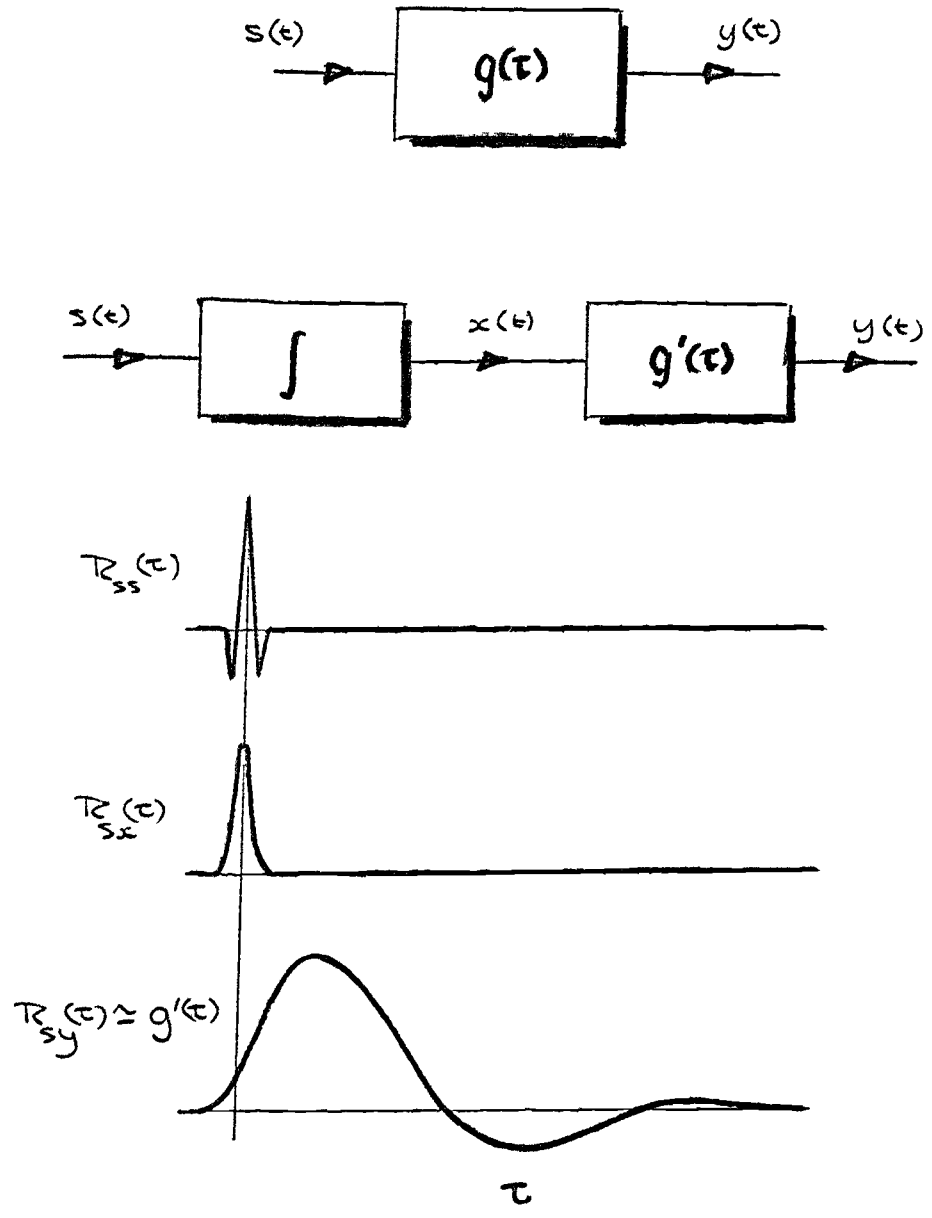

Figure 5.6 Using a clock modified sequence in the presence of an integrator

6. CONCLUSIONS

The application of correlation analysis to linear system identification has usually been restricted by the computing capacity required. Considerable attention is now being directed towards on-line measurement of system characteristics, where computing time is at a premium.

The technique of coarse quantisation has been used to reduce correlator complexity. A quantitative evaluation has been made of the errors introduced by the technique, with particular regard to the effects of finite averaging time. It has been demonstrated that a Gaussian random signal in one channel of a correlator can be adequately described by only three discrete levels, and that the additional statistical uncertainty amounts to an increase of only a few percent in the variance of the estimate. A correlator can therefore be constructed which uses a three level delay line, and in which multiplication is replaced by addition or subtraction. This form of correlator is sensitive to input level variations, and the effect of this has been derived directly from the equivalent gain technique used to analyse the quantiser.

A second form of correlator describes the input signal by the changes from one quantum level to the next. These changes can still be represented by a three level signal, even though the quantiser has many levels. This technique has been recognised as integration by parts, and it has been shown that it approximately doubles the uncertainty of an estimate.

In correlation analysis the effects of 'aliasing' do not need to be considered when choosing the sampling frequency. This has been applied to grading the sampling interval in a digital correlator, so that the sampling interval increases

with the delay required. This eliminates large amounts of storage, and saves an equivalent amount of computing time.

The coarse quantisation technique is applicable to systems having normal operating signals with Gaussian amplitude probability density functions. If a test signal can be injected into the system, then it can be tailored to suit the particular identification problem, and the prevailing noise environment, while still keeping the computing requirements to a minimum. One such signal is the periodic binary sequence, which has the useful features of 'white' noise without the disadvantages inherent in a random perturbation. The application of binary sequences to identification has been outlined, and some results presented demonstrating the choice of sequence parameters for any particular situation.

The cross correlation between periodic binary sequences has been studied, and it is concluded that if the sequences are the same length, they cannot be completely uncorrelated. However, a method is presented for obtaining a set of mutually uncorrelated sequences which are derived from a maximal length sequence, and may be useful for identification of multivariable systems.

The digital techniques described will enable greater use to be made of correlation analysis for measurement and subsequent control of dynamic systems. Also, the equivalent gain approach to the quantiser may be useful in digital measurement techniques other than correlation.

7. REFERENCES

1. BENDAT J.S.: 'Principles and applications of random noise theory', Wiley, 1958.
2. DOUCE, J.L.: 'An introduction to the mathematics of servomechanisms', E.U.P. 1963.
3. LEE, Y.W.: 'Statistical theory of communication', Wiley, 1960.
4. BOARDMAN, F.D , HARRINGTON, E.L.E.,CARSWELL, D.J.A.: 'A correlator for estimating dynamic parameters of nuclear reactors by fluctuation analysis', Radio and Electronic Engineer, 30, (3), September 1965.
5. GOODMAN, T.P., RESWICK, J.B.: 'Determination of system characteristics from normal operating records', ASME Trans. 78, pp. 259-271, February 1956.
6. WATTS, D.G.: 'A theory of amplitude quantisation with application to correlation determination', Proc. IEE 109c (15) p. 209, March 1962.
7. WATTS, D.G.: 'A study of amplitude quantisation with applications to correlation determination.' Ph.D. Thesis, London University, 1962.
8. BALCOMB, J.D., DEMUTH, H.B., GYFTOPOULOS, E.P.: 'A cross correlation method for measuring the impulse response of reactor systems', Nuclear Science & Engineering, 11, (2), October 1961, pp 159-166.
9. BRIGGS, P.A.M., HAMMOND P.H., HUGHES, M.T.G., PLUMB, G.O.: 'Correlation analysis of process dynamics using pseudo random binary test perturbations', Proc. I Mech. E., 1965, 179, (3H.), p37.
10. CORRAN, E.R., and CUMMINS, J.D.: 'Binary codes with impulse autocorrelation functions for dynamic experiments', U.K.A.E.A. Reactor Group report AEEW - R210, September 1962.

11. BARRET, J.F., and COALES, J.F.: 'Introduction to analysis of non-linear control systems with random inputs', Proc. IEE, 103C, p190.

12. ATHERTON, D.P.: 'The evaluation of the response of single valued non-linearities to several inputs', Proc. IEE, 109c, (15), p.146. (Mon 474M, October 1961).

13. SOMERVILLE, M.J., and ATHERTON, D.P.: 'Multigain representation for a single valued non-linearity with several inputs, and the evaluation of their equivalent gains by a cursor method', Proc. IEE, 105 C, (8), 1958, pp. 537-549.

14. ATHERTON, D.P.: 'Rapid evaluation of the autocorrelation function of the output of single valued non-linearities in response to sinusoidal and gaussian signals', Proc. IEE, 109C, September 1962, p656-664. (Mono, 533E, July 1962).

15. SHANNON, C.E.: 'A mathematical theory of communication', Bell Systems Tech. J., 27, (3) and (4), July and October 1948.

16. BLACKMAN, R.B., and TUKEY, J.W.: 'The measurement of power spectra from the point of view of communications engineering', Dover, 1959.

17. GIBSON J.E.: 'Non-linear automatic control' McGraw Hill.

18. COOPER, G.R., and LINDENLAUB, J.C.: 'Noise limitations of system identification techniques', Trans. IEEE, AC - 8 (1) January 1963, pp 43-48.

19. KERR, R.B., and SURBER, W.H.: 'Precision of impulse response identification based on short normal operating records', Trans. IRE, AC - 6, pp 173-182, May 1961.

20. CUMMINS, J.D.: 'A note on errors and signal to noise ratio of binary cross correlation measurements of system impulse response', U.K.A.E.A. Reactor Group report, AEEW-R329, 1964.

21. BIRDSALL, T.G., and RISTENBATT, M.P.: 'Introduction to linear shift register generated sequences', U.S. Government research report, PB 163 108, 1958.

22. CODRINGTON, R.S., and MAGNIN, J.P.: 'Legendre PCM synchronisation codes', IRE National Symposium on Space Electronics and Telemetry, 1962. Paper 2.5.

23. CORRAN, E.R., and CUMMINS, J.D.: 'Binary codes with impulse auto-correlation functions for dynamic experiments', UKAEA Reactor Group report AEEW-R210, September 1962.

24. ELSPAS, B.: 'The theory of autonomous linear sequential networks', Trans. IRE, CT - 6 (1), March 1959, p.45

25. GOLOMB, S.W. (editor): 'Digital communications with space applications', Prentice Hall, 1964.

26. PETERSON, W.W.: 'Error correcting codes', M.I.T. and Wiley, 1961.

27. ROE, G.M.: 'Pseudo random sequences for the determination of system response characteristics; sampled data systems', General Electric Research Lab., Schenectady, Report 63-RL - 334IE, June 1963.

28. ANDERSON, G.W., BULAND, R.N., COOPER, G.R.: 'The Aeronutronic self optimising automatic control system', WADC - TR 59-49, pp. 349 - 406, U.S. Government research report, PB142243.

29. CORRAN, E.R. and CUMMINS, J.D.: 'Impulse response measurements with an off line cross correlator', U.K.A.E.A. Reactor Group report, AEEW-R316, November 1963.

30. CORRAN E.R., and CUMMINS J.D.: 'Preliminary results of statistical dynamic experiments on a heat exchanger', U.K.A.E.A. Reactor Group report, AEEW-R255, August 1963.

31. HUGHES, M. T.G., and NOTON, A. R. M.: 'The measurement of control system characteristics by means of a cross correlator', Proc. IEE, 109B, (43), January 1962.

32. POORTVLIET, D.C.J.: 'The measurement of system impulse response by cross correlation with binary signals', Technical University, Delft, Netherlands, 1962.

33. STERN, J.E., VALAT, J., BLAQUIERE, A.: 'Reactivity measurement using pseudo random source excitation', Journal of Nuclear Energy (A, B), 16, pp499-508, 1962.

34. VAN DER GRINTEN, P.M.E.M., KRIJER, J.: 'Processing of the auto and cross correlation functions to step response', Ann. Assn. Int. Calcul Analogique, 5, pp. 160-161, July 1963.

35. STALDER, J.E., and CAHN, C.R.: 'Bounds for correlation peaks of periodic digital sequences', Proc. IEEE, October 1964.

36. HAMMOND, P.H., and ROBERTS, G.T.: Private communication, August 1964.

37. NORSWORTHY, K.: Private communication, February 1965.

38. HARMUTH, H.F.: 'On the transmission of information by orthogonal time functions', Trans. AIEE, 79, (1), Communication and Electronics, pp248-255, 1960.

39. BOULTON, P.I., and KAVANAGH, R.J.: 'A method of producing multiple non correlated random signals from a single gaussian noise source, IEEE Transactions on applications and Industry, 82, pp 46-52, March 1963.

40. WEST, J.C., DOUCE, J.L., and LEARY, B.G.: 'Frequency spectrum distortion of random signals in non-linear feedback systems', Proc. IEE, 108C, (13), p.259, 1961.

41. LANING, J.G., and BATTIN, R.H.: 'Random processes in automatic control', McGraw Hill, 1956.

42. ROBERTS, G.T.: 'Aspects of non-linear servomechanism analysis', Ph.D. Thesis, Manchester University, 1958.

43. DWIGHT, H.B.: 'Tables of integrals and other mathematical data', Macmillan, 1961.

44. PIERCE, R.L.: 'Properties of 2 element periodic sequences with some results on their cross correlation', General Electric Report, R62DSD55, June 1962.

APPENDICES

A.1.1. MEASURING THE IMPULSE RESPONSE OF A SYSTEM USING CORRELATION

The system in figure A.1.1 has an impulse response g(t) and is subjected to an input signal x(t). The true response z(t) of the system is contaminated by additive noise n(t), and the resulting output y(t) is to be cross correlated with x(t).

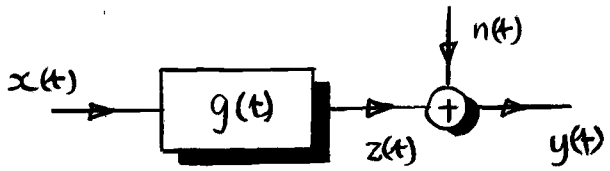

Figure A.1.1 A system with a random input and a random disturbance on the output.

$$R_{xy}(\tau) = \lim_{T\to\infty} \frac{1}{T}\int_0^T y(t)\,x(t-\tau)\,dt \qquad (A.1.1)$$

$$= \lim_{T\to\infty} \frac{1}{T}\int_0^T \left[z(t) + n(t)\right] x(t-\tau)\,dt \qquad (A.1.2)$$

$$= \lim_{T\to\infty} \frac{1}{T}\int_0^\infty z(t)\,x(t-\tau)\,dt + R_{xn}(\tau) \qquad (A.1.3)$$

If the system impulse response is g(t), then

$$z(t) = \int_0^\infty g(u)\,x(t-u)\,du \qquad (A.1.4)$$

Using (A.1.4) in (A.1.3)

$$R_{xy}(\tau) = \lim_{T\to\infty} \frac{1}{T}\int_0^T \int_0^\infty g(u)\,x(t-u)\,du \cdot x(t-\tau)\,dt + R_{xn}(\tau) \qquad (A.1.5)$$

Interchange the order of integration,

$$R_{xy}(\tau) = \int_0^\infty g(u) \lim_{T\to\infty} \frac{1}{T}\int_0^T x(t-u)\,x(t-\tau)\,dt\,du + R_{xn}(\tau) \qquad (A.1.6)$$

$$= \int_0^\infty g(u) \lim_{T\to\infty} \frac{1}{T}\int_0^T x(t)\,x(t-\tau+u)\,dt\,du + R_{xn}(\tau) \qquad (A.1.7)$$

$$= \int_0^\infty g(u)\,R_{xx}(\tau-u)\,du + R_{xn}(\tau) \qquad (A.1.8)$$

(A 1 8) can now be used to determine g(t) if $R_{xx}(\tau)$ and $R_{xn}(\tau)$ are known In particular this task is greatly simplified if

$$R_{xn}(\tau) = 0 \qquad \text{(A 1 9)}$$

$$R_{xx}(\tau) = \delta(\tau) \qquad \text{(A 1 10)}$$

In this case from (A 1 8) it can be seen that

$$R_{xy}(\tau) = g(\tau) \qquad \text{(A 1 11)}$$

This means that if the input signal x(t) is wideband, and if the disturbance n(t) is uncorrelated with x(t), then the impulse response may be measured directly from the cross correlation function (A 1 11)

A. 1. 2 THE VARIANCE OF CROSS CORRELATION FUNCTION ESTIMATES

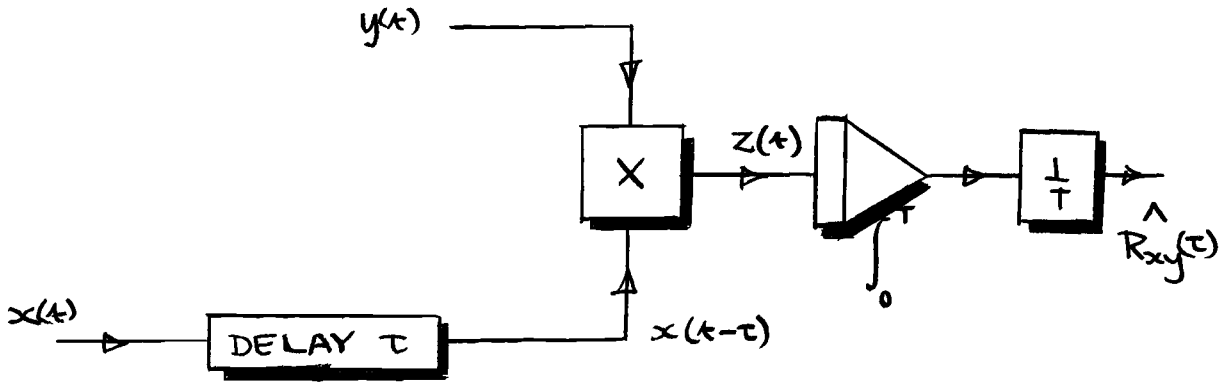

Figure A. 1. 2. Cross correlation using finite time integration

A correlator is illustrated in figure A. 1. 2. It is required to establish an expression for the variance of $\hat{R}_{xy}(\tau)$, in terms of the statistical properties of the input signals.

The true cross correlation function $R_{xy}(\tau)$ is the mean value of the signal z(t). The scatter on a set of estimates is due entirely to the a. c. component of z(t). Thus the integrator in figure A. 1. 2 could be replaced by a two channel device, figure A. 1. 3. One half accepts and integrates the mean value of z(t) to produce the true value of $R_{xy}(\tau)$, the other half integrates only the a. c. component, and gives rise to the uncertainty on the measurement, $R_e(\tau)$.

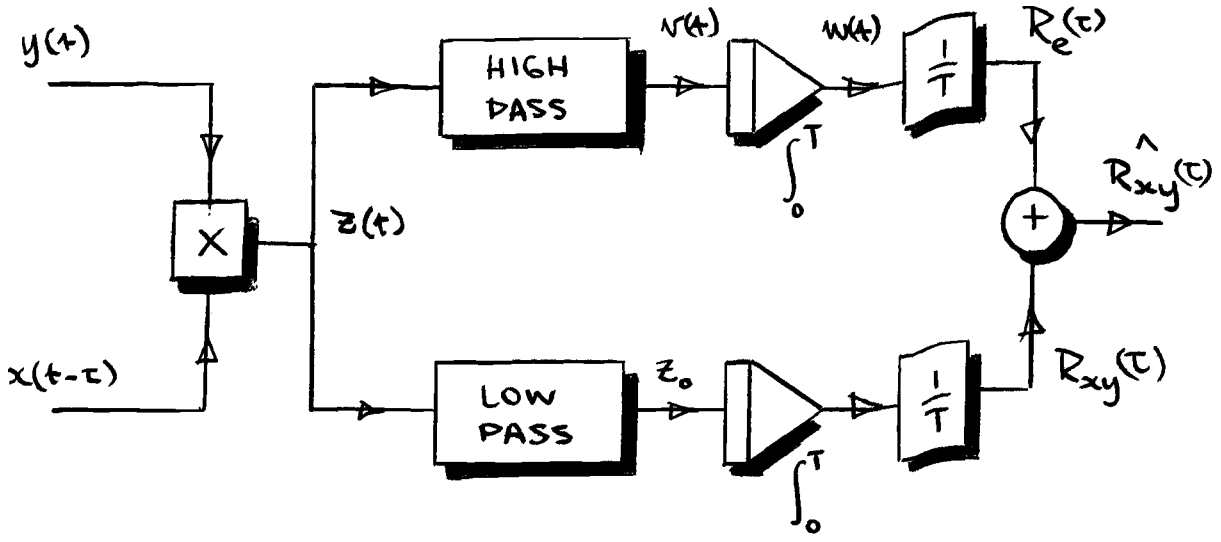

Figure A.1.3. Separating the components of $R_{xy}(\tau)$

It is apparent that to find the variance of $R_{xy}(\tau)$ only the a.c. component of z(t) need be considered. As a first step, consider figure A.1.4, where noise with zero mean is integrated for time T.

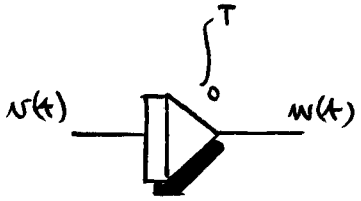

Figure A.1.4. Noise through an integrator

In figure A.1.4.

$$w(T) = \int_0^T v(t)\,dt \qquad \text{(A.1.12)}$$

$$w^2(T) = \int_0^T \int_0^T v(t_1)\,v(t_2)\,dt_1\,dt_2 \qquad \text{(A.1.13)}$$

let $t_1 = t_2 - u$

then

$$w^2(T) = \int_0^T \int_{t_2-T}^{t_2} v(t_2-u)\, v(t_2)\, du\, dt_2 \qquad \text{(A. 1. 14)}$$

$$E\left[w^2(T)\right] = \int_0^T \int_{t_2-T}^{t_2} E\left[v(t_2-u)\, v(t_2)\right] du\, dt_2 \qquad \text{(A. 1. 15)}$$

where E [ ] means 'expected value' or 'average'.

$$E\left[w^2(T)\right] = \int_0^T \int_{t-T}^{t} R_{vv}(u)\, du\, dt \qquad \text{(A. 1. 16)}$$

This double integral is illustrated in figure A 1. 5. The autocorrelation function is first integrated from t-T to t, to produce f(t). The function f(t) is finally integrated from 0 to T.

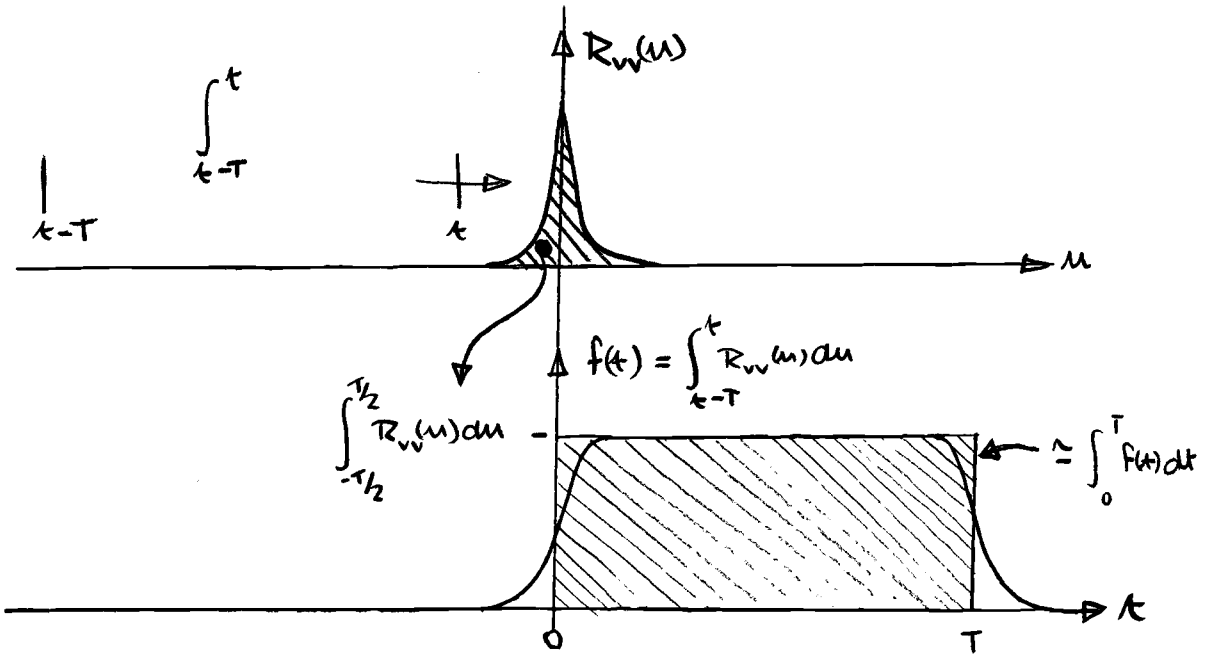

Figure A. 1. 5. Illustrating the double integral in (A. 1. 6)

If T is much larger than the decay time of $R_{vv}(\tau)$, the second integral can be closely approximated by the rectangle indicated in bottom half of figure A. 1. 5. Then

$$E\left[w^2(T)\right] \simeq T \int_{-T/2}^{T/2} R_{vv}(u)\, du \qquad \text{(A. 1. 17)}$$

$$E[w^2(T)] \simeq T\int_{-\infty}^{\infty} R_{vv}(u)\,du \qquad \text{(A. 1. 18)}$$

$$\simeq \pi G_v(0).T \qquad \text{(A. 1. 19)}$$

using (1. 3.).

(A. 1. 19) gives the variance of the output signal from the integrator, time T after switching on.

Returning to the correlator in figure A. 1. 3, the variance of the estimate $\hat{R}_{xy}(\tau)$ can be found.

In figure A. 1. 3

$$R_e(\tau) = \frac{1}{T}\int_0^T v(t)\,dt$$

$$= \frac{1}{T} w(T)$$

Thus the variance of $R_e(\tau)$ as a function of T is

$$v^2 = E[R_e^2(\tau)] = \frac{1}{T^2} E[w^2(T)] \qquad \text{(A. 1. 20)}$$

From (A. 1. 19)

$$v^2 \simeq \frac{\pi}{T} G_v(0) \qquad \text{(A. 1. 21)}$$

where $G_v(0)$ is the low frequency power per unit bandwidth of v(t) the a. c. component of z(t). From (1. 3)

$$G_v(0) = \frac{2}{\pi}\int_0^{\infty} R_{vv}(u)\,du \qquad \text{(A. 1. 22)}$$

$R_{vv}(u)$ can be found from

$$R_{zz}(u) = R_{vv}(u) + z_o^2$$

Now z_o is the mean value of z(t) = $R_{xy}(\tau)$. Hence

$$R_{vv}(u) = R_{zz}(u) - R_{xy}^2(\tau)$$

Using this expression in (A. 1. 22) gives

$$G_v(0) = \frac{2}{\pi}\int_0^\infty \left\{ E\left[z(t)\, z(t-u)\right] - R_{xy}^2(\tau) \right\} du \qquad \text{(A.1.23)}$$

$$= \frac{2}{\pi}\int_0^\infty \left\{ E\left[y(t)\, y(t-u)\, x(t-\tau)\, x(t-\tau-u)\right] - R_{xy}^2(\tau) \right\} du \qquad \text{(A.1.24)}$$

and so

$$v^2 = \frac{2}{T}\int_0^\infty \left\{ E\left[y(t)\, y(t-u)\, x(t-\tau)\, x(t-\tau-u)\right] - R_{xy}^2(\tau) \right\} du \qquad \text{(A.1.25)}$$

Let $$P_{xy}(u,\tau) = E\left[y(t)\, y(t-u)\, x(t-\tau)\, x(t-\tau-u)\right] \qquad \text{(A.1.26)}$$

The evaluation of $P_{xy}(u,\tau)$ has been treated by Bendat [1]. The two limiting cases of interest are when either x(t) and y(t) are completely uncorrelated or when x(t) = y(t)

Uncorrelated noise. If $R_{xy}(\tau) = 0$ it can be shown that [1]

$$P_{xy}(u,\tau) = R_{xx}(u)\, R_{yy}(u) \qquad \text{(A.1.27)}$$

Then

$$v^2 \simeq \frac{2}{T}\int_0^\infty R_{xx}(u)\, R_{yy}(u)\, du \qquad \text{(A.1.28)}$$

Now if y(t) is wide band compared with x(t), $R_{xx}(u)$ will appear to be constant and equal to $R_{xx}(0)$ over the range in which $R_{yy}(u)$ is significant. This means that

$$v^2 \simeq \frac{2}{T}\int_0^\infty R_{xx}(0)\, R_{yy}(u)\, du \qquad \text{(A.1.29)}$$

Using (1.3), and letting $R_{xx}(0) = \sigma_x^2$

$$v^2 \simeq \frac{2}{T}\,\sigma_x^2\,\frac{\pi}{2}\,G_y(0) \qquad \text{(A.1.30)}$$

$$v^2 \simeq \frac{\pi}{T} \sigma_x^2 G_y(0) \qquad \text{(A.1.31)}$$

when y(t) is an uncorrelated wideband signal.

Variance of Autocorrelation function. If $x(t) = y(t)$ then $R_{xy}(\tau) = R_{xx}(\tau)$ and it can also be shown that [1]

$$P_{xx}(u,\tau) = R_{xx}^2(u) + R_{xx}^2(\tau) + R_{xx}(\tau+u) R_{xx}(\tau-u) \qquad \text{(A.1.32)}$$

from which

$$v^2 \simeq \frac{2}{T} \int_0^\infty \{R_{xx}^2(u) + R_{xx}(\tau+u) R_{xx}(\tau-u)\}\, du \qquad \text{(A.1.33)}$$

If $\tau = 0$

$$v^2 \simeq \frac{2}{T} \int_0^\infty 2 R_{xx}^2(u)\, du \qquad \text{(A.1.34)}$$

Replacing $R_{xx}(u)$ by $\sigma_x^2 \rho_{xx}(u)$, we have

$$v^2 \simeq \frac{2\pi}{T} \sigma_x^2 \left[\frac{2}{\pi} \int_0^\infty \sigma_x^2 \rho_{xx}^2(u)\, du \right] \qquad \text{(A.1.35)}$$

If, for example, $\rho_{xx}(u) = \varepsilon^{-\alpha u}$, then

$$\rho_{xx}^2(u) = \varepsilon^{-2\alpha u}$$

It follows that $\sigma_x^2 \rho_{xx}^2(u)$ will be the autocorrelation function of a signal with approximately twice the bandwidth of x(t), but with the same total power. From this, and (1.3)

$$\frac{2}{\pi} \int_0^\infty \sigma_x^2 \rho_{xx}^2(u)\, du \simeq G_x(0)/2 \qquad \text{(A.1.37)}$$

so

$$v^2 \simeq \frac{\pi}{T} \sigma_x^2 G_x(0) \quad , \tau = 0 \qquad \text{(A.1.38)}$$

For τ large, either $R_{xx}(\tau+\mu)$ or $R_{xx}(\tau-\mu)$ will be zero and (A. 1. 32) reduces to

$$P_{xx}(\tau,\mu) = R_{xx}^2(\mu) + R_{xx}^2(\tau) \qquad \text{(A. 1. 39)}$$

From this, and from (A. 1. 25)

$$V^2 \simeq \frac{2}{T}\int_0^\infty R_{xx}^2(\mu)\, d\mu \qquad \text{(A. 1. 40)}$$

and from the same reasoning as for (A. 1. 38)

$$V^2 \simeq \frac{1}{2}\,\frac{\Pi}{T}\,\sigma_x^2\, G_x(0) \text{ , } \tau \text{ large.} \qquad \text{(A. 1. 41)}$$

Cross correlation. When x(t) and y(t) are partially correlated the analysis is more complicated, but approximation to the variance in a cross correlation estimate will be an expression of the same form

$$V^2 \simeq \frac{\Pi}{T}\,\sigma_x^2\, G_y(0) \qquad \text{(A. 1. 42)}$$

or

$$V^2 \simeq \frac{\Pi}{T}\,\sigma_y^2\, G_x(0) \qquad \text{(A. 1. 43)}$$

Effect of a wideband disturbance on a correlation estimate. If the signal $y(t) = y'(t) + n(t)$, where $y'(t)$ is the wanted signal, and $n(t)$ is a spurious disturbance,

$$R_{xy}(\tau) = \lim_{T\to\infty}\frac{1}{T}\int_0^T \left[\, y'(t)\,x(t-\tau) + n(t)\,x(t-\tau)\right] dt \qquad \text{(A. 1. 44)}$$

$$= R_{xy'}(\tau) + R_{xn}(\tau) \qquad \text{(A. 1. 45)}$$

The additional variance caused by n(t) can now be interpreted as that present on an estimate of $R_{xn}(\tau)$ alone. From (A. 1. 31) it follows that

$$V_N^2 \simeq \frac{\Pi}{T}\,\sigma_x^2\, G_n(0) \qquad \text{(A. 1. 46)}$$

A.1.3 COMPUTING CAPACITY REQUIRED FOR A CONVENTIONAL 50 CHANNEL CORRELATOR

Delay The basic requirement in a correlator is a means of delaying the signal. In a multi-channel correlator, the delay system must have tapping points at the required values of delay parameter. A digital correlator may use, for example, magnetic core store, which could contain quite easily 2047 samples, at a cost of around £1 per word of up to 20 bits. The maximum delay which can be obtained from such a store is not limited by any considerations of accuracy or drift. The minimum delay possible is only a few microseconds.

Analogue delay, on the other hand, is not easy to obtain, and is subject to severe limitations in terms of accuracy, and flexibility. The only practicable analogue method for obtaining long delay is magnetic recording on either tape or drum, using spatial separation of writing and reading heads to obtain time delay. There is clearly a limit in both directions, firstly to the smallest spacing of the heads and the maximum speed of the recording medium for short delays, and more important, to the maximum physical separation of the heads and the lowest usable recording speed, for long delays. If low frequency signals are being analysed the recording technique will usually be frequency modulation. The associated read and write electronics are complex, and limited both in accuracy and frequency response. The problems of pure analogue delay are so great that it is extremely difficult to give any estimate of likely cost, but this will greatly exceed the cost of digital storage. The most successful analogue system so far described [4] uses magnetic drum storage, but is not arranged for multichannel working.

Integration. The averaging process in a correlator is similar to the delay pro-

blem in that some form of storage is required. Digitally, the 50 locations required to store the different ordinates of the correlation function are trivial in comparison with the delay storage. In an analogue system each channel will require a separate analogue integrator which will be limited by drift and accuracy, and may cost upwards of £100.

Multiplication. Some of the advantages of a digital correlator are offset by the computing time required to multiply 50 pairs of samples together, and add them separately to the stored integrals, all within the time of a single sampling interval. The estimated computing times for these operations on two computers is shown in table A.1.1.

	Basic Instruction Time	Multiplication Time	Total Time for 50 Channels	Store	Cost
Atlas	1.6 μS	5 μS	405 μS		£500k
PDP-8	4.8 μS	334 μS *43 μS	17 mS *2.6 mS	4096 Basic	£6.5k

* with additional hardware

Table A.1.1 computing time for 50 channel correlation using a fast digital computer.

Atlas is a large, high speed, general purpose machine. PDP-8 is a much smaller, somewhat slower, scientific and data processing computer. The times are not in themselves restrictive, but they do represent a sizeable proportion of machine time, if other routines are intended to be time shared with the cross correlation.

An analogue multiplier may, in some cases, be faster than a digital machine,

but will not match the accuracy. It is also an expensive item (approximately £200-£500), and the cost of fifty channels may be prohibitive.

Analogue to digital converter. This device is peculiar to a digital system. The analogue signal must be sampled, and converted into an appropriate binary code for the computer. Conversion times as fast as 20 microseconds are possible, to at least 10 bit (.1%) resolution. This item can be expensive (£500-£2,000) but only one is necessary in a correlator. The converter may also be time shared with any other input lines connected to the computer.

A.2.1 DERIVATION OF THE EQUIVALENT GAIN OF A NON LINEARITY TO MINIMISE THE MEAN SQUARE DISTORTION

The non-linearity in figure A.2.1 is replaced by a gain K and distortion n(t). It will be shown that choosing K to minimise $\overline{n^2(t)}$, results in the distortion being uncorrelated with x(t).

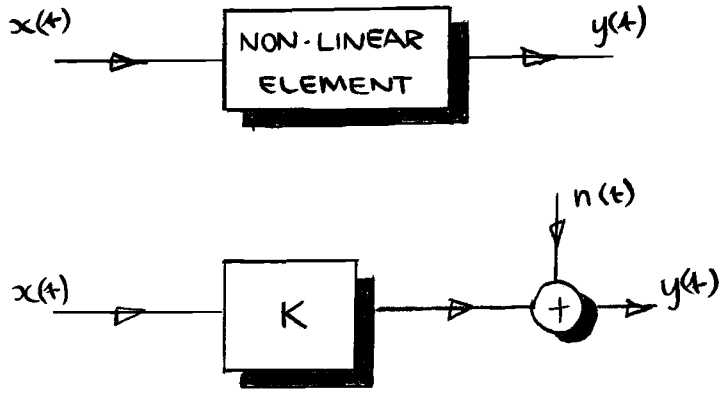

Figure A.21 A nonlinear element replaced by its equivalent gain

In figure A.2.1

$$n(t) = y(t) - Kx(t) \tag{A.2.1}$$

$$n^2(t) = y^2(t) - 2Kx(t)y(t) + K^2x^2(t) \tag{A.2.2}$$

Take averages, denoted by a bar.

$$\overline{n^2(t)} = \overline{y^2(t)} - 2K\,\overline{x(t)y(t)} + K^2\,\overline{x^2(t)} \tag{A.2.3}$$

$$\frac{d}{dK}\,\overline{n^2(t)} = 0 \tag{A.2.4}$$

then

$$-2\overline{x(t)\,y(t)} + 2K\,\overline{x^2(t)} = 0 \qquad \text{(A.2.5)}$$

and

$$K = \overline{x(t)\,y(t)} \,/\, \overline{x^2(t)} \qquad \text{(A.2.6)}$$

(A.2.6) may be used to calculate K for any non linear function f(x), if the input probability density function p(x) is known, since

$$\overline{x(t)\,y(t)} = \overline{x(t)\,f[x(t)]} \qquad \text{(A.2.7)}$$

$$= \int_{-\infty}^{\infty} x\,f(x)\,p(x)\,dx \qquad \text{(A.2.8)}$$

(A.2.8) is the average denoted in (A.2.7) taken over the ensemble of random signals x(t). Thus K is given by

$$K = \frac{1}{\sigma_x^2} \int_{-\infty}^{\infty} x\,f(x)\,p(x)\,dx \qquad \text{(A.2.9)}$$

where $\sigma_x^2 = \overline{x^2(t)}$, the mean square value of the input.

The cross correlation between x(t) and n(t) is given for τ=0 by (A.2.10), by multiplying (A.3.1) by x(t) and averaging.

$$\overline{n(t)\,x(t)} = \overline{x(t)\,y(t)} - K\,\overline{x^2(t)} \qquad \text{(A.2.10)}$$

Substitute the value of K given by (A.2.6)

$$\overline{n(t)\,x(t)} = \overline{x(t)\,y(t)} - \frac{\overline{x(t)\,y(t)}}{\overline{x^2(t)}} \cdot \overline{x^2(t)} \qquad \text{(A.2.11)}$$

$$= 0 \qquad \text{(A.2.12)}$$

(A.2.12) shows that n(t) is uncorrelated with x(t) for $\tau = 0$. It can also be shown that, when x(t) is Gaussian.

$$\overline{n(t)\, x(t-\tau)} = 0 \qquad \text{(A.2.13)}$$

for all values of τ. [39, 40].

A.2.2 EQUIVALENT GAIN OF A QUANTISER

Figure A.2.2 shows the non-linear characteristic associated with a quantiser. There are M positive levels, and N negative levels, equally spaced by a step q. The input probability density distribution p(x) is also shown in relation to the quantiser.

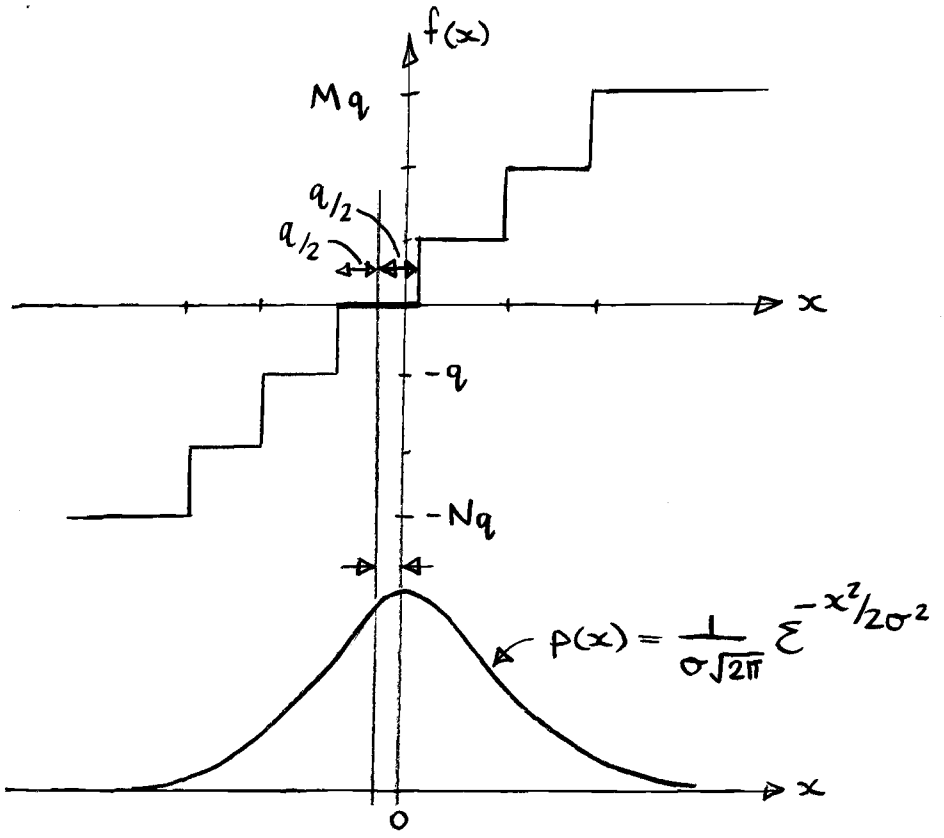

Figure A.2.2 Quantiser characteristic and input probability density function

From (A.2.9)

$$K = \frac{1}{\sigma^2}\int_{-\infty}^{\infty} x f(x) p(x)\, dx \qquad \text{(A.2.14)}$$

In figure A.2.2

$$\left.\begin{aligned} f(x) &= -Nq \qquad x+x_0 < (-N+\tfrac{1}{2})q \\ &= rq \qquad (r-\tfrac{1}{2})q < x+x_0 < (r+\tfrac{1}{2})q \\ &= Mq \qquad (M-\tfrac{1}{2})q < x+x_0 \end{aligned}\right\} \qquad \text{(A.2.15)}$$

where r is taken from -(N-1) to M-1,

and

$$p(x) = \frac{1}{\sigma\sqrt{2\pi}}\,\varepsilon^{-x^2/2\sigma^2} \qquad \text{(A. 2. 16)}$$

Putting these expressions into (A. 2. 14) gives

$$K = \frac{q}{\sigma^3\sqrt{2\pi}}\left[-N \int_{-\infty}^{(-N+\frac{1}{2}-x_0/q)q} x\,\varepsilon^{-x^2/2\sigma^2}\,dx \right.$$

$$+ \sum_{-(N-1)}^{M-1} r \int_{(r-\frac{1}{2}-x_0/q)q}^{(r+\frac{1}{2}-x_0/q)q} x\,\varepsilon^{-x^2/2\sigma^2}\,dx$$

$$\left. + M \int_{(M-\frac{1}{2}-x_0/q)q}^{\infty} x\,\varepsilon^{-x^2/2\sigma^2}\,dx \right] \qquad \text{(A. 2. 17)}$$

$$= -\frac{q}{\sigma\sqrt{2\pi}} \left\{ \sum_{-N}^{M-1} r\,\varepsilon^{-\frac{1}{2}\left[(r+\frac{1}{2}-x_0/q)q/\sigma\right]^2} \right.$$

$$\left. - \sum_{-(N-1)}^{M} r\,\varepsilon^{-\frac{1}{2}\left[(r-\frac{1}{2}-x_0/q)q/\sigma\right]^2} \right\} \qquad \text{(A. 2. 18)}$$

The summations in (A. 2. 18) reduce to give

$$K = \frac{q}{\sigma\sqrt{2\pi}} \sum_{-N}^{M-1} \varepsilon^{-\frac{1}{2}\left[(r+\frac{1}{2}-x_0/q)q/\sigma\right]^2} \qquad \text{(A. 2. 19)}$$

A program has been written to evaluate K as a function of σ/q and x_0/q, for

quantisers with various numbers of levels (Table A. 2. 1). Some results are tabulated in table A. 2. 2 and these have been used to construct figures 2. 8 and 2. 13 in the text.

```
begin
real a,b,c,x,y,z
integer i,j,r,L,M,N
1: read(L)
newlines(6)
stop if L=-1
->2 if parity(L)>0
M=(L-1)/2
->3
2: M=L/2
3: N=L-M-1
print(L,2,0)
caption #level#quantiser
newlines(2)
caption ##A
spaces(5)
caption s/q
spaces(8)
caption Keq
newlines(2)
cycle i=0,1,5
a=0.1i
->4 unless parity(L)>0
print(0.5-a,1,1)
->5
4: print(a,1,1)
5: spaces(3)
cycle j=1,1,10
b=0.1j
print(b,1,2)
spaces(4)
x=1/(b*sqrt(2π))
y=1/b
z=0
c=0.5-a
cycle r=-N,1,M-1
z=z+exp(-0.5*((r+c)*y)↑2)
repeat
print(z*x,2,3)
newline
spaces(7) unless j=10
repeat
newline
repeat
newlines(3)
->1
end of program

21  2  3  4  5  6  7
-1
```

Table A.2.1

Program to evaluate the equivalent gain of an L level quantiser, for y /q = 0,0.1,0.5 and /q = 0,0.1,1.0

The data lists the number of levels, followed by -1.

Number of Levels	σ/q	x_o/q					
		0.0	0.1	0.2	0.3	0.4	0.5
Multilevel	0.10	0.000	0.001	0.044	0.540	2.420	3.989
	0.20	0.175	0.292	0.652	1.211	1.760	1.995
	0.30	0.663	0.727	0.894	1.103	1.274	1.340
	0.40	0.915	0.931	0.974	1.026	1.069	1.085
	0.50	0.986	0.988	0.996	1.004	1.012	1.014
	0.60	0.998	0.999	0.999	1.001	1.001	1.002
	0.70	1.000	1.000	1.000	1.000	1.000	1.000
	0.80	1.000	1.000	1.000	1.000	1.000	1.000
	0.90	1.000	1.000	1.000	1.000	1.000	1.000
	1.00	1.000	1.000	1.000	1.000	1.000	1.000
3	0.10	0.000	0.001	0.044	0.540	2.420	3.989
	0.20	0.175	0.292	0.652	1.211	1.760	1.995
	0.30	0.663	0.727	0.894	1.103	1.273	1.335
	0.40	0.913	0.929	0.969	1.015	1.046	1.041
	0.50	0.968	0.968	0.966	0.958	0.940	0.906
	0.60	0.940	0.936	0.923	0.902	0.872	0.831
	0.70	0.883	0.879	0.866	0.844	0.814	0.775
	0.80	0.820	0.817	0.805	0.786	0.760	0.727
	0.90	0.760	0.757	0.747	0.731	0.709	0.682
	1.00	0.704	0.701	0.694	0.681	0.663	0.641
5	0.10	0.000	0.001	0.044	0.540	2.420	3.989
	0.20	0.175	0.292	0.652	1.211	1.760	1.995
	0.30	0.663	0.727	0.894	1.103	1.274	1.340
	0.40	0.915	0.931	0.974	1.026	1.069	1.085
	0.50	0.986	0.988	0.996	1.004	1.012	1.014
	0.60	0.998	0.998	0.999	1.000	1.000	0.999
	0.70	0.998	0.998	0.997	0.996	0.994	0.990
	0.80	0.992	0.992	0.990	0.987	0.983	0.977
	0.90	0.981	0.980	0.978	0.973	0.967	0.959
	1.00	0.963	0.962	0.959	0.954	0.947	0.939
7	0.10	0.000	0.001	0.044	0.540	2.420	3.989
	0.20	0.175	0.292	0.652	1.211	1.760	1.995
	0.30	0.663	0.727	0.894	1.103	1.274	1.340
	0.40	0.915	0.931	0.974	1.026	1.069	1.085
	0.50	0.986	0.988	0.996	1.004	1.012	1.014
	0.60	0.998	0.999	0.999	1.001	1.001	1.002
	0.70	1.000	1.000	1.000	1.000	1.000	1.000
	0.80	1.000	1.000	1.000	1.000	1.000	1.000
	0.90	1.000	0.999	0.999	0.999	0.999	0.998
	1.00	0.998	0.998	0.998	0.997	0.996	0.995

Table A.2.2 Equivalent gain as a function of σ/q and x_o/q for 3, 5, 7 and multilevel quantisers.

Number of Levels	σ/q	x_o/q					
		0.0	0.1	0.2	0.3	0.4	0.5
2	0.10	3.989	2.420	0.540	0.044	0.001	0.000
	0.20	1.995	1.760	1.210	0.648	0.270	0.088
	0.30	1.330	1.258	1.065	0.807	0.547	0.332
	0.40	0.997	0.967	0.880	0.753	0.605	0.457
	0.50	0.798	0.782	0.737	0.666	0.579	0.484
	0.60	0.665	0.656	0.629	0.587	0.532	0.470
	0.70	0.570	0.564	0.547	0.520	0.484	0.442
	0.80	0.499	0.495	0.483	0.465	0.440	0.410
	0.90	0.443	0.441	0.432	0.419	0.402	0.380
	1.00	0.399	0.397	0.391	0.381	0.368	0.352
4	0.10	3.989	2.420	0.540	0.044	0.001	0.000
	0.20	1.995	1.760	1.211	0.652	0.292	0.175
	0.30	1.340	1.274	1.103	0.894	0.727	0.663
	0.40	1.085	1.069	1.026	0.974	0.931	0.914
	0.50	1.014	1.011	1.003	0.993	0.984	0.977
	0.60	0.996	0.995	0.992	0.987	0.979	0.969
	0.70	0.981	0.979	0.975	0.967	0.956	0.941
	0.80	0.955	0.953	0.948	0.938	0.924	0.906
	0.90	0.921	0.919	0.913	0.903	0.889	0.870
	1.00	0.883	0.881	0.875	0.865	0.851	0.834
6	0.10	3.989	2.420	0.540	0.044	0.001	0.000
	0.20	1.995	1.760	1.211	0.652	0.292	0.175
	0.30	1.340	1.274	1.103	0.894	0.727	0.663
	0.40	1.085	1.069	1.026	0.974	0.931	0.915
	0.50	1.014	1.012	1.004	0.996	0.988	0.986
	0.60	1.002	1.001	1.000	0.999	0.999	0.998
	0.70	1.000	1.000	1.000	1.000	0.999	0.999
	0.80	0.999	0.999	0.999	0.998	0.997	0.996
	0.90	0.997	0.996	0.996	0.994	0.993	0.990
	1.00	0.991	0.990	0.989	0.987	0.985	0.981

Table A. 2. 2 (continued) Equivalent gain of 2, 4 and 6 level quantisers

A.2.3 MEAN VALUE AT OUTPUT OF QUANTISER

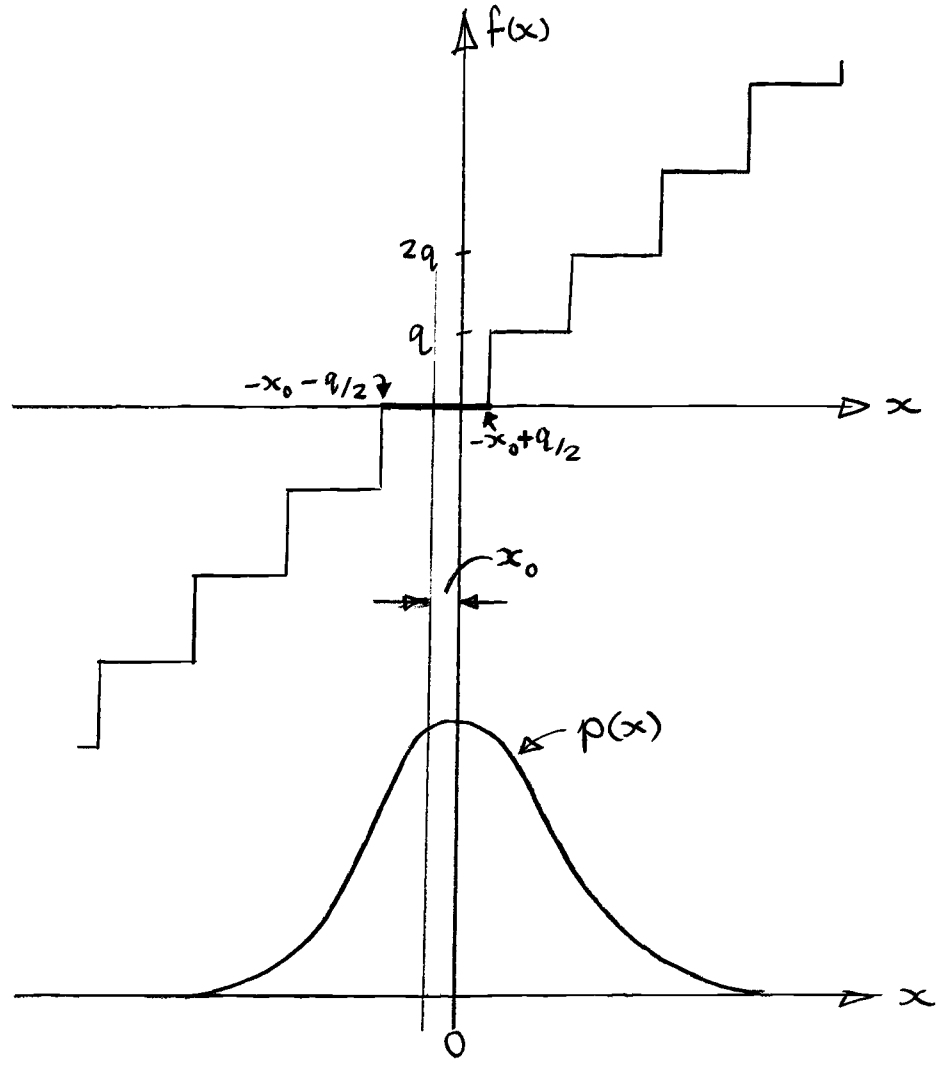

Figure A.2.3 Quantiser characteristic without limiting

For simplicity a non-saturating characteristic is considered. In figure A.2.3 the probability that the output y has the value rq is the probability that $(r-\frac{1}{2})q-x_0 < x < (r+\frac{1}{2})q-x_0$. If this probability is P(rq) then the mean value of the output is

$$y_0 = \sum_{r=-\infty}^{\infty} rq\, P(rq) \qquad \text{(A.2.20)}$$

P(rq) is given by

$$P(rq) = \int_{(r-\frac{1}{2})q - x_0}^{(r+\frac{1}{2})q - x_0} p(x)\, dx \qquad \text{(A.2.21)}$$

$$\int_{(r-\frac{1}{2}-x_0/q)q}^{(r+\frac{1}{2}-x_0/q)q} \frac{1}{\sigma\sqrt{2\pi}}\, \varepsilon^{-x^2/2\sigma^2}\, dx \qquad \text{(A.2.22)}$$

From A.2.20

$$y_{0/q} = \sum_{r=-\infty}^{\infty} r \int_{(r-\frac{1}{2}-x_0/q)q}^{(r+\frac{1}{2}-x_0/q)q} \frac{1}{\sigma\sqrt{2\pi}}\, \varepsilon^{-x^2/2\sigma^2}\, dx \qquad \text{(A.2.23)}$$

substitute $u = x/\sigma$

$$y_{0/q} = \frac{1}{\sqrt{2\pi}} \sum_{r=-\infty}^{\infty} r \int_{(r-\frac{1}{2}-x_0/q)q/\sigma}^{(r+\frac{1}{2}-x_0/q)q/\sigma} \varepsilon^{-u^2/2}\, du \qquad \text{(A.2.24)}$$

This expression can be evaluated using tables of the probability integral.

Figure A.2.4 shows y_0/q as a function of x_0/q and σ/q, for $0 < x_0/q < \frac{1}{2}$. Figure A.2.5 illustrates what happens when the d.c. component is outside this range.

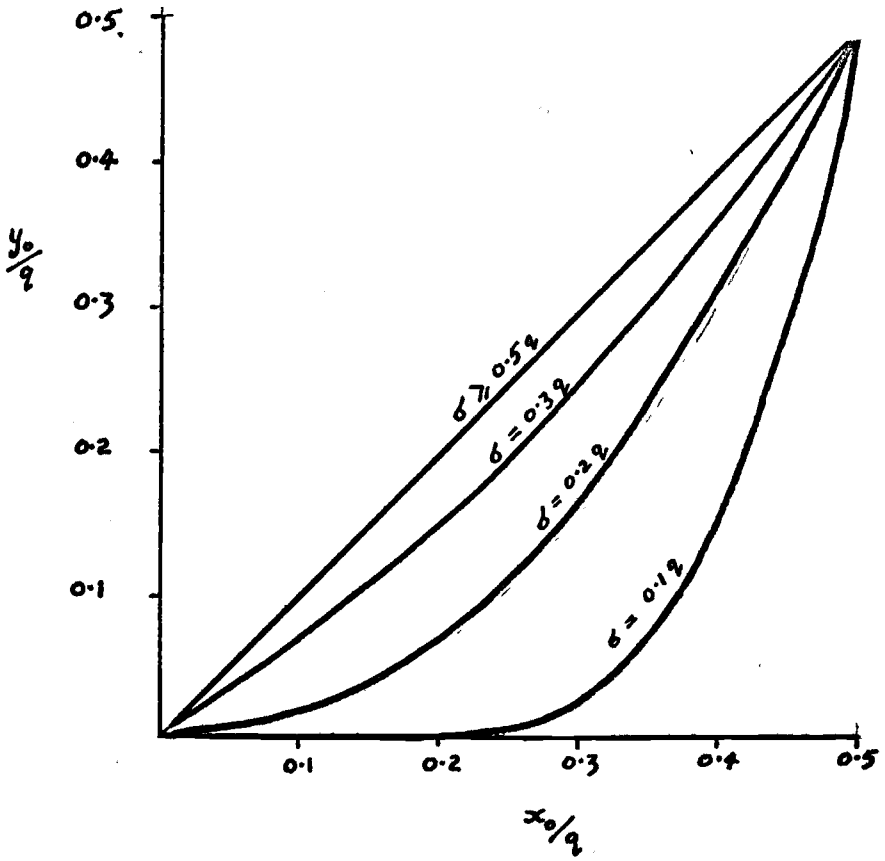

Figure A.2.4 Mean value of quantiser output for input d.c. level between 0 and $\frac{1}{2}$.

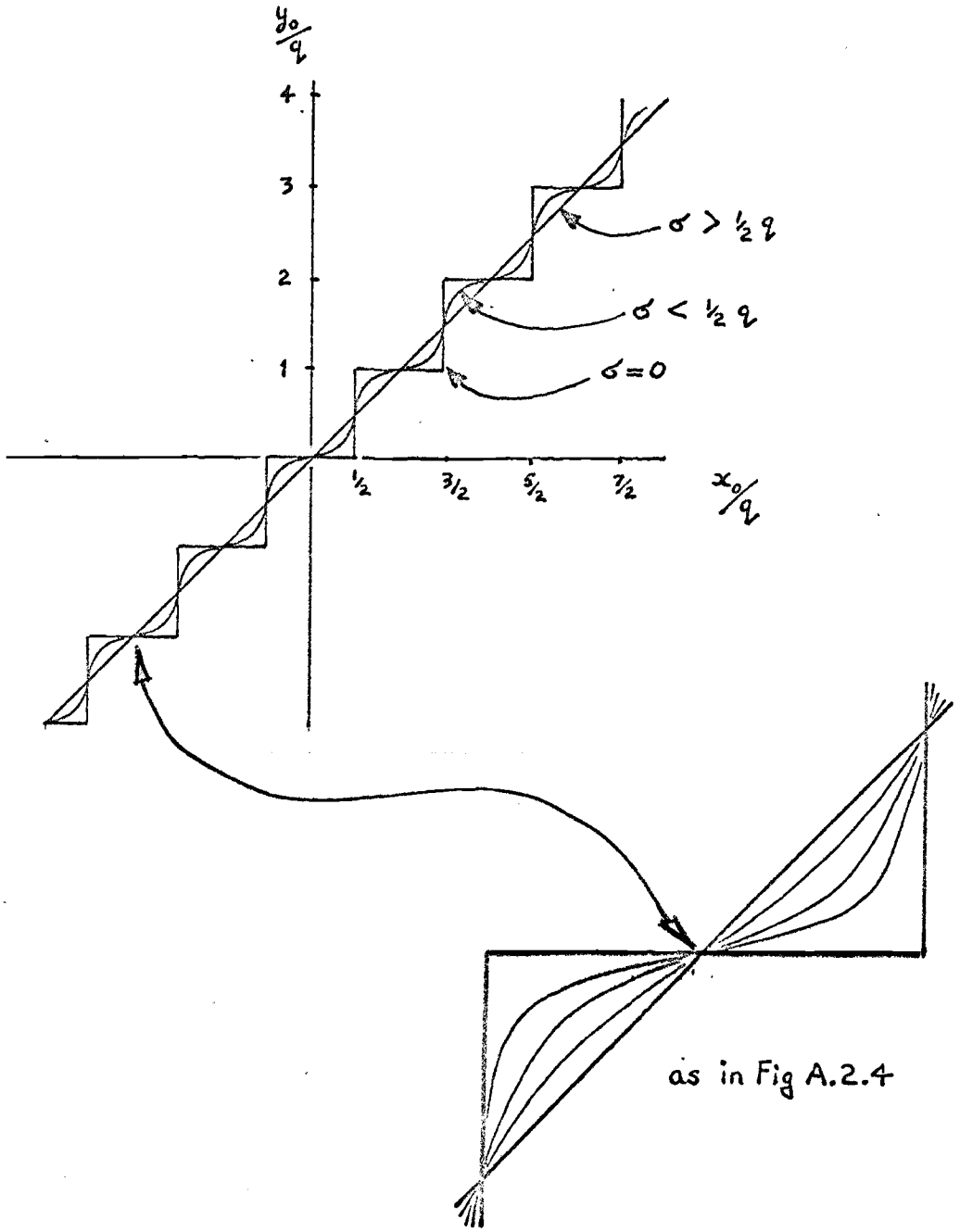

Figure A.2.5 Mean value of quantiser output as a function of input d.c. level.

A.2.4 EVALUATION OF QUANTISER NOISE AUTOCORRELATION FUNCTION BY THE POWER SERIES METHOD

It can be shown that the autocorrelation function of the output from a single valued non-linearity can be represented by a power series [14, 41, 42].

$$R_{yy}(\tau) = \sum_{n=0}^{\infty} \alpha_n^2 \rho^n \qquad \text{(A.2.25)}$$

where $\rho = R_{xx}(\tau)/\sigma_x^2$ is the normalised autocorrelation function of the input, and α_n is given by

$$\alpha_n = \frac{1}{\sigma^n} \int_{-\infty}^{\infty} f(x)\, H_n(x/\sigma)\, p(x)\, dx \qquad \text{(A.2.26)}$$

In (A.2.26) f (x) is the non linear function,

and p(x) is the p.d.f. of the input.

and

$$H_n(u) = (-1)^n \varepsilon^{u^2/2} \frac{d^n}{du^n} \varepsilon^{-u^2/2} \qquad \text{(A.2.27)}$$

is a Hermite polynomial of order n.

For the quantiser, assuming $x_0 = 0$ (figure A.2.3)

$$f(x) = rq \quad , \quad (r-\tfrac{1}{2})q \leq x \leq (r+\tfrac{1}{2})q \qquad \text{(A.2.28)}$$

and

$$p(x) = \frac{1}{\sigma\sqrt{2\pi}} \varepsilon^{-x^2/2\sigma^2} \qquad \text{(A.2.29)}$$

From (A. 2. 26)

$$\alpha_n = \frac{1}{\sigma^n} \sum_{-\infty}^{\infty} \frac{rq}{\sqrt{2\pi}} \int_{(r-\frac{1}{2})q}^{(r+\frac{1}{2})q} H_n\left(\frac{x}{\sigma}\right) \mathcal{E}^{-x^2/2\sigma^2} \frac{dx}{\sigma} \qquad \text{(A. 2. 30)}$$

Let $t = x/\sigma$

$$\frac{\alpha_n}{q} = \frac{1}{\sigma^n} \sum_{-\infty}^{\infty} r \frac{1}{\sqrt{2\pi}} \int_{(r-\frac{1}{2})q/\sigma}^{(r+\frac{1}{2})q/\sigma} H_n(t) \mathcal{E}^{-t^2/2} dt \qquad \text{(A. 2. 31)}$$

Using the integral

$$\int H_n(t) \mathcal{E}^{-t^2/2} dt = - H_{n-1}(t) \mathcal{E}^{-t^2/2} \qquad \text{(A. 2. 32)}$$

(A. 2. 31) becomes

$$\frac{\alpha_n}{q} = \frac{1}{\sigma^n \sqrt{2\pi}} \sum_{-\infty}^{\infty} r \left\{ H_{n-1}\left[(r-\tfrac{1}{2})q/\sigma\right] \mathcal{E}^{-(r-\frac{1}{2})^2 q^2/2\sigma^2} - H_{n-1}\left[(r+\tfrac{1}{2})q/\sigma\right] \mathcal{E}^{-(r+\frac{1}{2})^2 q^2/2\sigma^2} \right\} \qquad \text{(A. 2. 33)}$$

This summation reduces to give

$$\frac{\alpha_n}{q} = \frac{1}{\sigma^n} \sum_{-\infty}^{\infty} \frac{1}{\sqrt{2\pi}} \mathcal{E}^{-(r+\frac{1}{2})^2 q^2/2\sigma^2} H_{n-1}\left[(r+\tfrac{1}{2})q/\sigma\right] \qquad \text{(A. 2. 33)}$$

If n is even, then $\alpha_n = 0$, since H_{n-1} is then odd. Also

$$\alpha_1 = \frac{q}{\sigma\sqrt{2\pi}} \sum_{-\infty}^{\infty} \mathcal{E}^{-(r+\frac{1}{2})^2 q^2/2\sigma^2} \qquad \text{(A. 2. 34)}$$

$$\alpha_1 = K \qquad \text{(A. 2. 35)}$$

where K is the equivalent gain, from (A. 2. 19) with $M = N = \infty$

Autocorrelation of Quantiser Noise.

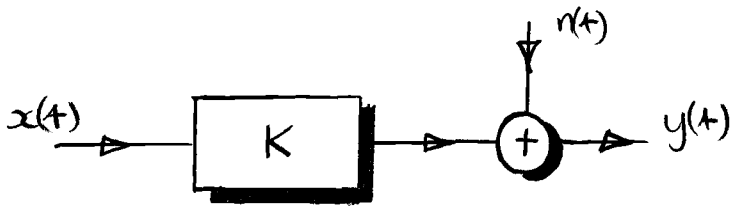

Figure A. 2. 6 Equivalent gain and noise representation of the nonlinearity

In figure A. 2. 6

$$y(t) = K x(t) + n(t) \qquad \text{(A. 2. 36)}$$

and

$$R_{yy}(\tau) = K^2 R_{xx}(\tau) + R_{nn}(\tau) \qquad \text{(A. 2. 37)}$$

$$R_{nn}(\tau) = R_{yy}(\tau) - K^2 R_{xx}(\tau) \qquad \text{(A. 2. 38)}$$

Comparing (A. 2. 38) with (A. 2. 25) and using the fact that $\alpha_1 = K$

$$R_m(\tau) = \sum_{n=3}^{\infty} \alpha_n^2 \rho^n(\tau) \quad , \text{ for } n = 3, 5, \ldots \qquad \text{(A. 2. 39)}$$

The coefficients α_3^2 , α_5^2 , etc. in (A. 2. 39) have been evaluated using a digital computer, and figure A. 2. 7 shows the envelope of these coefficients for various ratios of σ/q . It can been seen that the subsequent computation of $R_{nn}(\tau)$ from (A. 2. 39) is unlikely to be satisfactory in view of the powers involved. As there is a more useable technique available (appendix 2. 5) the power series approach is not taken any further here.

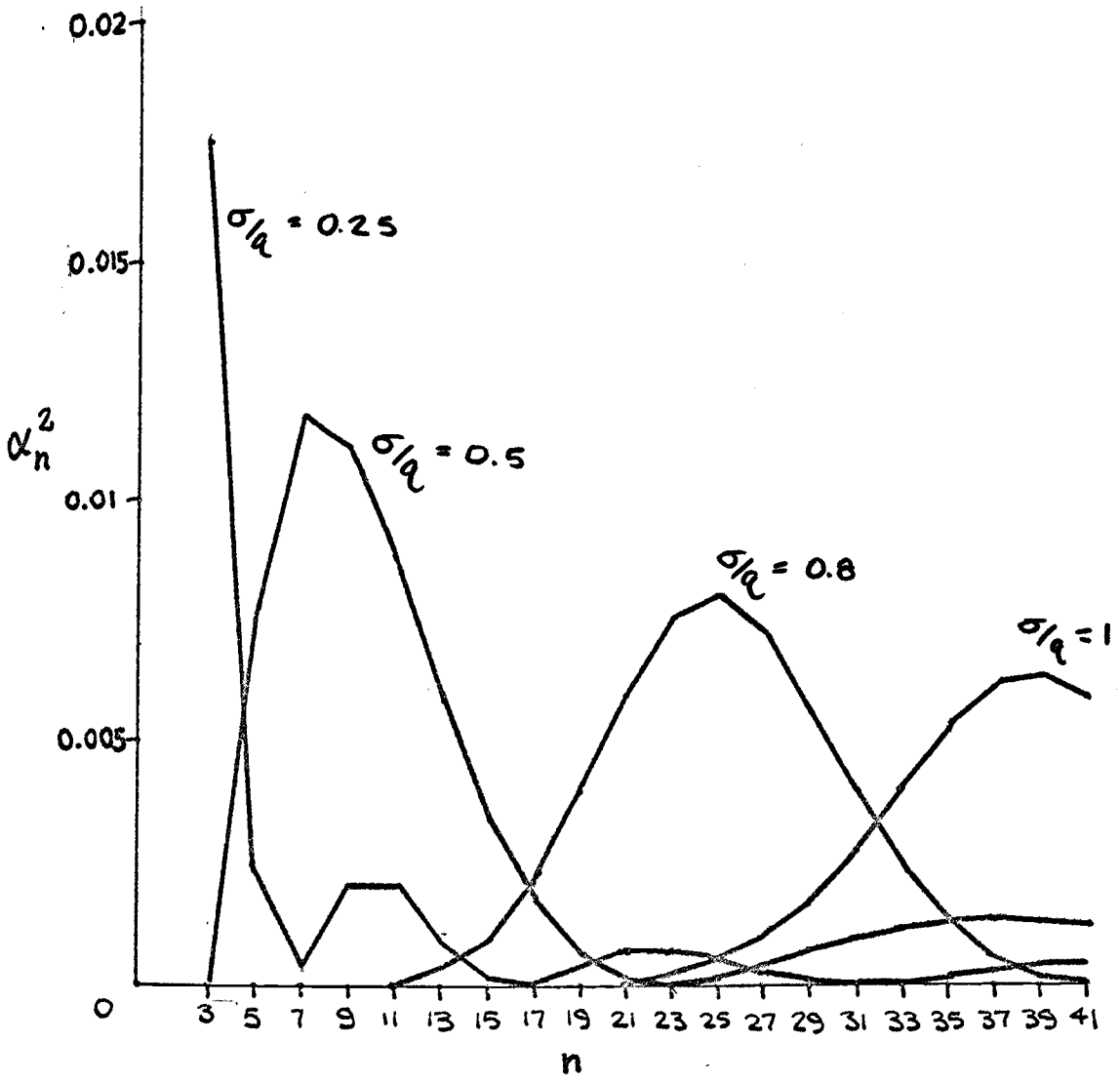

Figure A.2.7 Envelope of the coefficients α_n^2 in the quantiser noise power series expansion

$$R_{nn}(\tau) = \alpha_3^2\rho^3 + \alpha_5^2\rho^5 + \ldots\ldots\ldots$$

A.2.5 POWER SPECTRUM OF QUANTISATION NOISE

Watts' expression for the noise autocorrelation function is [7].

$$\frac{R(\tau)}{q^2} = -\frac{1}{4\pi^2}\sum_{K\neq 0}\sum_{m\neq 0}\frac{(-1)^{k+m}}{km}\,\varepsilon^{-j2\pi(k+m)a}\,\varepsilon^{-2\pi^2\left(\frac{\sigma}{q}\right)^2[k^2+m^2+2\rho km]} \qquad \text{(A.2.40)}$$

where ρ is $\rho(\tau)$, the normalised autocorrelation function of the input. When ρ is positive, only terms with k = -m contribute. When ρ is negative, only terms with k = +m contribute. In both cases, when the d.c. level term a = 0, or i/2, i any integer

$$\frac{R(\tau)}{q^2} = \frac{1}{2\pi^2}\sum_{k=1}^{\infty}\frac{1}{k^2}\,\varepsilon^{-4\pi^2\left(\frac{\sigma}{q}\right)^2 k^2(1-|\rho|)} \qquad \text{(A.2.41)}$$

The power spectrum is the Fourier transform of this.

$$\frac{G(\omega)}{q^2} = \frac{2}{\pi}\int_0^{\infty}\frac{R(\tau)}{q^2}\cos\omega\tau\,d\tau \qquad \text{(A.2.42)}$$

$$= \frac{1}{\pi^3}\sum_{1}^{\infty}\frac{1}{k^2}\int_0^{\infty}\varepsilon^{-Ak^2(1-|\rho|)}\cos\omega\tau\,d\tau \qquad \text{(A.2.43)}$$

where $$A = 4\pi^2(\sigma/q)^2 \qquad \text{(A.2.44)}$$

$\varepsilon^{-Ak^2(1-|\rho|)}$ falls away rapidly for $\tau > 0$ and is only significant for τ near zero. In this region $|\rho| = \rho$, and ρ can be represented by the first two

terms in the Maclaurin series. This gives.

$$\int_0^\infty \varepsilon^{-Ak^2(1-|\rho|)} \cos\omega\tau \, d\tau \simeq \int_0^\infty \varepsilon^{+Ak^2 \rho''(0)\, \tau^2/2} \cos\omega\tau \, d\tau \qquad \text{(A.2.45)}$$

Note that $\rho''(0)$ is negative.

The integral on the right hand side of (A.2.45) is known [43] and is given by

$$I = \int_0^\infty \varepsilon^{Ak^2 \rho''(0)\tau^2/2} \cos\omega\tau \, d\tau$$

$$= \sqrt{\frac{\pi}{2Ak^2[-\rho''(0)]}} \cdot \varepsilon^{-\omega^2/2Ak^2[-\rho''(0)]} \qquad \text{(A.2.46)}$$

substitute (A.2.44)

$$I = \frac{1}{2\sqrt{2\pi}(\sigma/q)} \cdot \frac{1}{\pi} \cdot \frac{1}{k} \cdot \frac{1}{\sqrt{-\rho''(0)}} \cdot \varepsilon^{-\omega^2/8\pi^2(\sigma/q)^2 k^2(-\rho''(0))}$$

(A.2.47)

Finally the expression for the power spectrum is

$$\frac{G(\omega)}{q^2} = \frac{1}{\pi^4} \frac{1}{2\sqrt{2\pi}(\sigma/q)N_0} \sum_{k=1}^{\infty} \frac{1}{k^3} \varepsilon^{-\omega^2/k^2\omega_n^2} \qquad \text{(A.2.48)}$$

where $N_0 = \sqrt{-\rho''(0)}$, the average number of zero crossings of the input signal per second, and $\omega_n = 2\sqrt{2}\,\pi^2 N_0 (\sigma/q)$

A. 2.6 EFFECT OF QUANTISATION NOISE ON ESTIMATE OF AN AUTOCORRELATION FUNCTION

In appendix 1.2 it is shown that the variance on an estimate of the autocorrelation function of a signal x(t) is approximately

$$V_R^2 \simeq \frac{\pi}{T} \sigma_x^2 G_x(0) \qquad \text{(A.2.49)}$$

where T is the averaging time.

The additional variance due to a disturbing wideband noise has been shown in appendix 1.2 to be

$$V_N^2 \simeq \frac{\pi}{T} \sigma_x^2 G_n(0) \qquad \text{(A.2.50)}$$

so

$$\frac{V_N^2}{V_R^2} \simeq \frac{G_n(0)}{G_x(0)} \qquad \text{(A.2.51)}$$

Consider a second order spectrum

$$G_x(\omega) = \frac{G_x(0)}{\left[1+(\omega/\omega_x)^2\right]^2} \qquad \text{(A.2.52)}$$

The total power σ_x^2 is the integral of this spectrum

$$\sigma_x^2 = \int_0^\infty G_x(\omega)\, d\omega \qquad \text{(A.2.53)}$$

$$= G_x(0) \int_0^\infty \frac{1}{\left[1+(\omega/\omega_x)^2\right]^2}\, d\omega \qquad \text{(A.2.54)}$$

$$\sigma_x^2 = G_x(0)\,\omega_x \frac{\pi}{4} \tag{A.2.55}$$

so that

$$G_x(0) = \frac{4}{\pi}\frac{\sigma_x^2}{\omega_x} \tag{A.2.56}$$

From appendix A.2.5

$$\frac{G_n(0)}{q^2} = \frac{1}{\pi^4}\frac{1}{2\sqrt{2\pi}\left(\frac{\sigma_x}{q}\right)N_0}\sum_1^\infty \frac{1}{k^3} \tag{A.2.57}$$

where

$$\sum_1^\infty \frac{1}{k^3} = 1.202 \tag{A.2.58}$$

and

$$N_0 = \sqrt{-\rho''(0)} \tag{A.2.59}$$

is the average number of zero crossings per second of x(t).

It can also be shown that [1]

$$N_0 = \frac{1}{\pi}\left[\frac{\int_0^\infty \omega^2 G(\omega)\,d\omega}{\int_0^\infty G(\omega)\,d\omega}\right]^{\frac{1}{2}} \tag{A.2.60}$$

$$\int_0^\infty \omega^2 G(\omega)\,d\omega = G_x(0)\int_0^\infty \frac{\omega^2}{\left[1+(\omega/\omega_x)^2\right]^2}\,d\omega \tag{A.2.61}$$

$$= G_x(0)\,\omega_x^3 \frac{\pi}{4} \tag{A.2.62}$$

Hence

$$N_0 = \frac{1}{\pi}\left[\frac{G_x(0)\,\omega_x^3\,\pi/4}{G_x(0)\,\omega_x\,\pi/4}\right]^{\frac{1}{2}} \tag{A.2.63}$$

$$= \frac{\omega_x}{\pi} \tag{A.2.64}$$

From (A.2.57)

$$\frac{G_n(0)}{q^2} = \frac{1}{\pi^4}\,\frac{1.202}{2\sqrt{2\pi}\,(\sigma_x/q)(\omega_x/\pi)} \tag{A.2.65}$$

and so

$$\frac{V_N^2}{V_R^2} \simeq \frac{\dfrac{1.202\,q^2}{\pi^4\,2\sqrt{2\pi}\,(\sigma_x/q)(\omega_x/4\pi)}}{(4/\pi)(\sigma_x^2/\omega_x)} \tag{A.2.66}$$

$$\simeq \left(\frac{q}{\sigma_x}\right)^3 \times \frac{1.202}{8\pi^2\sqrt{2\pi}} \tag{A.2.70}$$

$$\simeq .0061\,(q/\sigma_x)^3 \tag{A.2.71}$$

A.2.7 CORRELATION USING INTEGRATION BY PARTS

Figure A.2.9 shows a correlator in which the delay channel is differentiated, and the other signal is integrated. The estimate of the correlation function by this technique is represented by $R'_{xy}(\tau)$

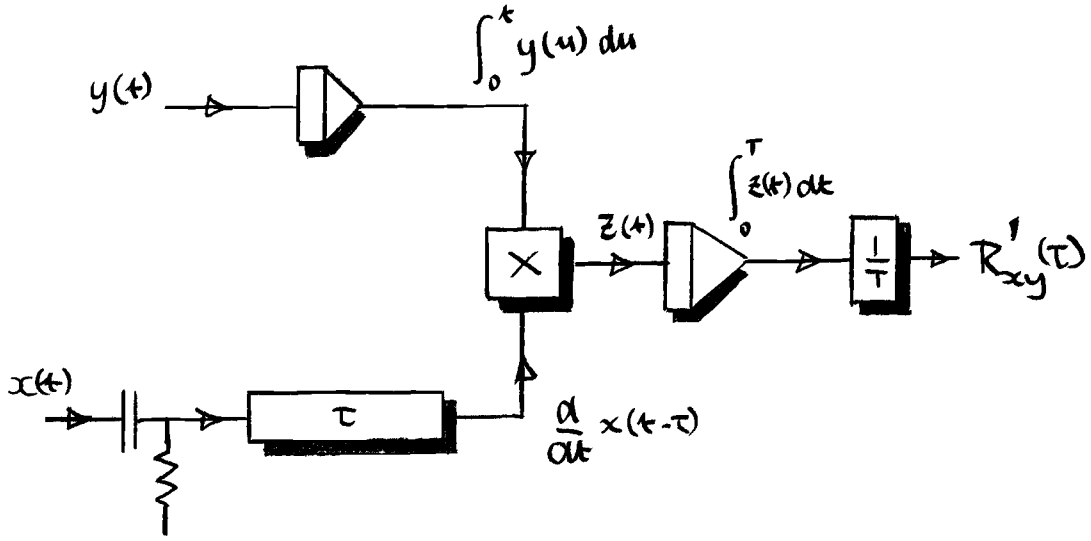

Figure A.2.9 Integration by parts in a correlator

The integrators in figure A.2.9 are both clamped with zero output for $t < 0$. Then for $t > 0$.

$$R'_{xy}(\tau) = \frac{1}{T}\int_0^T z(t)\,dt \qquad \text{(A.2.72)}$$

$$= \frac{1}{T}\int_0^T \left[\int_0^t y(u)\,du\right] \frac{d}{dt}\left[x(t-\tau)\right] dt \qquad \text{(A.2.73)}$$

Integrate (A.2.73) by parts.

$$R'_{xy}(\tau) = \frac{1}{T}\left[\int_0^t y(u)\,du \cdot x(t-\tau)\right]_0^T - \frac{1}{T}\int_0^T x(t-\tau)\,y(t)\,dt \qquad \text{(A.2.74)}$$

The second term in (A.2.74) can be recognised as $R_{xy}(\tau)$, the true estimate.

The first term represents the error.

$$\frac{1}{T}\left[\int_0^t y(u)\,du \,.\, x(t-\tau)\right]_0^T = \frac{1}{T}\left[\int_0^T y(u)\,du \,.\, x(T-\tau)\right] \qquad \text{(A.2.75)}$$

$$= x(T-\tau)\,\frac{1}{T}\int_0^T y(u)\,du \qquad \text{(A.2.76)}$$

as $T \to \infty$ the second part of this product is the mean value of the signal y(t). In a practical system the mean value of y(t) should be zero in order to prevent the integrator in this channel going off range. In this case, the error term in (A.2.76) $\to$ 0 as $T \to \infty$. It remains to discover what the effect of this term is on the variance of the estimate. This is given by

$$V_T^2 = E\left[\left(\frac{1}{T}x(T)\int_0^T y(t)\,dt\right)^2\right] \qquad \text{(A.2.77)}$$

where E [ ] represents the mean value.

Using the fact that $\overline{ab} < \bar{a}.\bar{b}$ [1],

$$E\left[\left(\frac{1}{T}x(T)\int_0^T y(t)\,dt\right)^2\right] \leq E\left[x^2(T)\right].E\left[\left(\frac{1}{T}\int_0^T y(t)\,dt\right)^2\right] \qquad \text{(A.2.78)}$$

From appendix 1.2

$$E\left[\left(\frac{1}{T}\int_0^T y(t)\,dt\right)^2\right] = \frac{\pi}{T}\,G_y(0) \qquad \text{(A.2.79)}$$

also

$$E\left[x^2(T)\right] = \sigma_x^2 \qquad \text{(A.2.80)}$$

Finally

$$V_T^2 \leq \frac{\pi}{T}\,\sigma_x^2\,G_y(0) \qquad \text{(A.2.81)}$$

(A. 2. 81) gives the additional variance introduced by integration by parts. There will already be some uncertainty on the true estimate which has been shown in Appendix 1. 2 to be approximately

$$V_K^2 \simeq \frac{\pi}{T} \sigma_x^2 G_y(0) \qquad \text{(A. 2. 82)}$$

(A. 2. 81) and (A. 2. 82) show that integration by parts approximately doubles the variance of the estimate, due to the error introduced by end conditions of the integration. If a continuous averaging circuit is used instead of a clamped integrator then it is expected that the effectively non-zero initial conditions will give rise to a further increase in the variance.

A.2.8. DESCRIPTION OF AN ON-LINE DIGITAL CORRELATOR

The instrument to be described accepts analogue signals x(t) and y(t), one of which is digitised to 8 bit resolution, and the other is quantised to three levels. The cross correlation function $R_{xy}(\tau)$ is computed for fifty different values of delay and the averaging is performed by a low pass digital filter.

An ultrasonic delay line is used to store a total of fifty 18 bit words. 16 of these bits represent the value of $R_{xy}(\tau)$ in two's complement binary form, with a guard bit which is used to indicate overflow from the most significant (sign) bit. The remaining two bits of the eighteen are the value of the three level delayed signal, according to the truth table given in table A.2.3

y(t)	01	±
+q	1	0
0	0	
-q	1	1

Table A.2.3 Truth table for 3 level signal

The word format is shown in figure A.2.10, together the arrangement in the store. The y (delayed) samples are located immediately in front of the corresponding $R(\tau)$ word.

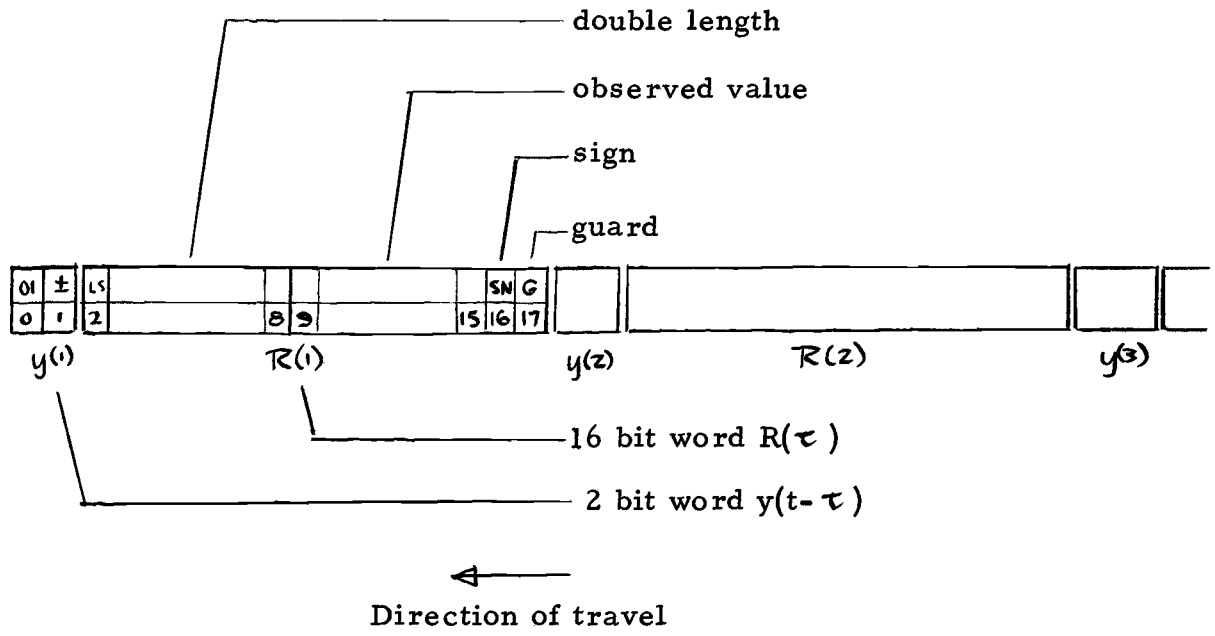

Figure A.2.10 Word and store format

The y samples are delayed by shunting each one into a temporary store, and re-inserting it immediately after the R word. This is illustrated in figure A.2.11. The y samples 'precess' round the delay line.

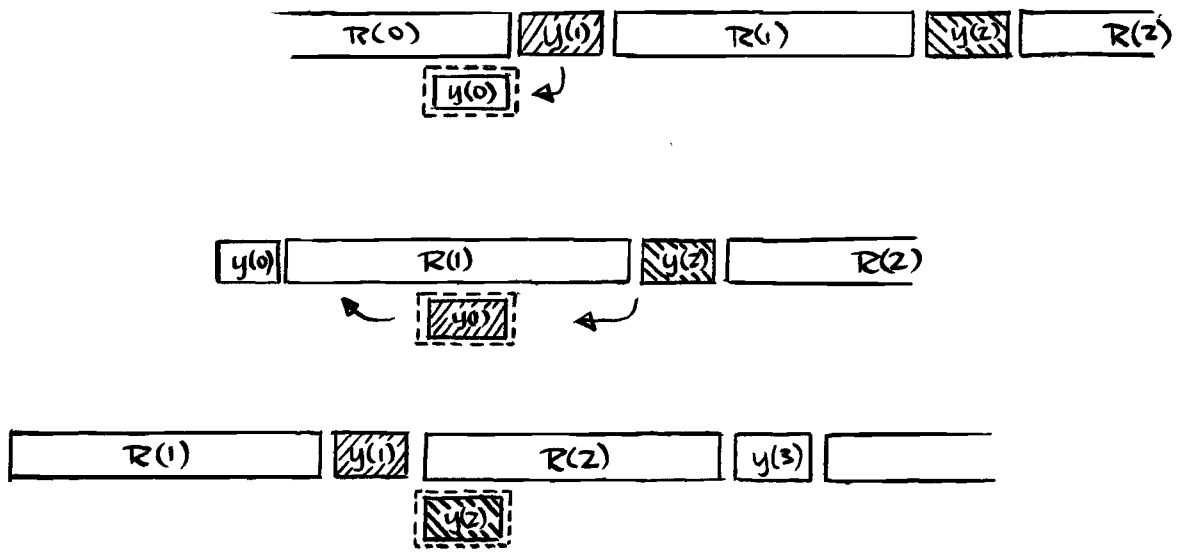

Figure A.2.11 Precessing of delayed samples

Integration The basic instrument arrangement is shown in figure A.2.12. The signal x(t) is sampled and converted to 8 bit binary data, which is held for at least a complete cycle time of 3.2 milliseconds. This parallel data is serialised and fed to the complementer. The signal y(t) is quantised to only three levels, and also serialised.

If switch S1 is at A, the three level data is read into the temporary store and held there. The complementer then acts on the O1, ± commands, and provides x, 0, or -x to the adder. This is added serially to the value of R(O), which is appearing at the other input of the adder. During this time S1 is at A, and the new sum R(O) is fed to the delay line. S1 and S2 now change to B, the present y sample is fed in behind R(O), and the first delayed y sample appears in the temporary store from the delay line shift register. This is held, S2 returns to A, and ±x, or O is added to R(1). The sequence of operations continues for all fifty words, and stops, storing the current values of the R's and y's until the next sample instruction.

The routine above is a single step in the integration of the product xy for all values of delay. It may be repeated an appropriate number of times to obtain the final estimate of $R_{xy}(\tau)$. The digital integrators will eventually overflow, however, and it is useful to be able to introduce a low pass filter, which can average the data without overflow, and allows any changes in $R_{xy}(\tau)$ with time to be followed.

Filtering A division circuit is used to obtain a small fraction of the integral R in the store, which is then subtracted from R. This mechanises the equation $R_0(\tau) = R_1(\tau)\,\varepsilon^{-\Delta}$.

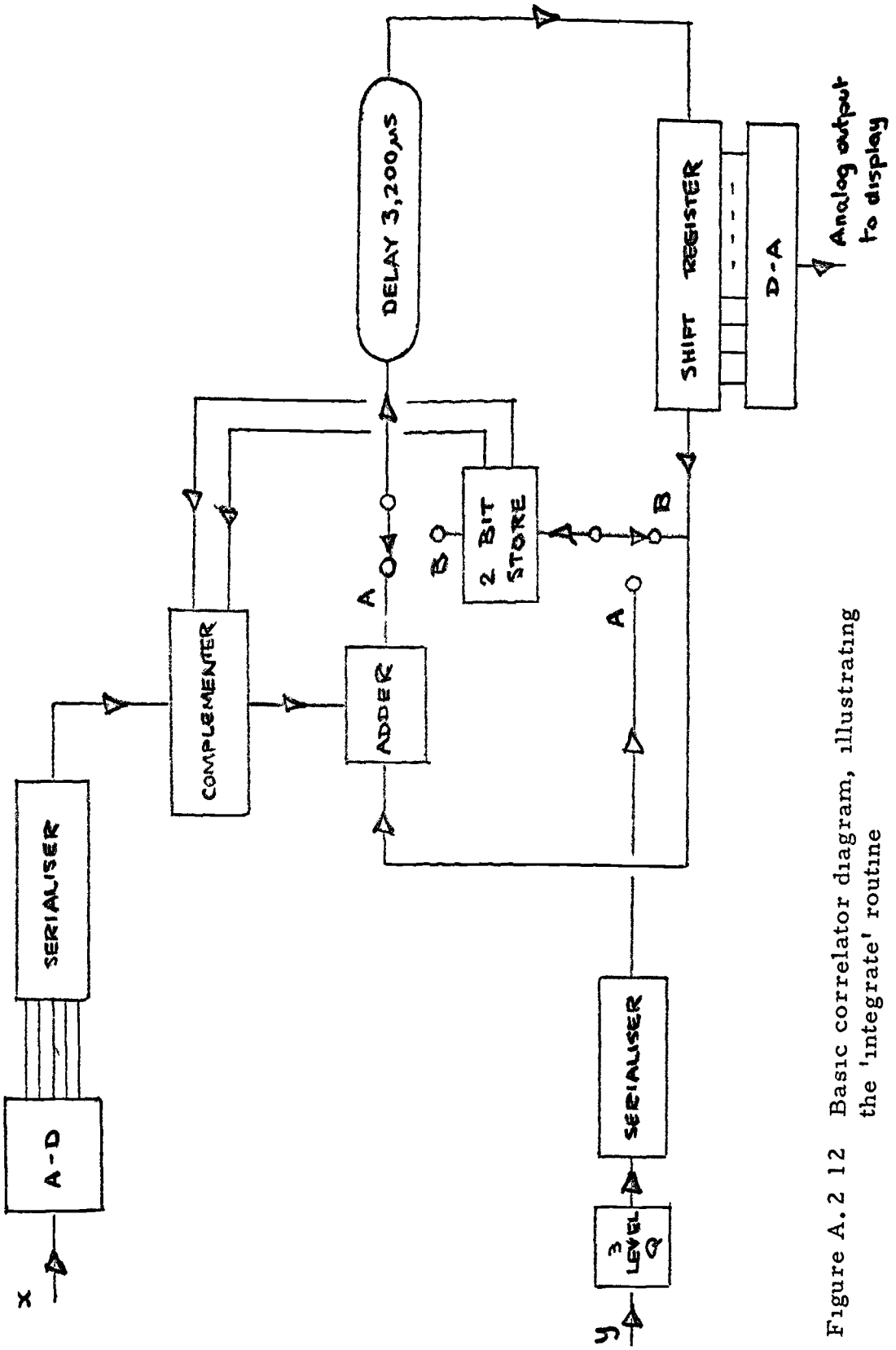

Figure A.2 12 Basic correlator diagram, illustrating the 'integrate' routine

The integrate step can be interlaced with this operation to realise an overall equation

$$R_0(\tau) = R_{-1}(\tau)\,\varepsilon^{-\Delta} + x_0 y_0(t-\tau)$$

which can be recognised as the difference equation for a single exponential decay. The correlator 'divide' routine is illustrated in figure A.2.13. Each value of $R(\tau)$ is reduced by approximately 1% each time this routine is called. The frequency with which it is called determines the filter time constant. For example, a frequency of 5 per second means that the initial slope of the decay is approximately 5% per second, so that the time constant is 100/5 seconds = 20 seconds.

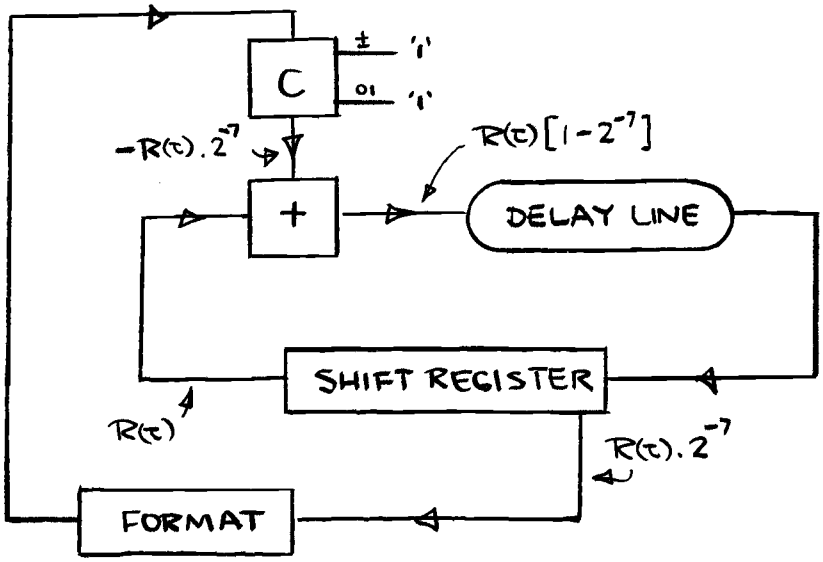

Figure A.2.13 The 'divide' routine

Grading the sampling interval It is possible to use grading in the instrument. Referring to figure A.2.12, S2 is in position A during an 'integrate' cycle, and is connected to B for the 01, ± bits to precess. If halfway down a cycle this switch is prevented from going to B, the 01, ± bits do not precess. If this inhibit is provided every second integrate cycle, then the effect is to sample at half the basic rate from the point in the cycle selected, in this case halfway.

Hardware The complete block diagram is shown in figure A.2.15, and the individual circuit diagrams are given in figures A.2.16 to A.2.34. The important features are covered in the following notes.

Components All units directly connected with the delay line are 2 MHz logic elements (Ferranti LCE200G series). Lower speed circuits use 100 kHz elements (Mullard circuit blocks).

The delay line is a Mullard type YL2108, with a total delay of 3,200 microseconds.

Logic Levels The d.c. logic levels are 0 volts for '0', and -6 volts for a '1'. Flip-flops are triggered by positive edges, or by d.c. levels, whichever is suited to the circuit and timing requirements.

Timing The entire timing system in the correlator relies on gating the appropriate clock pulse by a succession of wider pulses, figure A.2.14. Two phases of clock pulse are used to achieve this. Gating pulses from the counter are synchronised with the first clock pulse, and changes of the data occur on the delayed clock pulse.

The clock frequency required for the correlator is 278.25 kHz. The tolerance should be $\pm$ 0.5 kHz to be within the range of adjustment of the delay line. The stability required is 0.01%.

The count down from the clock is in two stages. A count of 18 identifies each bit, and a further count of 50 provides a word index.

Arithmetic Two's complement arithmetic is used, and a consequence of this is the need to watch format when numbers are shifted (e.g. in the divide unit). If at any time the actual word available stops short of the most significant position in the machine, i.e. the sign and guard bits, 16 and 17, then the sign bit of that word should be copied into the remaining places. This feature is provided in the input serialiser and divider units.

If overflow from the most significant bit occurs, the guard and sign bit become different. This state is detected by an 'exclusive or' circuit which compares the sign and guard bits of every word as it passes through the delay line shift register. A warning lamp is lit if overflow is detected.

Control functions The basic mode of the machine without the two control units is 'integrate'. This is the condition when the 'st' and 'div' lines are at '1'. Raising the appropriate line to 'O' puts the machine into 'store' or 'divide'.

Control unit 1 provides these signals synchronised to the beginning of each cycle. In addition the logic is arranged so that the basic mode with control unit connected is 'store'. The two inputs to control unit 1 are interpreted according to table A.2.4, below.

'int'	'f/s'	instruction
0	0	integrate
	1	
1	0	filter
	1	store

Control unit 2 is a latch circuit which arranges that the correlator goes into the 'integrate' or 'filter' routine for a single cycle after an edge on the 'sample' or 'filter' input lines. The 'sample' and 'filter' commands are obtained from external oscillators. To take care of simultaneous commands on these lines the 'filter' routine is arranged to wait until the next 'integrate' cycle has finished.

Data inputs The input y serialiser is connected to the 01, $\pm$ outputs of the three level quantiser or the Stieltjes decoder (the Stieltjes decoder takes successive differences of the three level signal). The sampling pulse 'spa' is timed so as not to allow the data to change while being read.

Input x is also held during the time when it is being read into the machine. The serialiser connections P2 to P9 are for minimum gain while still using all eight bits. Advancing these one step (i.e. P3 to P10) will double the gain. If a reduction of gain is necessary, some of the least signigicant bits must be dropped, since P2 is the machine's least significant position. PO and Pl are the 01, $\pm$ positions.

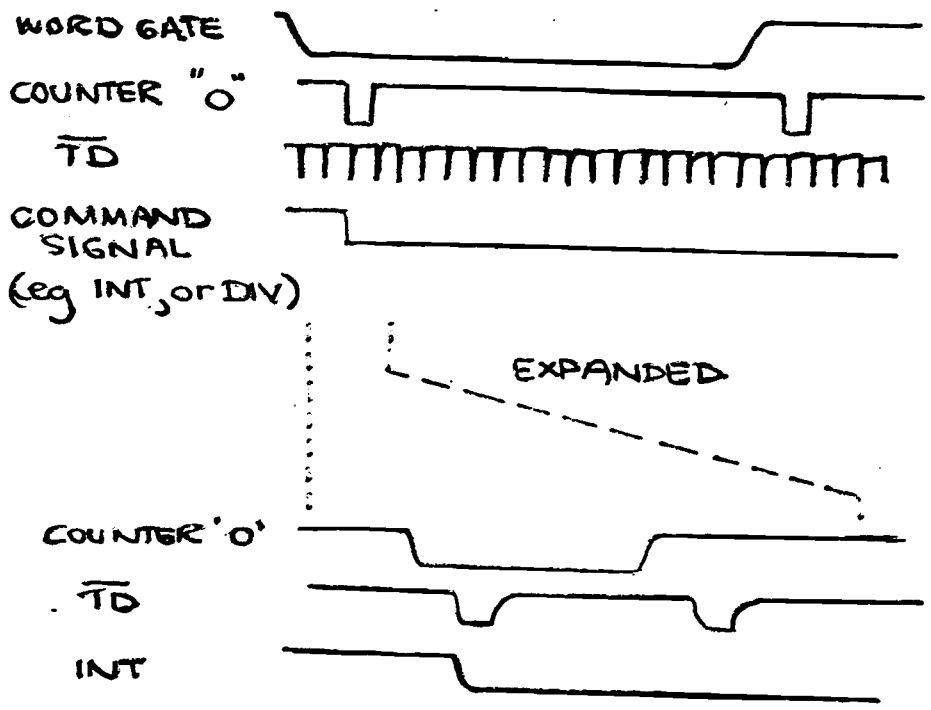

Figure A.2.14 (a) Timing wave-forms. All changes of 'routine' e.g. from 'store' to 'integrate', or 'integrate' to 'filter' take place on the transition from word 50 to word 0 . There is no 'dead word' space and the change takes 100 nanoseconds.

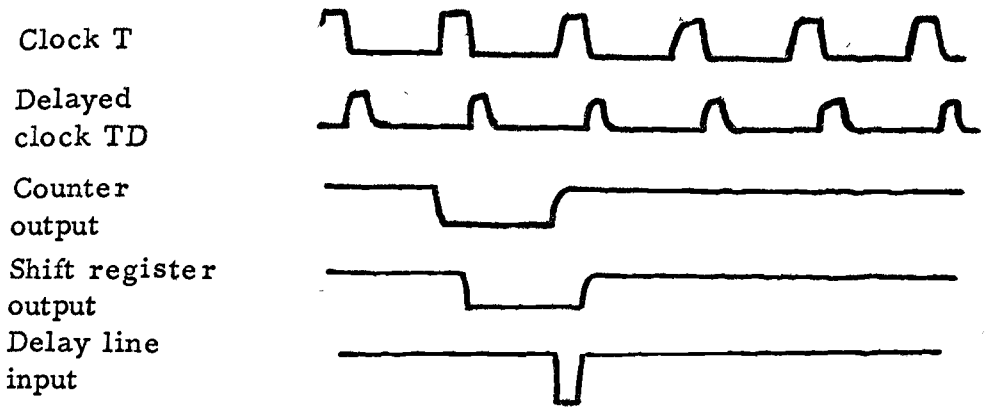

Figure A.2.14 (b)

(i) and (ii) Clock wave forms.
(iii) Counter triggers on leading edge of T.
(iv) Shift register shifts on leading edge of TD.
(v) Adder output is strobed by T to give a negative going drive to the delay line near the end of the bit.

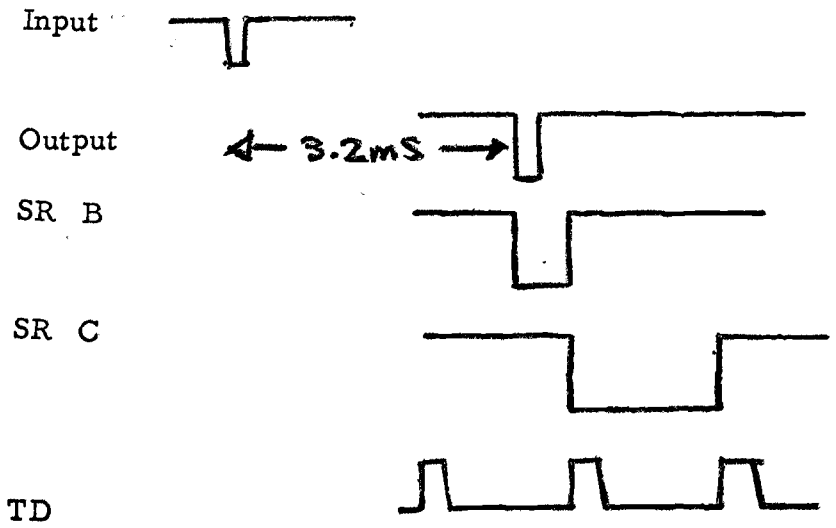

Figure A.2.14 (c). Delay line wave-forms. The delay line output sets shift register B. Shift pulse TD clears B and shifts its value into shift register C.

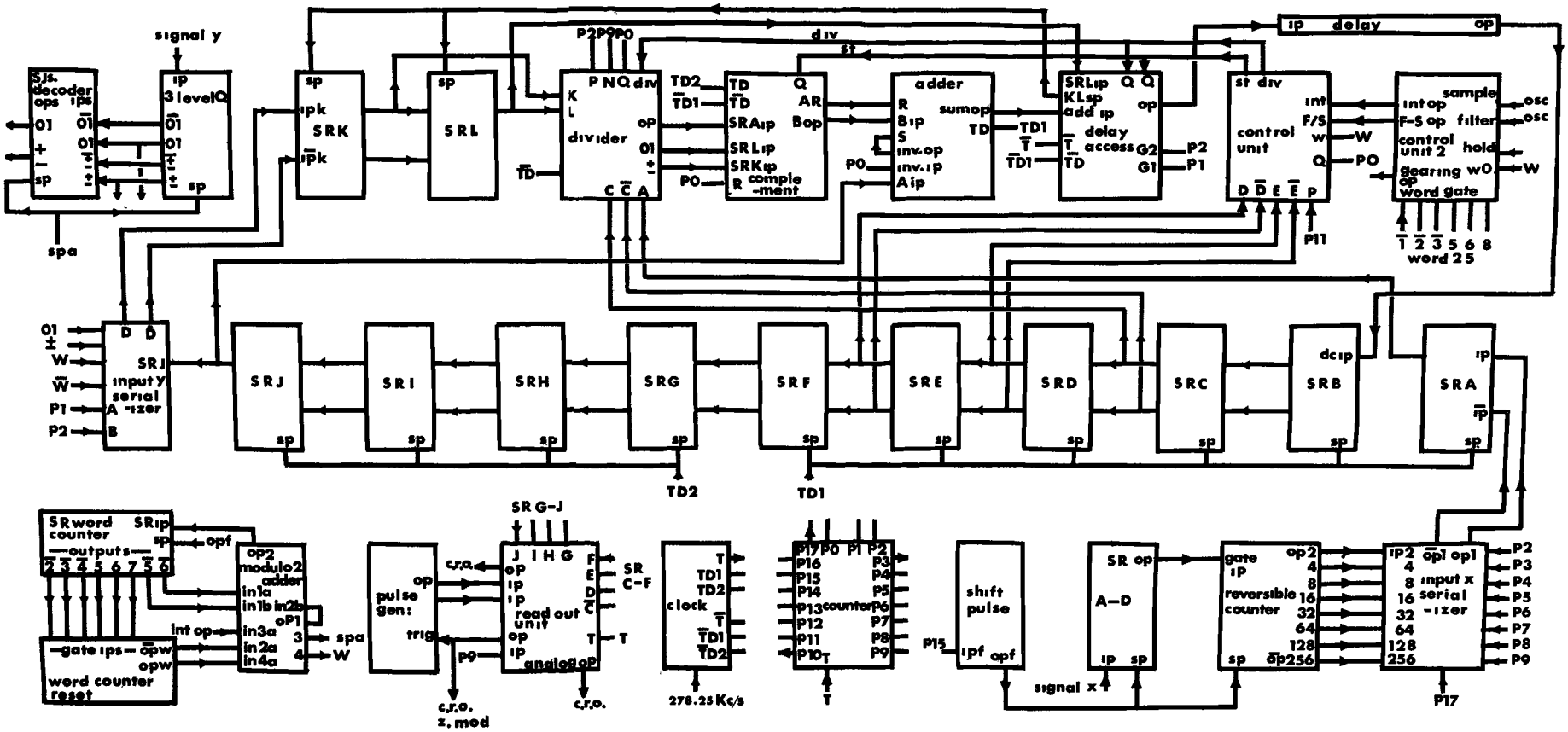

Figure A.2.15 Correlator block diagram

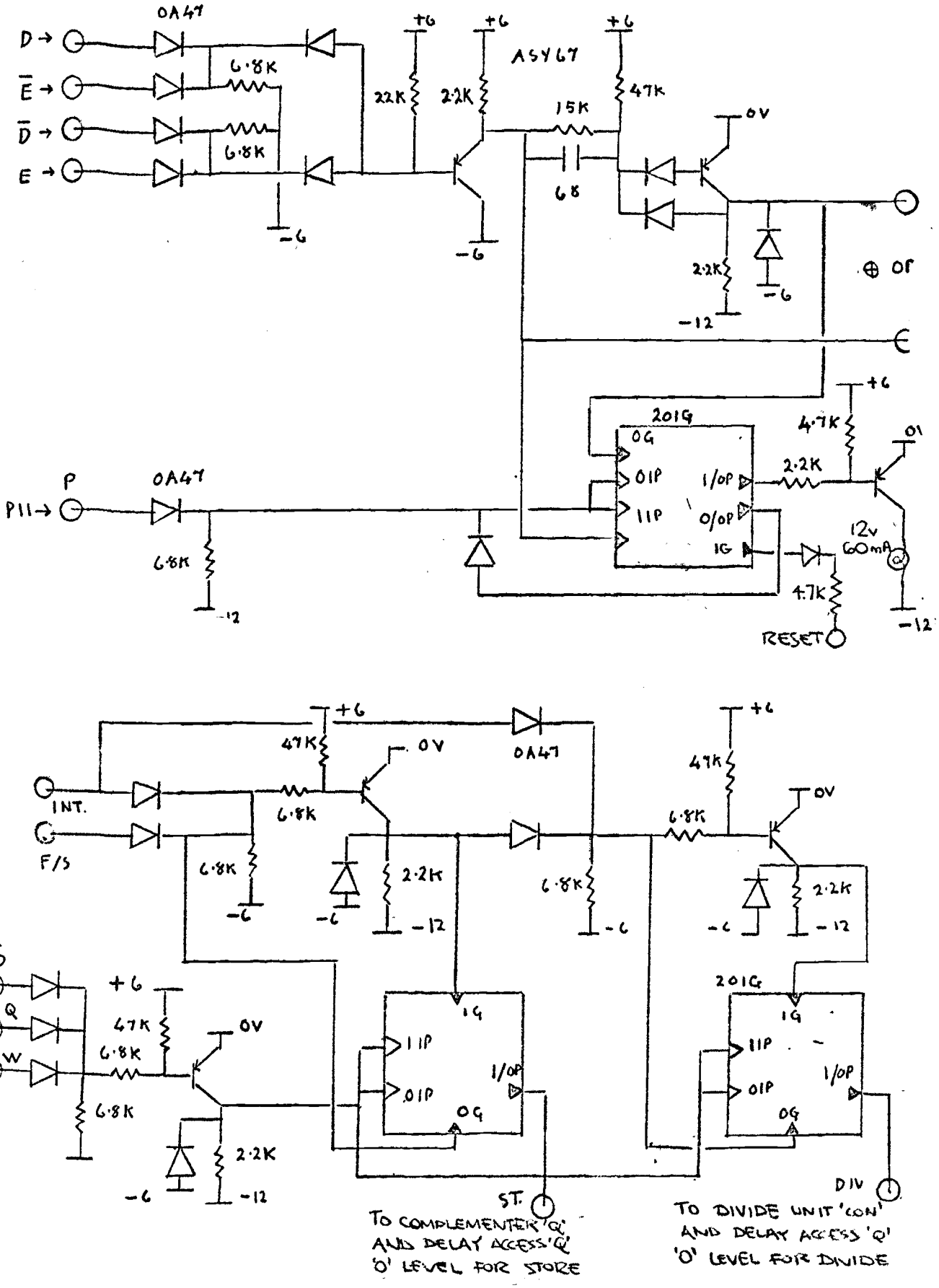

Figure A.2.16 Control unit 1. Top, overflow detector. Bottom, control logic.

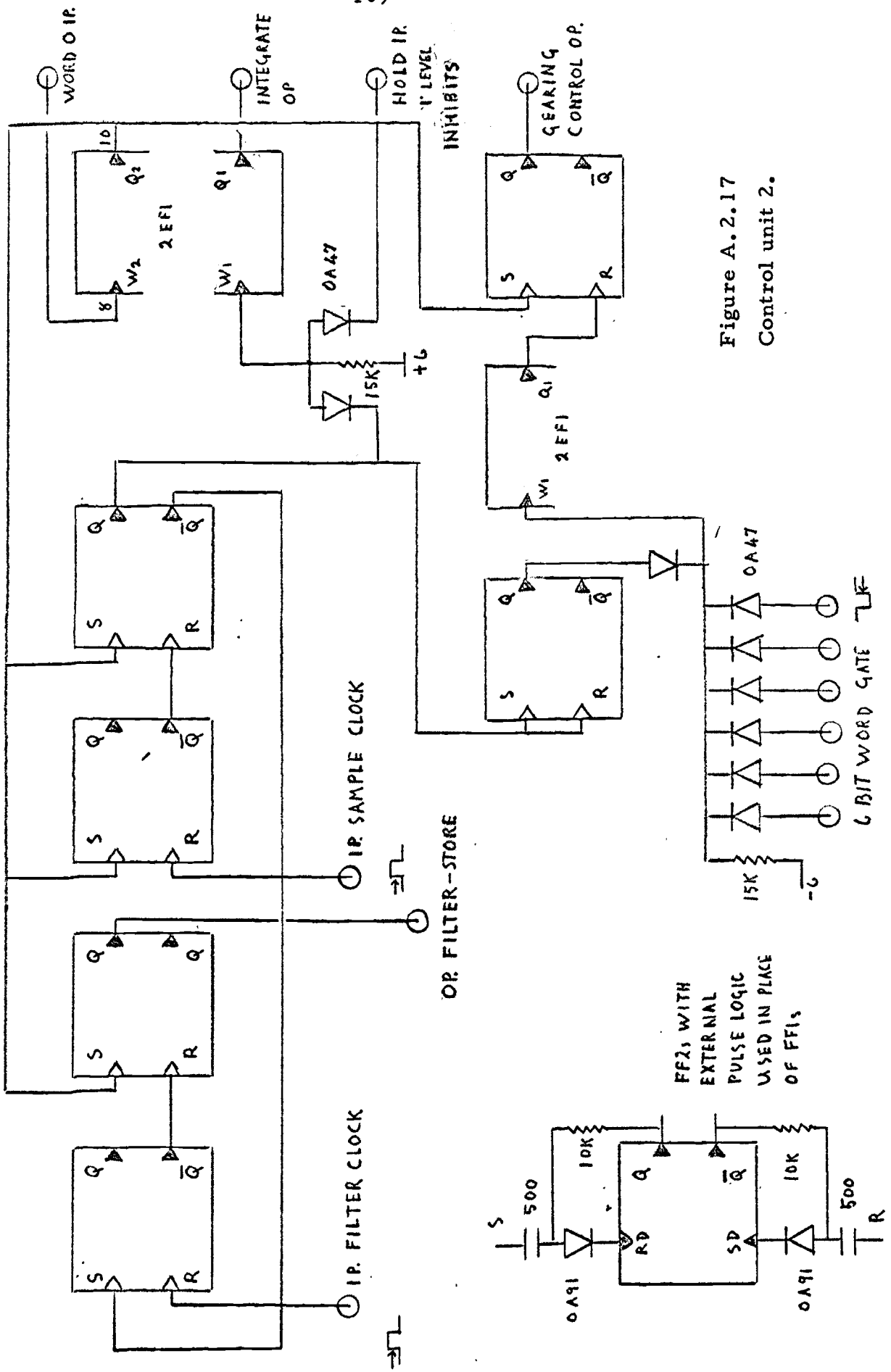

Figure A.2.17
Control unit 2.

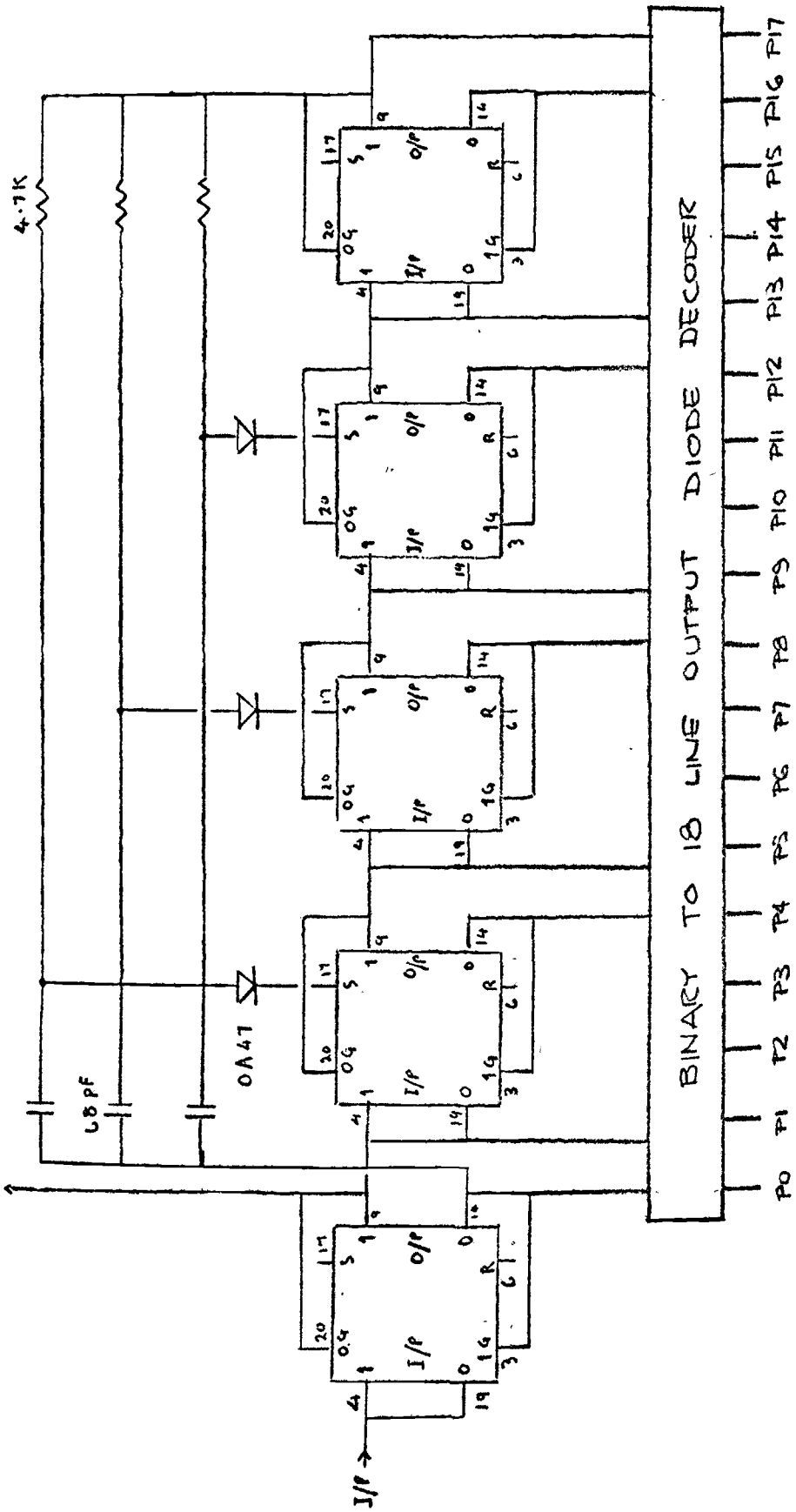

Figure A.2.18 Count of 18 circuit

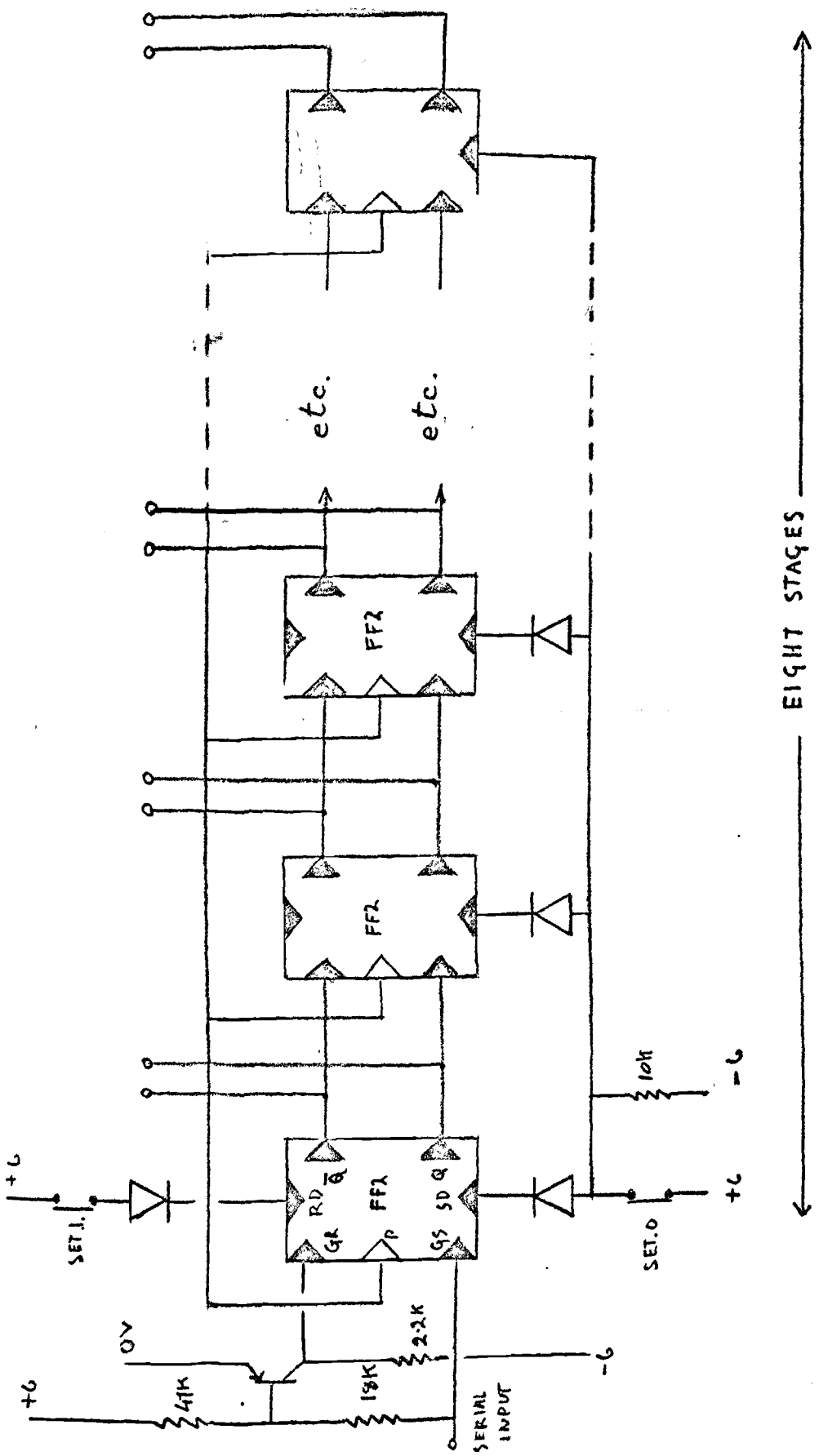

Figure A.2.19 100 kHz shift register used in word counter

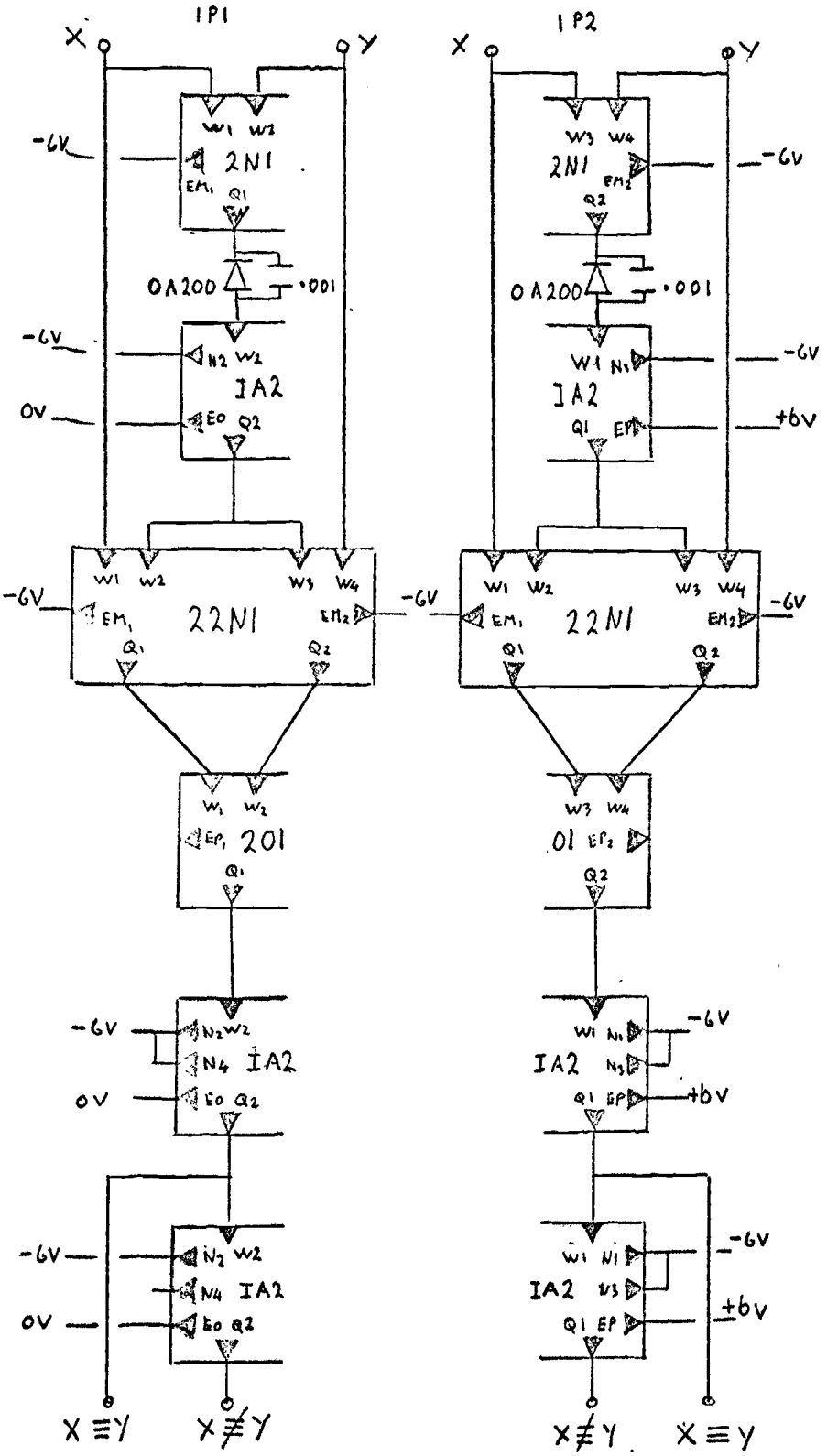

Figure A.2.20 Modulo two adder unit, used in word counter.

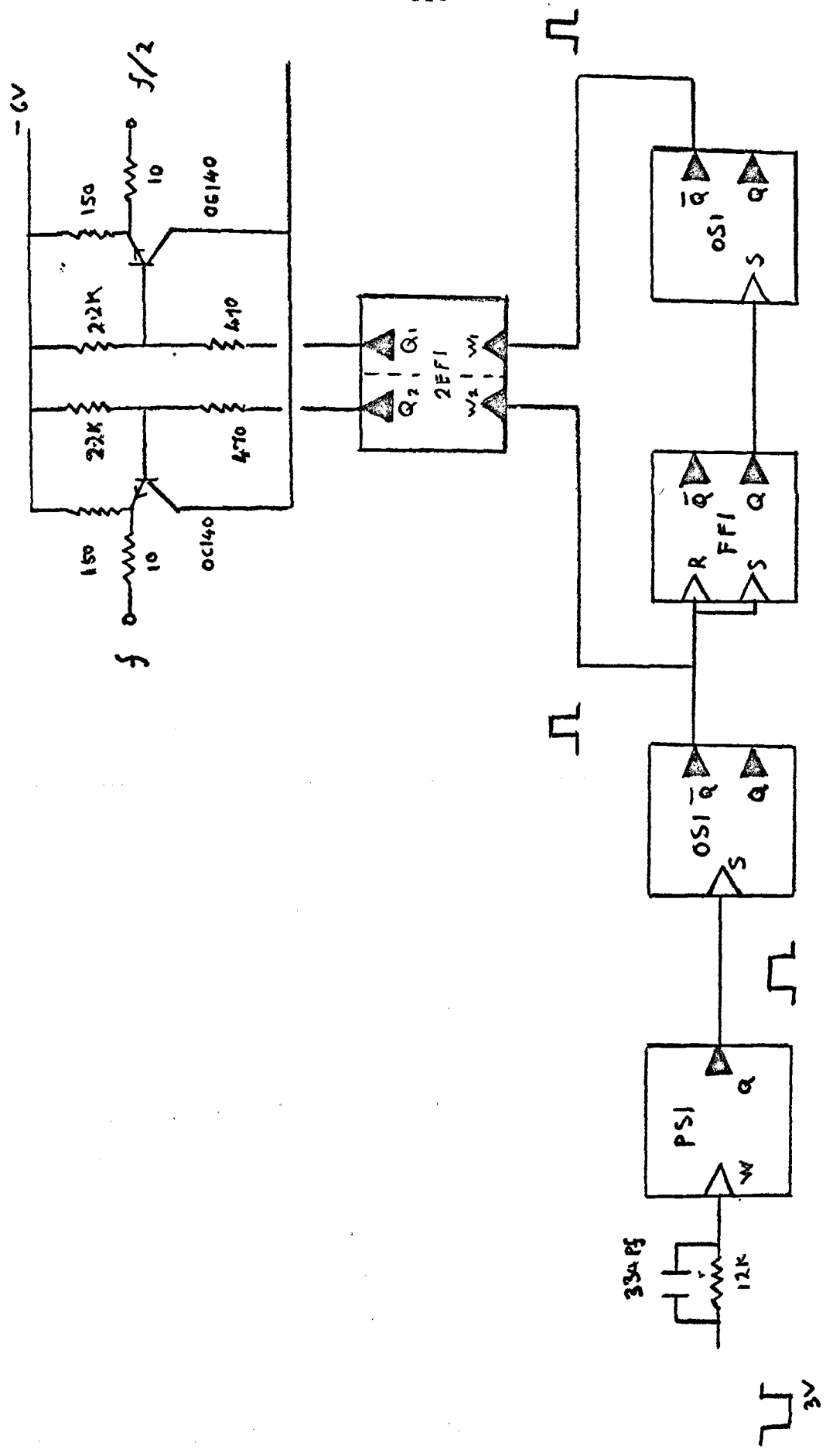

Figure A.2.21 Pulse generator for driving 100kHz circuit blocks.

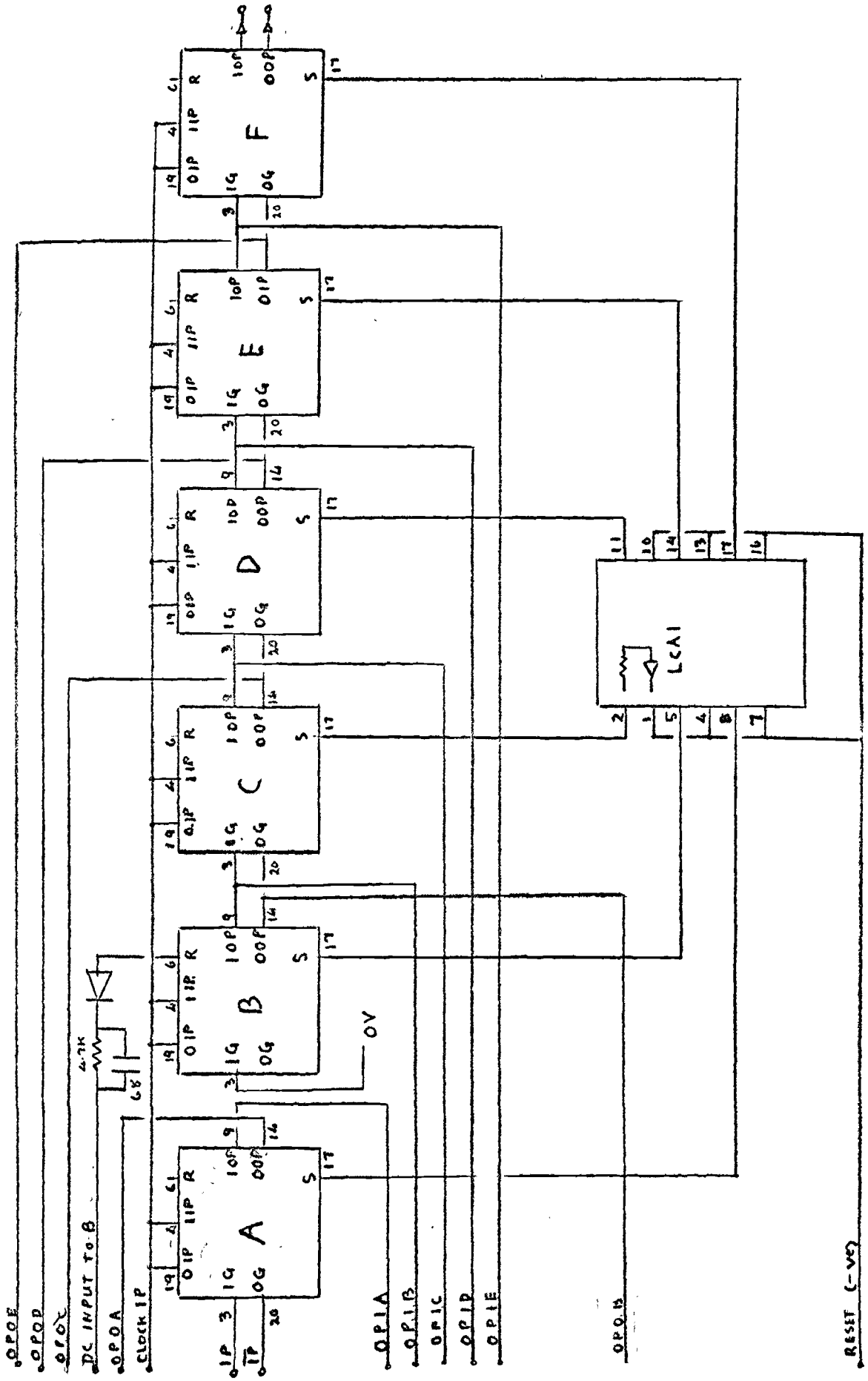

Figure A.2.22 Shift registers A-F

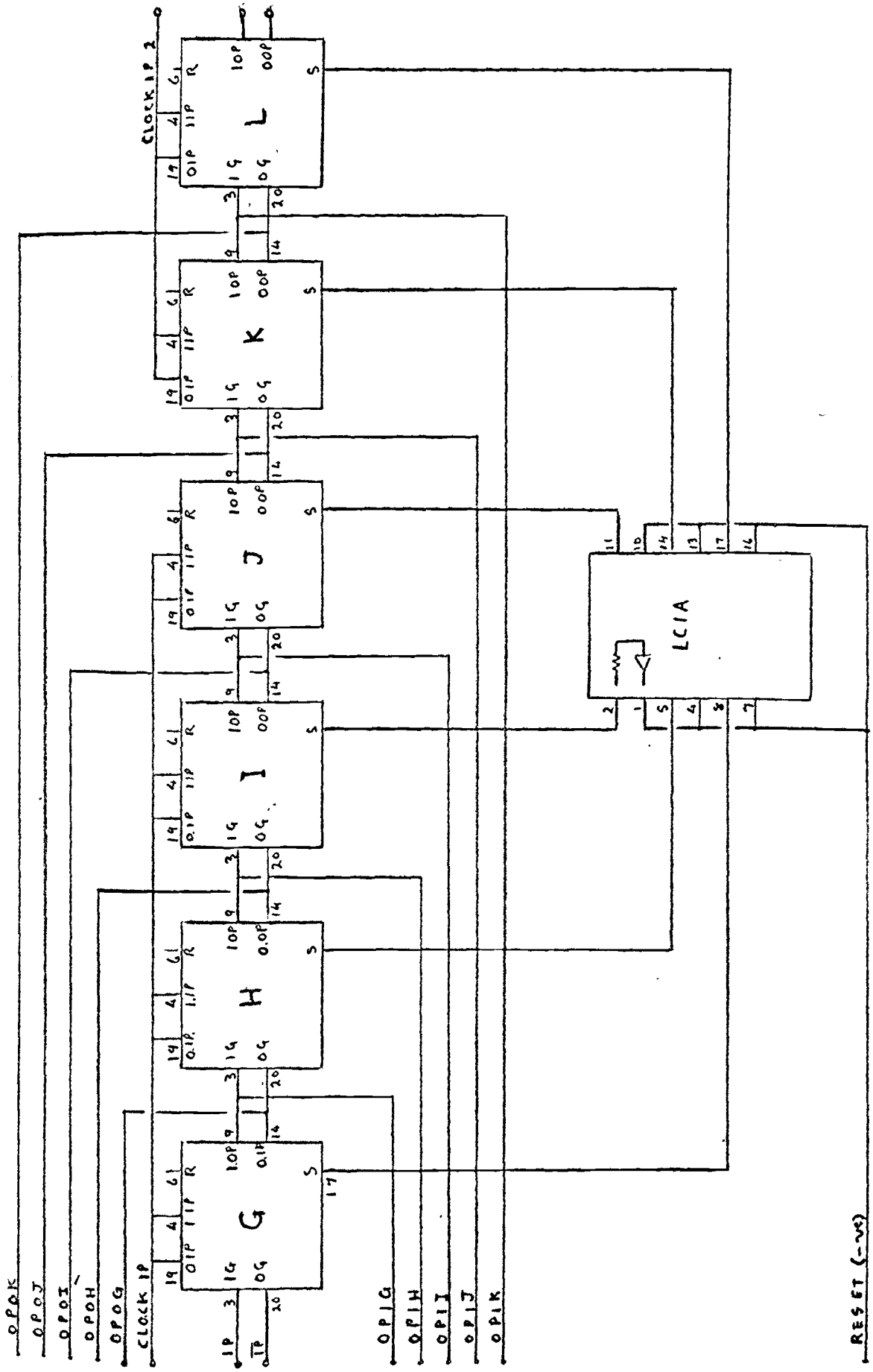

Figure A.2.23 Shift registers G-L

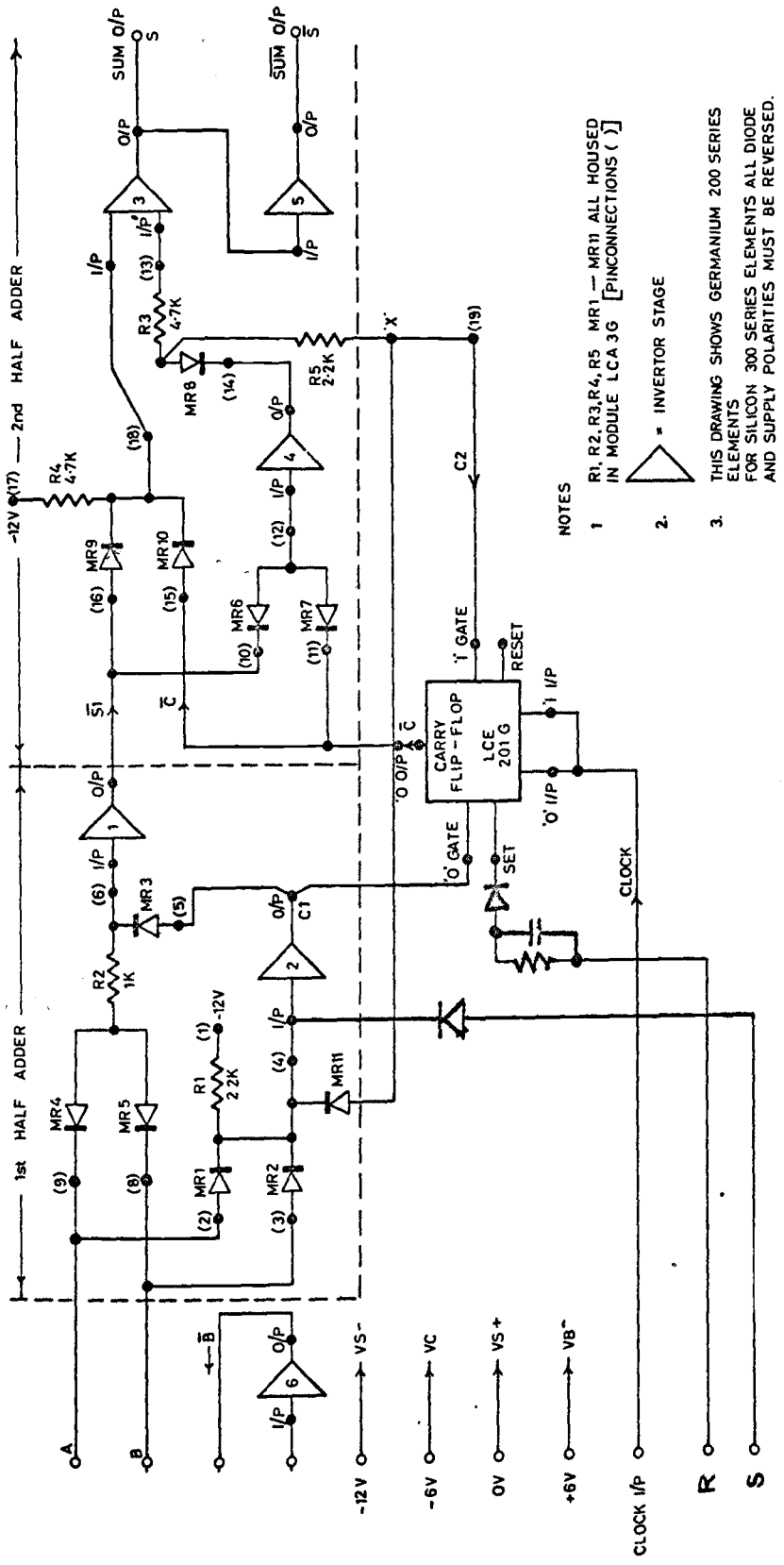

Figure A.2.24 Serial adder circuit. (Modification of standard Ferranti card; Ferranti application report No. 105).

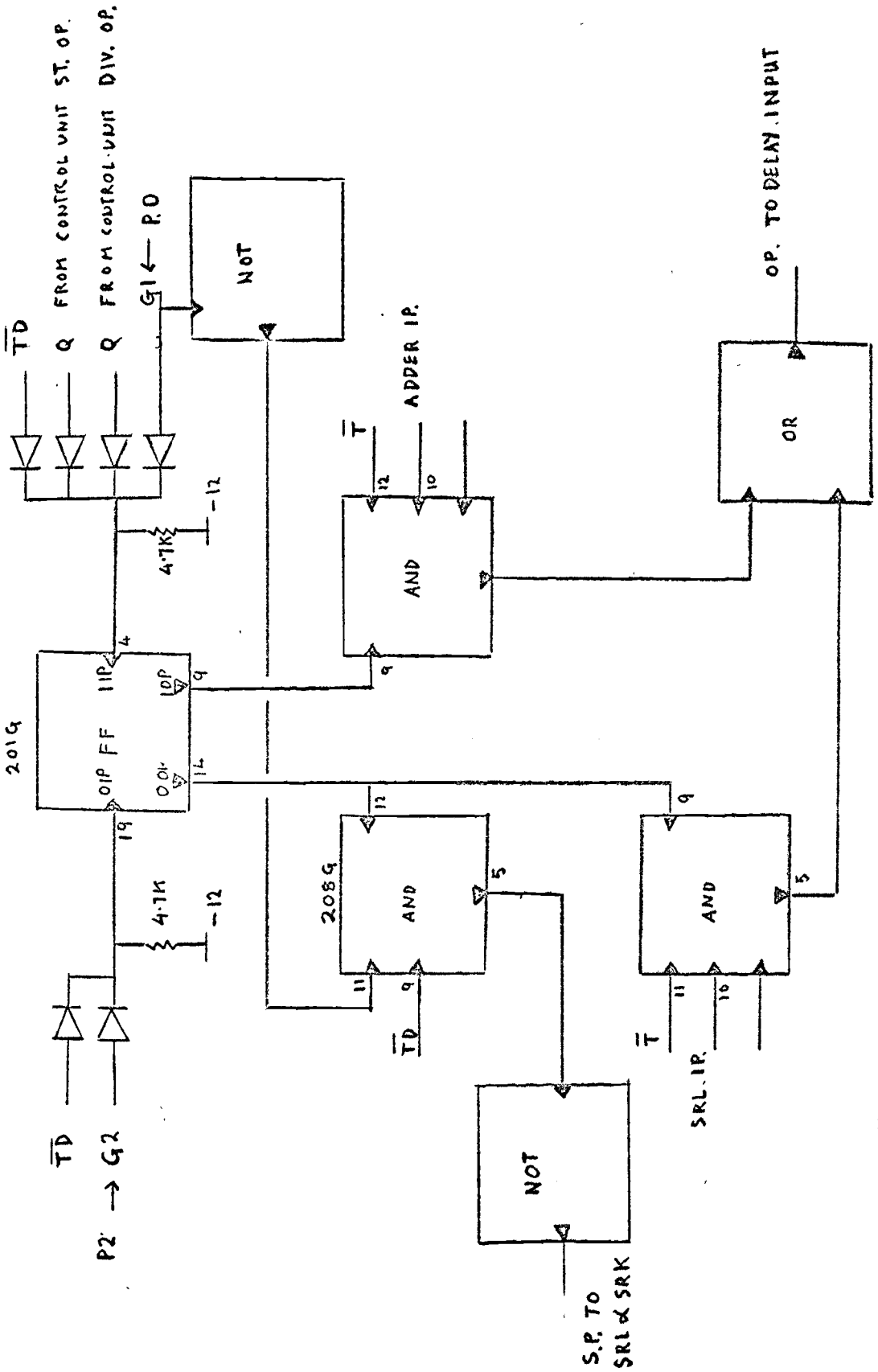

Figure A. 2. 25 Delay access unit

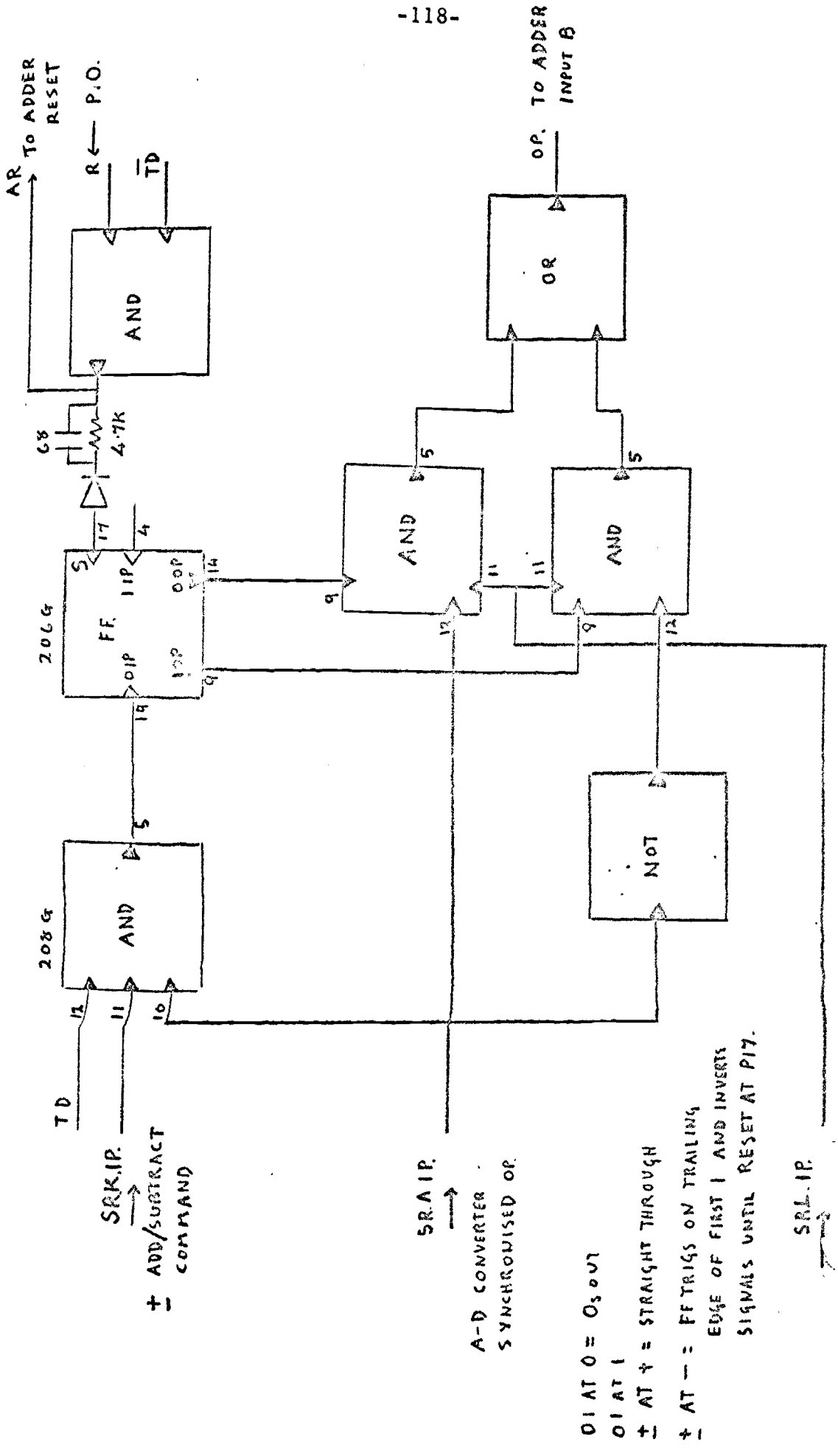

Figure A.2.26 Complement circuit

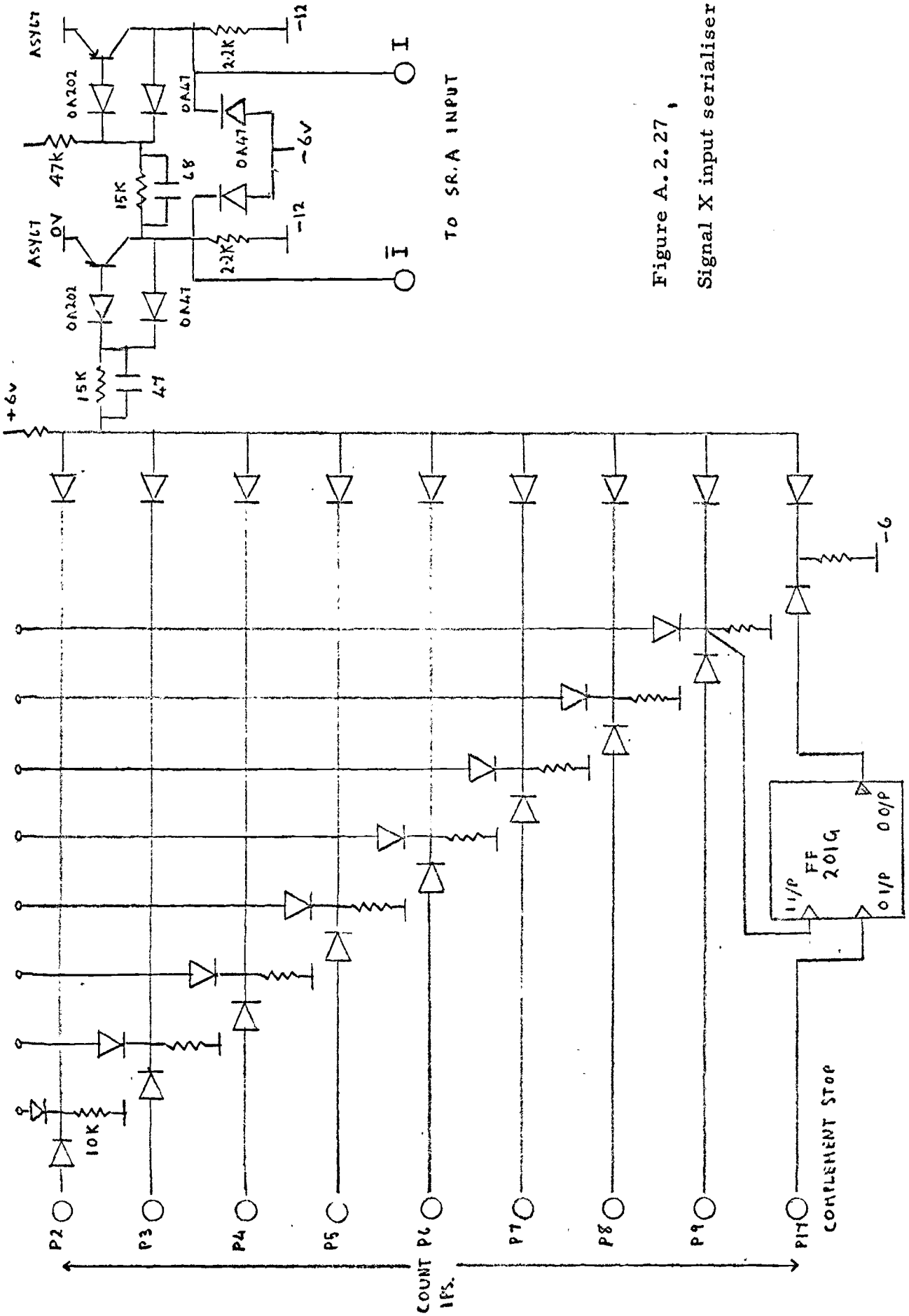

Figure A.2.27 Signal X input serialiser

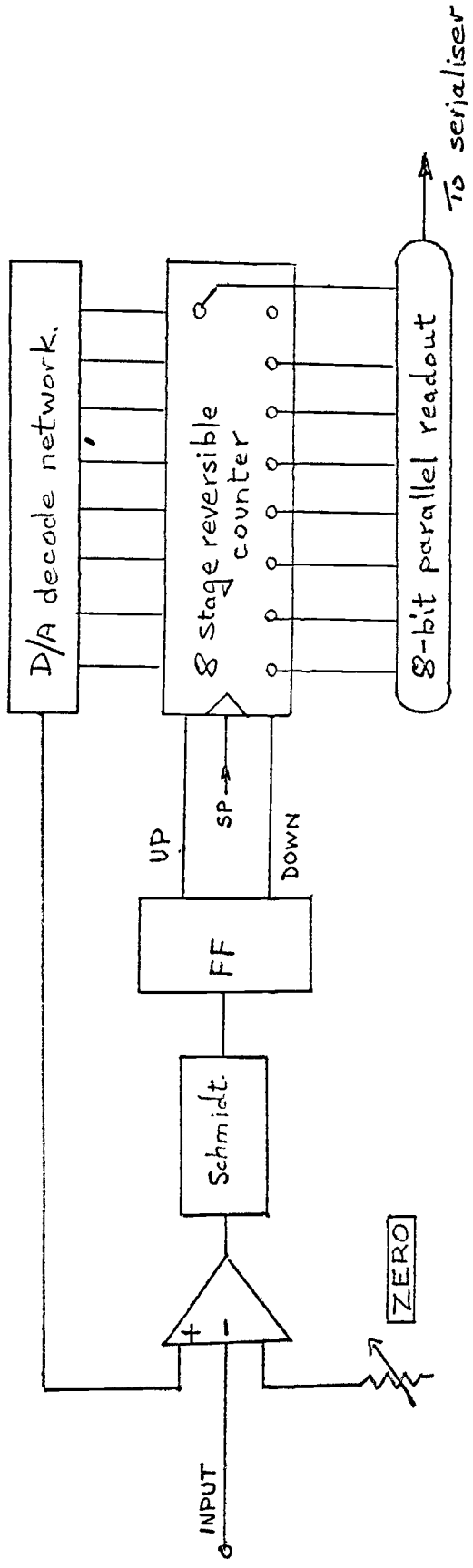

Figure A.2.28 Analogue to two's complement binary converter. The most significant counter bit is inverted to form the two's complement sign bit.

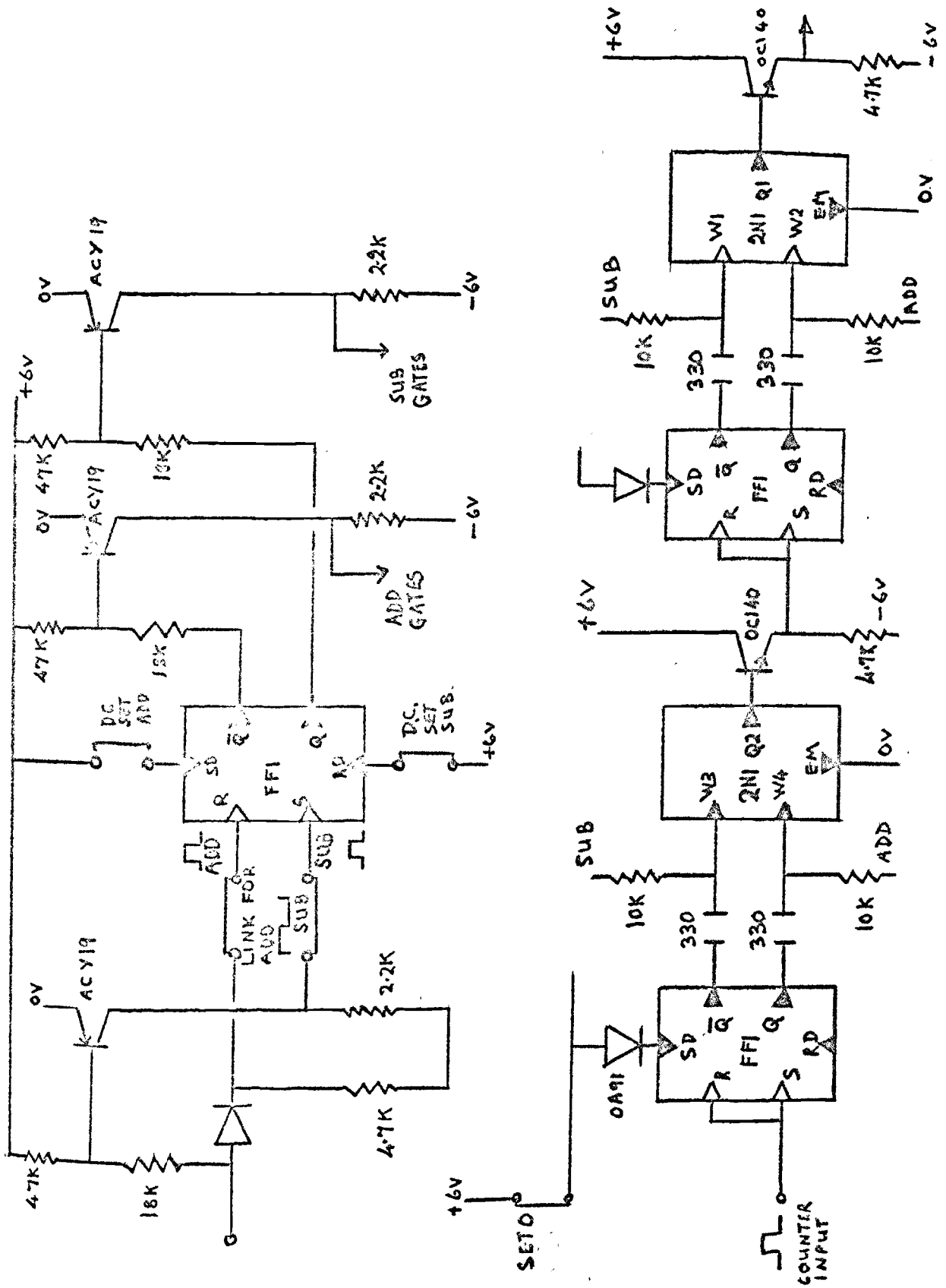

Figure A.2.29 Reversible counter circuit (Add/subtract gate, and two stages shown).

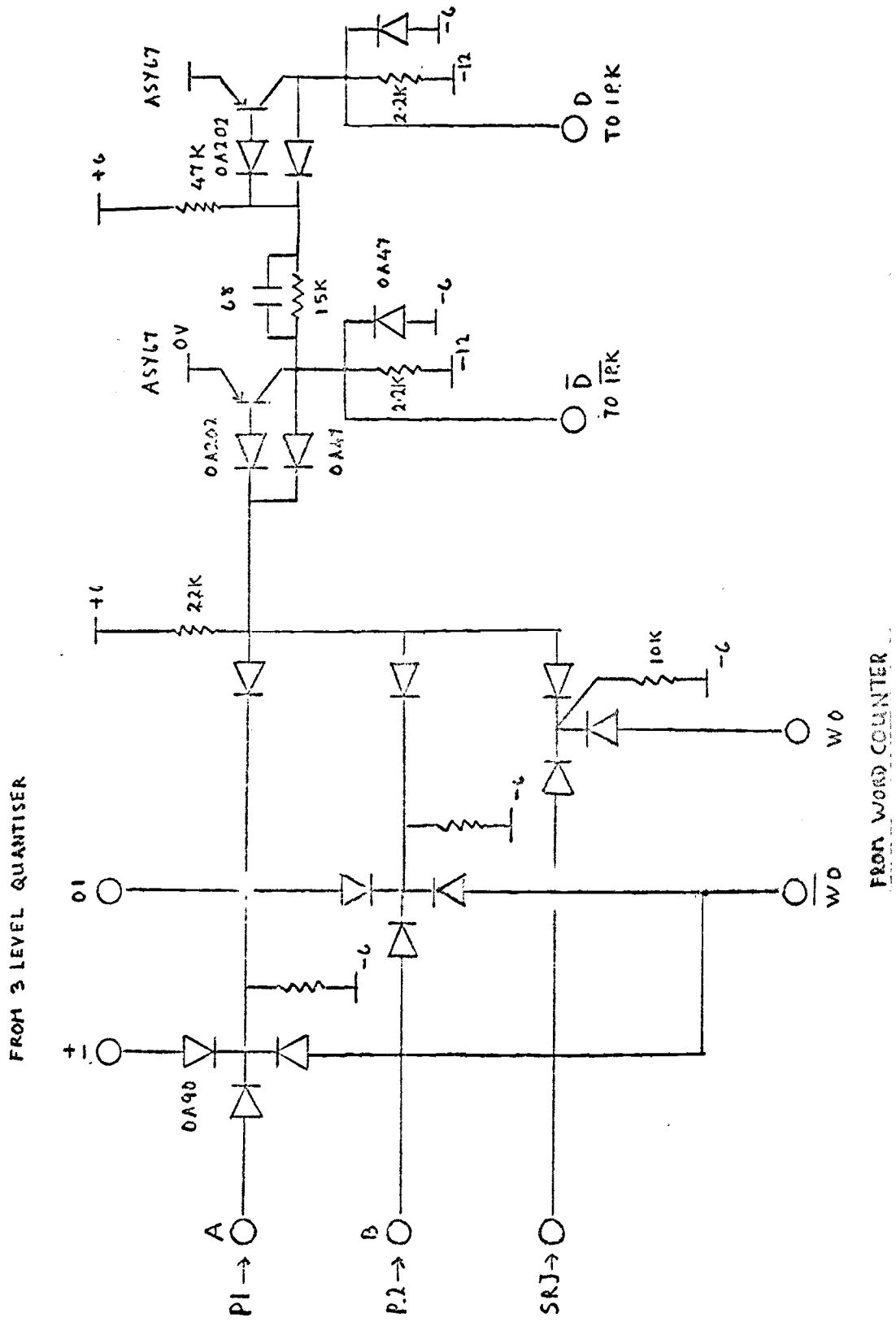

Figure A.2.30 Signal y input serialiser

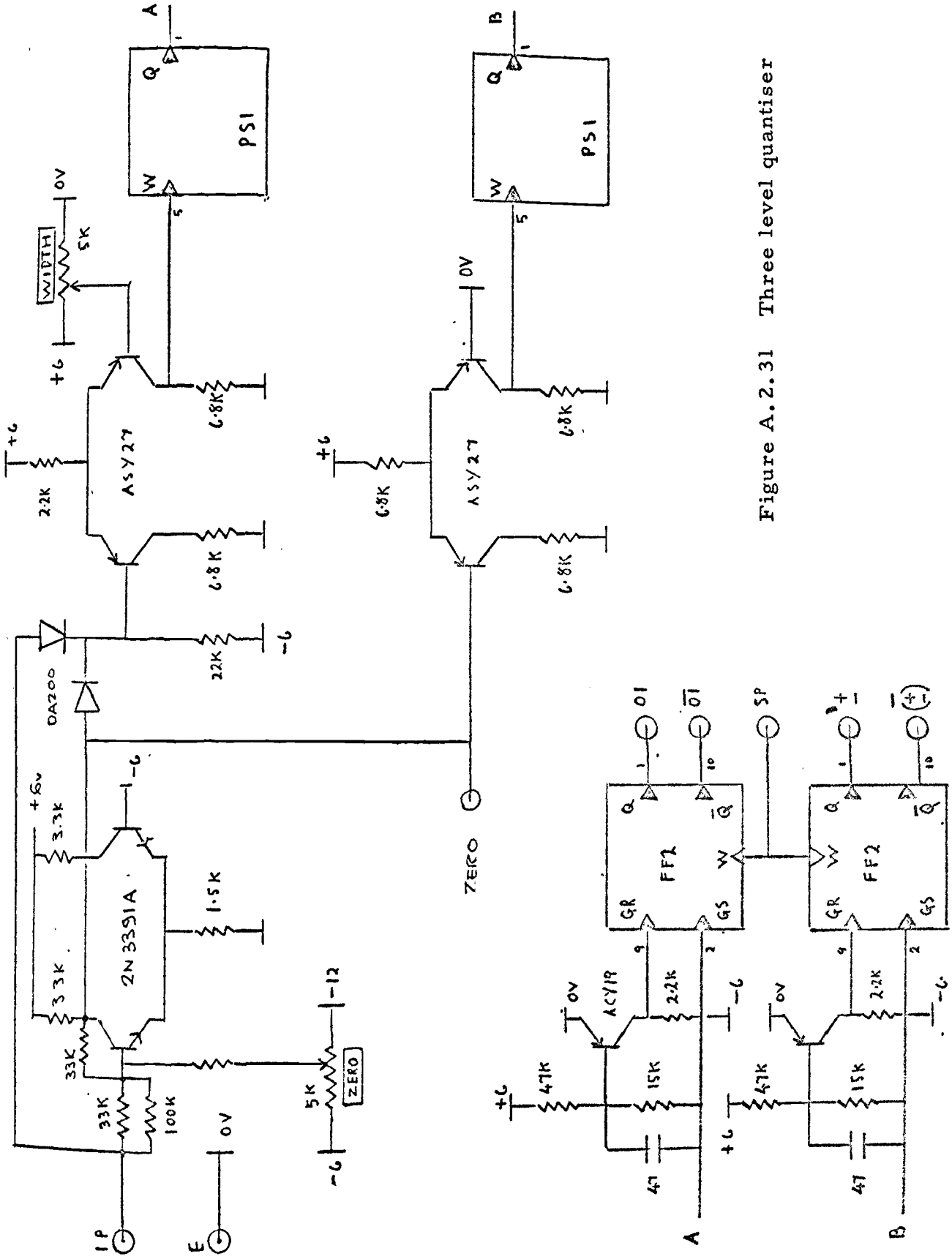

Figure A.2.31 Three level quantiser

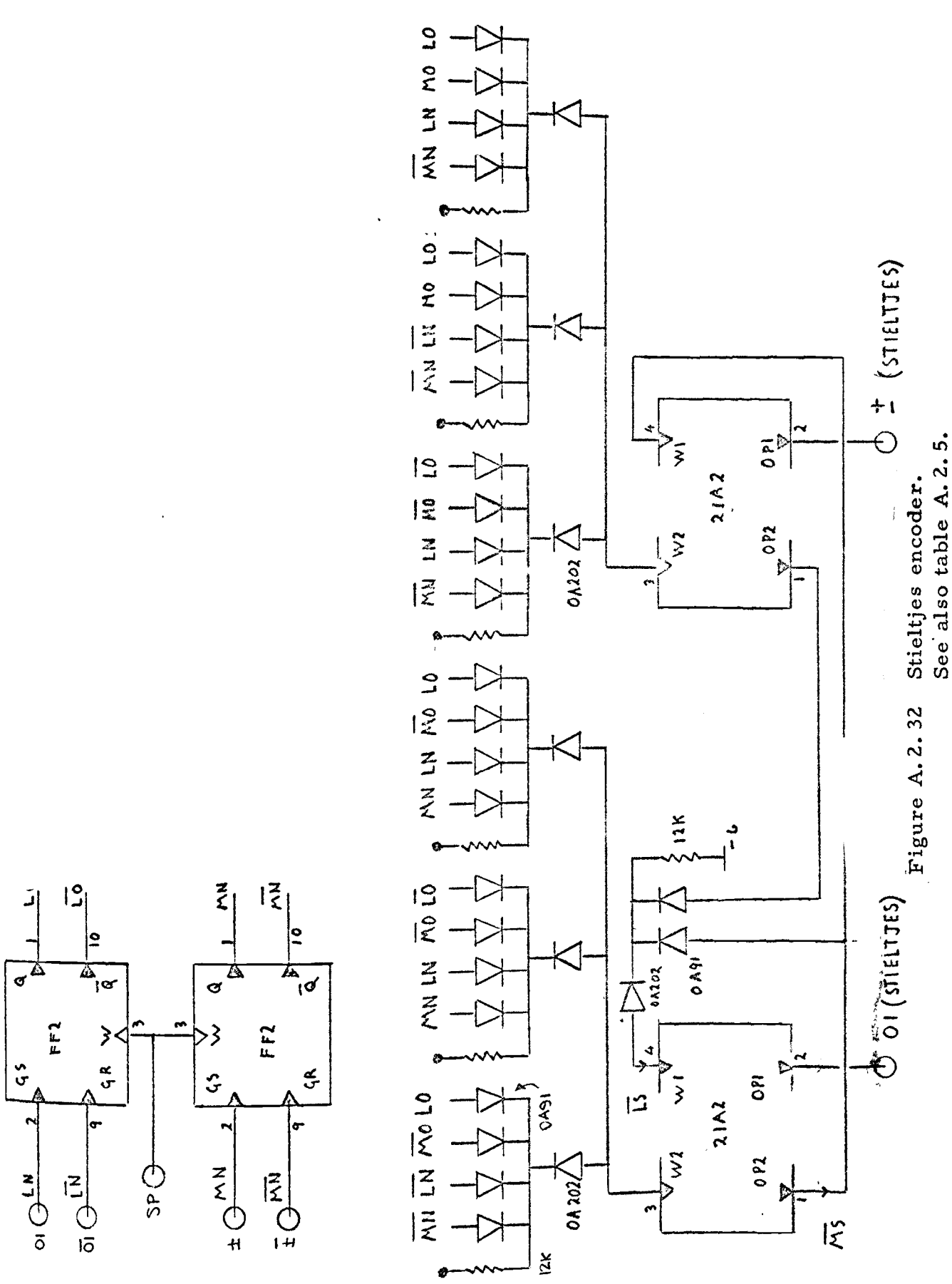

Figure A.2.32 Stieltjes encoder.
See also table A.2.5.

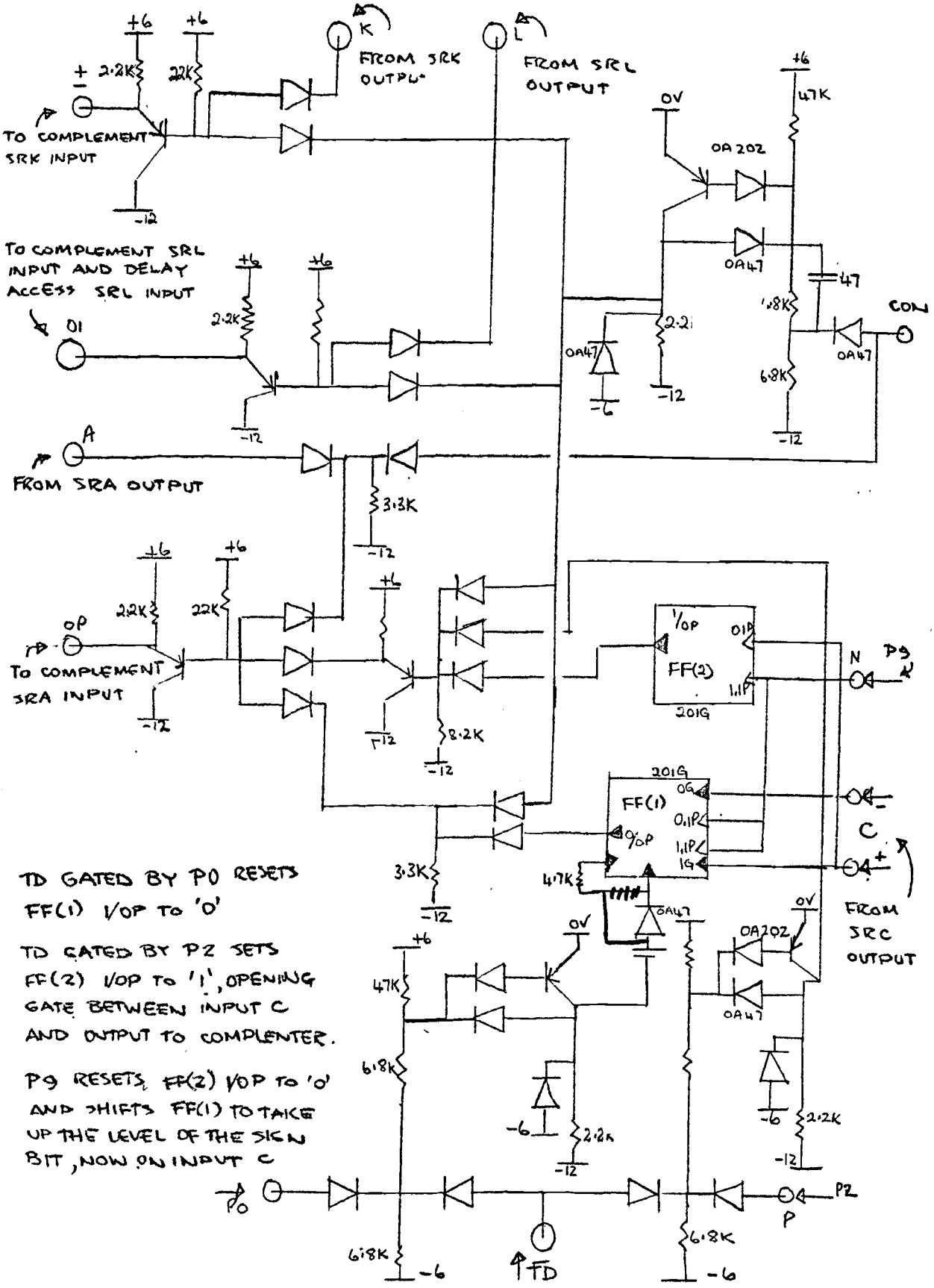

Figure A.2.33 Divide format circuit.

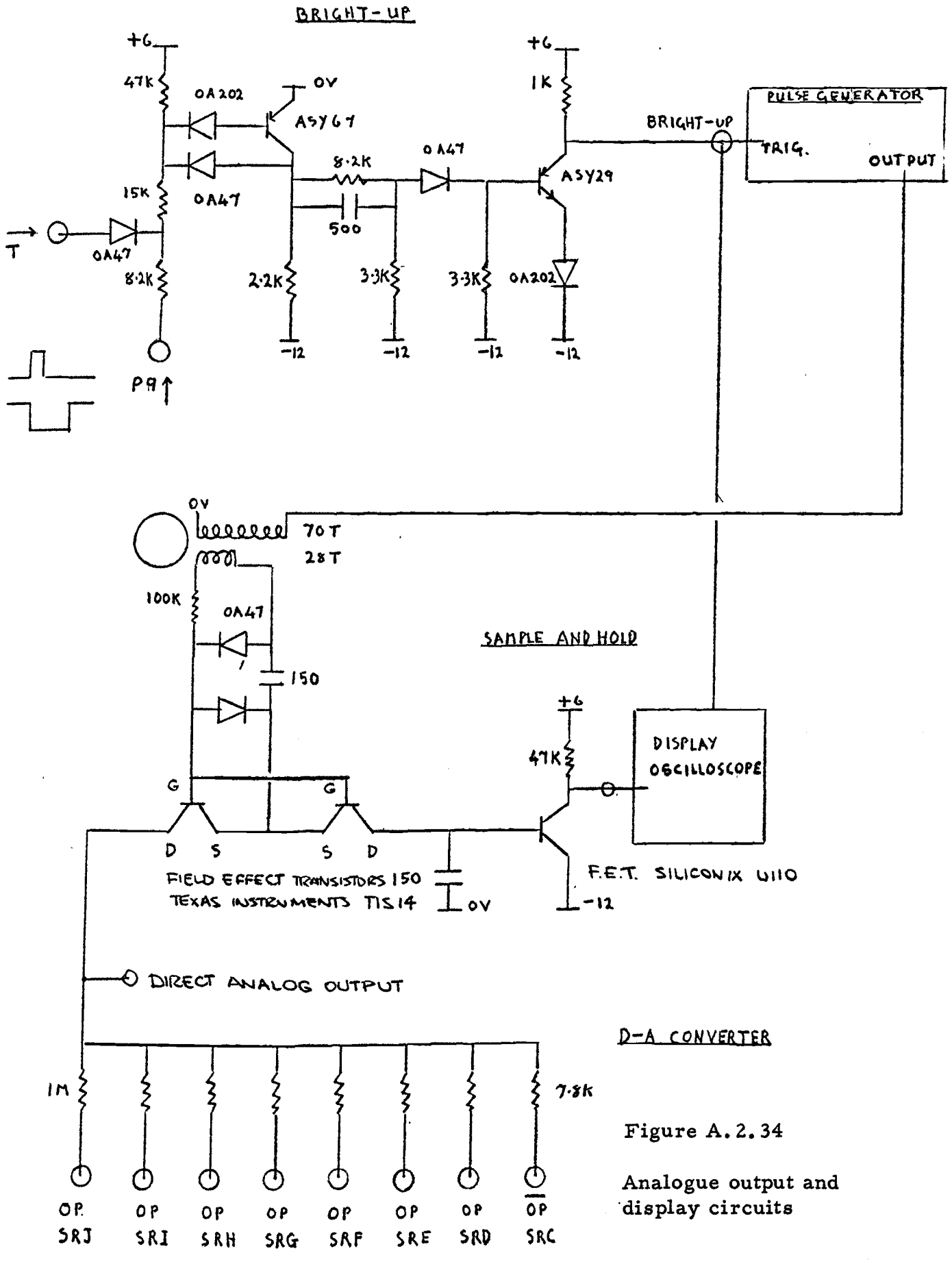

Figure A.2.34

Analogue output and display circuits

Analogue levels			3 level codes		Stieltjes	
Old	New	Change	Old MO LO	New MN LN	Code MS LS	Interpretation
-1	-1	0	1 1	1 1	X 0	no change
-1	0	+1	1 1	X 0	0 1	up one
-1	+1	+2	1 1	0 1	0 1	up one
0	0	0	X 0	X 0	X 0	no change
0	+1	+1	X 0	0 1	0 1	up one
0	-1	-1	X 0	1 1	1 1	down one
+1	+1	0	0 1	0 1	X 0	no change
+1	0	-1	0 1	X 0	1 1	down one
+1	-1	-2	0 1	1 1	1 1	down one

Table A.2.5 Truth table for the Stieltjes encoder, figure A.2.32, in terms of successive differences of a three level quantised signal. X denotes either 0 or 1.

A.3.1 THE EFFECT OF COARSE SAMPLING ON A CORRELATION ESTIMATE

The correlation function is estimated by averaging a large number, N, of sample products $z(kT_s) = x(kT_s - \tau)y(kT_s)$. The variance of this average is shown by Lee [3] to be

$$V^2 = \sum_{\kappa=-(N-1)}^{N-1} \frac{N-|k|}{N^2} R_{vv}(kT_s) \qquad (A.3.1)$$

where $R_{vv}(kT_s)$ is the autocorrelation function of $v(kT_s)$, the a.c. component of $z(kT_s)$, as in appendix 1.2. For large T_s, only the term in (A.3.1.) with $k = 0$ contributes, and

$$V^2 = \sigma_v^2/N \qquad (A.3.2.)$$

The number of samples in a fixed averaging time T will be T/T_s. In this case, for T large

$$V^2 = \sigma_v^2 T_s/T \qquad (A.3.3.)$$

As T_s is reduced, so will V^2, by (A.3.3.), until a stage is reached when successive samples are no longer independent, and more terms in (A.3.1.) are required. The effect of this is to make the variance tend to be almost constant for small T_s. This is illustrated in figure A.3.1. which shows how (A.3.1.) is affected by T_s when

$$N = T/T_s \qquad (A.3.4.)$$

and

$$R_{vv}(u) = \sigma_v^2 \varepsilon^{-\omega_v u} \qquad (A.3.5.)$$

To apply this result to correlation it is necessary to use the expression for $R_{vv}(u)$ previously used in Appendix 1.2.

$$R_{vv}(u) = P_{xy}(u,\tau) - R_{xy}^2(\tau) \qquad (A.3.6)$$

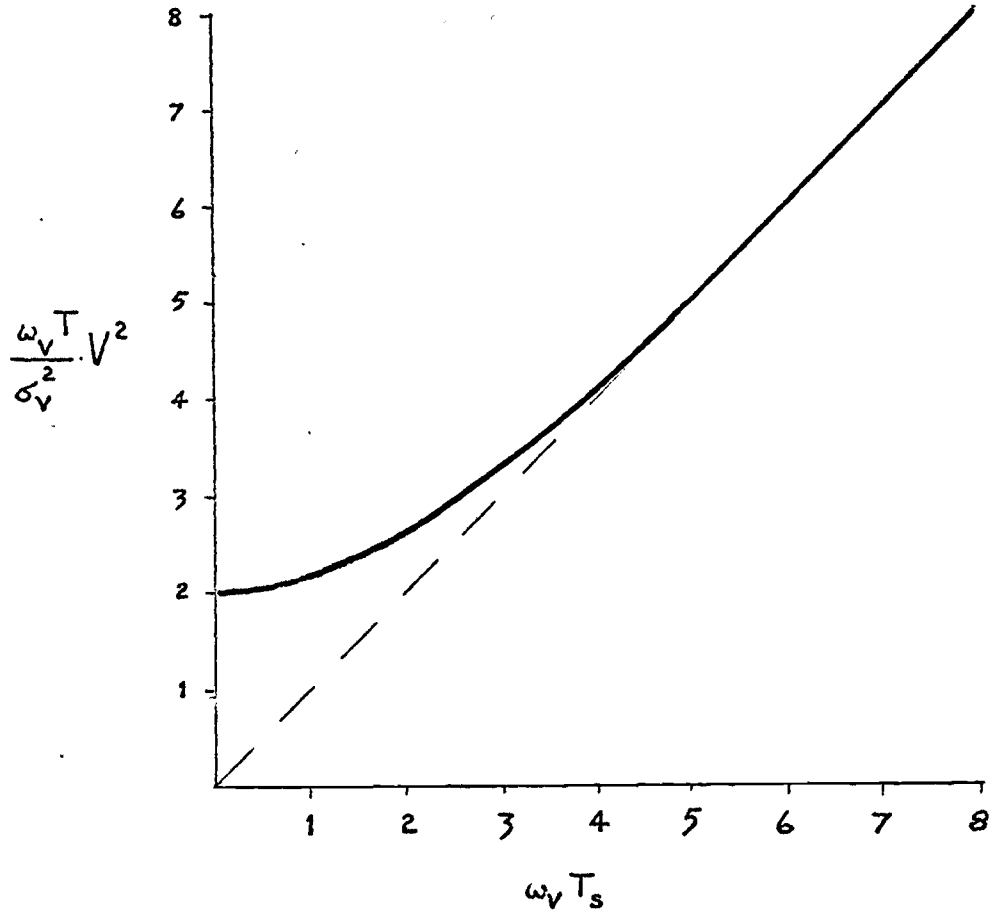

Figure A.3.1. Effect of sampling interval on variance of an estimate in a fixed time T.

A particular example will be developed here. The purpose of the coarse sampling technique is to allow such sampling on the tail of the correlation function. It was shown in appendix 1.2 that for τ large, and $x(t) = y(t)$,

$$P_{xx}(u,\tau) - R_{xx}^2(\tau) \simeq R_{xx}^2(u) \qquad \text{(A.3.7.)}$$

If, for example,

$$R_{xx}(u) = \sigma_x^2 \, \varepsilon^{-\alpha u} \qquad \text{(A.3.8.)}$$

then

$$R_{vv}(u) = R_{xx}^2(u) = \sigma_x^4 \, \varepsilon^{-2\alpha u} \qquad \text{(A.3.9.)}$$

from which

$$\omega_v = 2\alpha \qquad \text{(A.3.10)}$$

$$\sigma_v^2 = \sigma_x^4 \qquad \text{(A.3.11)}$$

For continuous signals, from figure A.3.1

$$V^2 \simeq \frac{2}{\omega_v T} \sigma_v^2 \qquad \text{(A.3.12)}$$

$$\simeq \frac{1}{\alpha T} \sigma_x^4 \qquad \text{(A.3.13)}$$

If we sample at, say $T_s = \frac{1}{\alpha}$, then $\omega_v T_s = 2$

and from figure A.3.1.

$$V^2 \simeq \frac{2.3}{\alpha T} \sigma_x^4 \qquad \text{(A.3.14)}$$

which shows a 30% increase over the finely sampled situation.

A.4.1 SUMMARY OF THE ALGEBRA OF DIGITAL SEQUENCES AND CIRCUITS

The algebra related to shift register generated sequences has been given by several authors [9, 21, 24]. For completeness a summary is given here, together with some conclusions on the cross correlation properties of two sequences.

1. Sequences. A sequence $\{u\}$ will be regarded as a succession of integers modulo 2.

$$\{u\} = u_0, u_1, u_2, \ldots u_n, \ldots \qquad (A.4.1.)$$

The algebraic operations to be used, addition modulo 2 and multiplication, are defined by table A.4.1.

+	0	1
0	0	1
1	1	1

(a)

X	0	1
0	0	0
1	0	1

(b)

Table A.4.1. Modulo 2 (a) addition (b) multiplication.

It can be seen that the practical realisation of a modulo 2 adder is the 'not equivalent' or 'exclusive or' function. A multiplier is simply an 'and' gate, and multiplication by a constant coefficient 1, or 0 is simply the presence of a connection, or not.

A further operation required is delay by an integral interval Δ, e.g. u_k would become $u_{k-\Delta}$. This is treated in the next section.

2. The delay operator D. The operator D, and its inverse are defined by

$$D(u_k) = u_{k-1} \quad \text{and} \quad D^{-1}(u_{k-1}) = u_k \qquad (A.4.2.)$$

Note also that

$$D^r(u_k) = u_{k-r} \qquad (A.4.3)$$

The operation can equally well be used on the entire sequence $\{u\}$ to shift every element, and the equation implying this is

$$D\{u_k\} = \{u_{k-1}\} \qquad \text{(A.4.4)}$$

For a sequence with elements appearing at intervals in time the delay operation can be realised physically by a shift register stage, the present output of which is the previous value of the input, figure A.4.1.

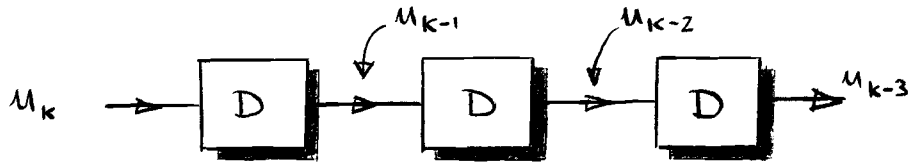

Figure A.4.1. Delay stages in cascade

3. Sequential circuits. Delay stages, adders, and coefficient multipliers may be connected to form a circuit which will produce an output sequence $\{u\}$ in response to an input $\{v\}$. Figure A.4.2. shows a possible configuration.

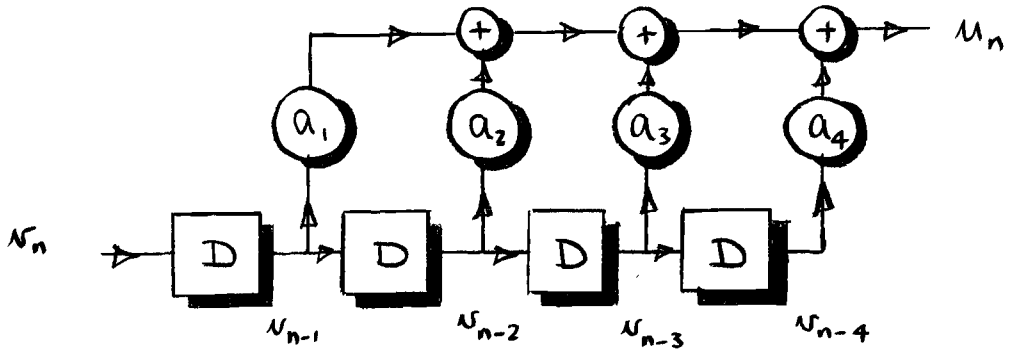

Figure A.4.2. A sequential circuit

In figure A.4.2.

$$u_n = a_1 v_{n-1} + a_2 v_{n-2} + a_3 v_{n-3} + a_4 v_{n-4}$$

where the coefficients a_1, a_2, etc. are either '0' or '1'. In a general expression

$$u_n = \sum_{i=1}^{r} a_i v_{n-i} \qquad \text{(A.4.5)}$$

This expression is linear.

An interesting network results if the output of a circuit such as figure A.4.2 is fed back to the input as in figure A.4.3

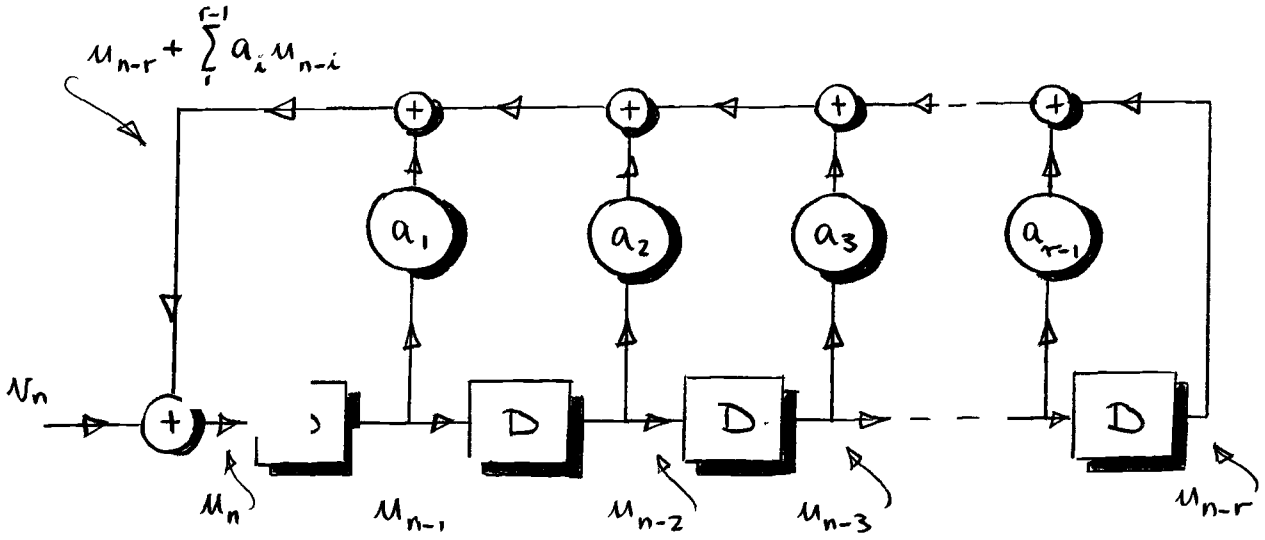

Figure A.4.3 A feedbac cuit

In figure A.4.3,

$$u_n = v_n + u_{n-r} + \sum_{i=1}^{r-1} a_i u_{n-i} \qquad \text{(A.}$$

let $\{v\} = \{0\}$

$$u_n = u_{n-r} + \sum_{i=1}^{r-1} a_i u_{n-i} \qquad \text{(A.4.7)}$$

A sequence which is a solution of the linear difference equation (A.4.7) will be maintained in this network in the absence of an input. This is a situation typical of a feedback system.

(A.4.7) can be re-written using the operator D

$$u_n = D^r u_n + \left(\sum_1^{r-1} a_\lambda D^\lambda \right) u_n \qquad \text{(A.4.8)}$$

Hence

$$u_{n-r} = D^r u_n = \left(-\sum_1^{r-1} a_\lambda D^\lambda + 1 \right) u_n \qquad \text{(A.4.9)}$$

This expression (7) gives u_{n-r} in terms of its future r values.

From (A.4.9)

$$\left(D^r + \sum_1^{r-1} a_\lambda D^\lambda + 1 \right) u_n = 0 \qquad \text{(A.4.10)}$$

If $u_n = 0$ for all n, then the sequence $\{u\}$ is the sequence $\{0\}$ and this is a trivial solution to equation (A.4.10). Otherwise $u_n \neq 0$ for all n, and so

$$D^r + \sum_1^{r-1} a_\lambda D^\lambda + 1 = 0 \qquad \text{(A.4.11)}$$

This is an important relation involving D.

4. <u>The advance operator A</u>. It is useful to determine a similar relation to (A.4.11) for the advance operator, defined by (A.4.12).

$$A = D^{-1} \qquad \text{(A.4.12)}$$

Then

$$A u_{n-1} = D^{-1} u_{n-1}$$

$$= u_n$$

Then, from (A.4.8)

$$A u_{n-1} = D^r u_n + \left(\sum_1^{r-1} a_\lambda D^\lambda \right) u_n$$

$$= D^{r-1} u_{n-1} + \left(\sum_1^{r-1} a_\lambda D^{\lambda-1} \right) u_{n-1}$$

$$= \left(D^{r-1} + \sum_1^{r-1} a_\lambda D^{\lambda-1} \right) u_{n-1} \qquad \text{(A.4.13)}$$

Hence

$$A = D^{r-1} + \sum_{1}^{r-1} a_i D^{i-1} \qquad \text{(A.4.14)}$$

$$= A^{-(r-1)} + \sum_{1}^{r-1} a_i A^{-(i-1)}$$

Multiply by A^{r-1}, and collect terms to the left hand side.

$$A^r - \sum_{1}^{r-1} a_i A^{r-i} - 1 = 0 \qquad \text{(A.4.15)}$$

Notice that the coefficients of the polynomial in A on the L.H.S. of (A.4.15) are the coefficients of the polynomial in D from equation (A.4.11), but in reverse order, and of opposite sign except for the leading term. From (A.4.15)

$$u_{n+r} = A^r u_n$$

$$= \left(\sum_{1}^{r-1} a_i A^{r-i} + 1 \right) u_n \qquad \text{(A.4.16)}$$

This gives u_{n+r} in terms of its previous values.

5. <u>The cyclic property.</u> Let the polynomial (A.4.15) be p(A).

$$p(A) = \left(A^r - \sum_{1}^{r-1} a_i A^{r-i} - 1 \right) = 0 \qquad \text{(A.4.17)}$$

Then, from the theory of polynomials, there will be some integer k such that p(A) will divide the polynomial $A^k - 1$ without remainder.

That is

$$A^k - 1 = p(A) g(A) \qquad \text{(A.4.18)}$$

where g(A) is some polynomial in A, of order k-r.

But, from (A.4.17)

$$p(A) = 0$$

Hence, from (A. 4. 18)

$$A^k = 1$$

and so

$$\left.\begin{aligned} A^k u_n &= u_n \\ u_{n+k} &= u_n \end{aligned}\right\} \qquad \text{(A. 4. 19)}$$

The sequence $\{u\}$ is therefore cyclic with period k.

For example, the sequence with the recurrence relation

$$u_{n+5} + u_{n+4} + u_n = 0 \qquad \text{(A. 4. 20)}$$

has a corresponding polynomial

$$A^5 + A^4 + 1 \qquad \text{(A. 4. 21)}$$

and

$$(A^5 + A^4 + 1)(A^{16} + A^{15} + A^{14} + A^{13} + A^{12} + A^{10} + A^8 + A^5 + A^4 + 1)$$

$$= A^{21} + 1 \qquad \text{modulo 2}$$

$$= A^{21} - 1 \qquad \text{modulo 2}$$

The sequences which satisfy (A. 4. 20) are therefore cyclic with a period of 21.

Similarly $A^5 + A^3 + 1$ divides $A^{31} - 1$, modulo 2, showing that the solution of

$$u_{n+5} + u_{n+3} + u_n = 0$$

has period 31.

6. Maximal length sequences. If p(A) divides $A^k - 1$ for some k such that

$$k = 2^r - 1 \qquad \text{modulo 2}$$

the resulting sequence is of maximal length, i. e. one cycle of such a sequence, contains all combinations of successive elements with the exception of r successive zeros, giving a total of $2^r - 1$.

A result of this is that of the 2^r-1 elements in the sequence there will be $2^r/2$ non zero elements, and one less than this number of zeros. In the example in section 5, where

$$p(A) = A^5 + A^3 + 1$$

we have

$$r = 5$$

$$k = 2^r - 1 = 31$$

There will be 16 elements '1' and 15 elements '0'.

All possible initial conditions of the network realising the polynomial p(A) are contained in a maximal length sequence. It follows that the non-zero solutions to the associated difference equation can only be the maximal length sequence, or other sequences which are identical to it, except for a shift.

Any linear combination of solutions to a difference equation must also be a solution. A linear combination of shifted versions of a maximal length sequence will therefore produce either the all zero sequence or another shifted version of the same sequence.

That is

$$\left(\sum_m b_m A^m\right)\{u_n\} = A^j\{u_n\} \qquad \text{modulo 2} \qquad \text{(A.4.22)}$$

for some j, or

$$\left(\sum_m b_m A^m\right)\{u_n\} = \{0\} \qquad \text{modulo 2} \qquad \text{(A.4.23)}$$

7. Autocorrelation for a binary maximal length sequence. Define a sequence $\{u'\}$ as the sequence which results from replacing '0' by (+1) and '1' by (-1) in the sequence $\{u\}$, a maximal length sequence with period N. → (A.4.24)

The Autocorrelation function

$$R(\Delta) = \frac{1}{N} \sum_{\lambda=0}^{N-1} u'_\lambda u'_{\lambda+\Delta}$$

is also cyclic with period N.

The product $u'_\lambda u'_{\lambda+\Delta}$ can be related to the original sequence of '0's and '1's by comparing the truth table for modulo 2 addition with that of multiplication of +1 and -1, table A.4.2.

+	0	1
0	0	1
1	1	0

(a)

×	+1	-1
+1	+1	-1
-1	-1	+1

(b)

Table A.4.2. Truth tables for (a) modulo 2 addition, and (b) multiplication of ± 1

It is apparent that a product of elements from the +1, -1 sequence $\{u'\}$ can be found by returning to the original sequence $\{u\}$ and adding the elements modulo 2. The resulting sum is then transformed by using (A.4.24). This enables the results of section 6 to be used to evaluate $R(\Delta)$.

If $\Delta = 0$, or kN, where N is the period,

$$u_i + u_i = 2u_i$$

$$= 0 \qquad \text{modulo 2}$$

for each i. This is the condition expressed by (A.4.23). The equivalent term in the sequence $u'_i u'_i$ will be (+1) for all i,

Hence for $\Delta = 0$, or kN

$$R(0) = \frac{1}{N} \sum_{0}^{N-1} (+1) = 1 \qquad \text{(A.4.25)}$$

When $\Delta \neq 0$, then from (A. 2. 23)

$$u_i + u_{i+\Delta} = u_{j+i}$$

for some j, and the sequence $\{u'_i u'_{i+\Delta}\}$ will be the sequence $\{u'_{j+i}\}$. The autocorrelation function becomes

$$R(\Delta) = \frac{1}{N} \sum_{0}^{N-1} u'_{j+i}$$

In the sequence $\{u'\}$ there is one more -1 element +1 element (from section 6), and it follows that for $\Delta \neq 0$

$$R(\Delta) = -\frac{1}{N} \qquad \text{(A. 4. 26)}$$

(A. 4. 25) and (A. 4. 26) demonstrate that the autocorrelation function of a maximal length sequence has an impulse like form, figure A. 4. 4.

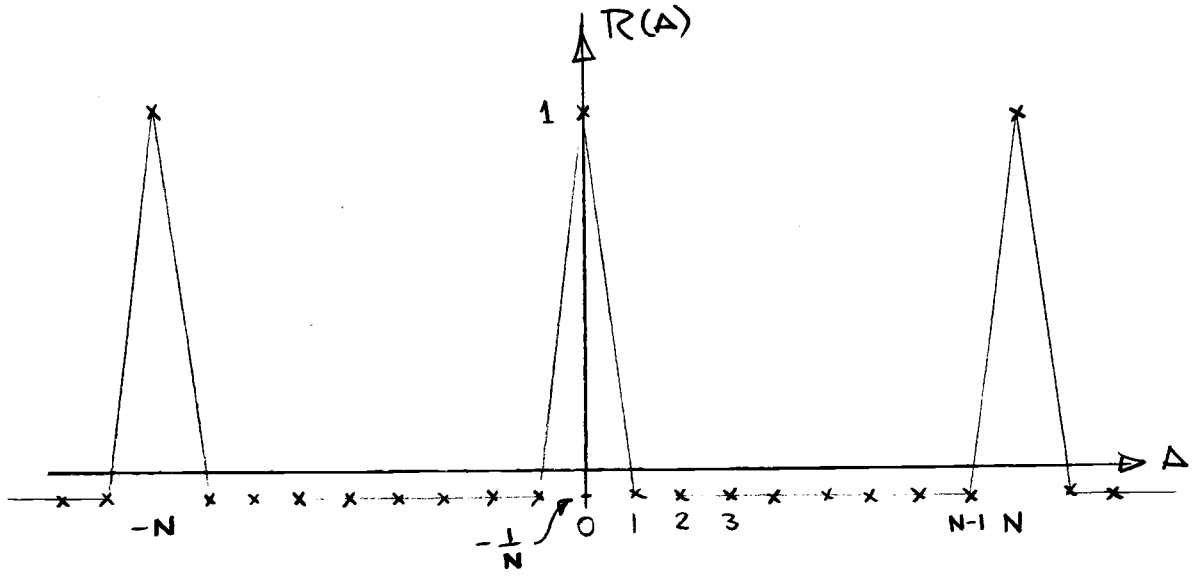

Figure A. 4. 4 Autocorrelation function of a maximal length sequence

8. Factorable polynomials. The example (A. 4. 21) in section 5, $A^5 + A^4 + 1$, which generates sequences with a period of 21, can be factorised

$$A^5 + A^4 + 1 = (A^2 + A + 1)(A^3 + A + 1) \qquad \text{modulo 2} \qquad \text{(A. 4. 27)}$$

Sequences which satisfy

$$A^5 + A^4 + 1 = 0 \qquad \text{(A.4.28)}$$

are those sequences which make either of the two factors zero,

$$A^2 + A + 1 = 0 \qquad \text{(A.4.29)}$$

$$A^3 + A + 1 = 0 \qquad \text{(A.4.30)}$$

These do not factorise further, and so the only solutions to (A.4.29) and (A.4.30) are the two maximal length sequences with periods $2^2 - 1$, and $2^3 - 1$ respectively, their shifted versions, and the all-zero sequence.

Additional solutions of (A.4.28) will be linear combinations of the solutions to (A.4.29) and (A.4.30). The combination of all-zero's with any other sequence produces no new solutions, since the sequence is unchanged. The combination of the two maximal length sequences will only give rise in this case to one new cyclic sequence and its associated shifts, which have a period equal to the lowest common multiple of 3 and 7, namely 21. This bears out the earlier statement about the periodicity of solutions to (A.4.28).

The separate non-zero solutions, allowing shifted versions, will be

21 sequences of length 21

3 sequences of length 3

7 sequences of length 7

The total number is 31. The order k of $A^5 + A^4 + 1$ is 5. Thus the total number of solutions coincides with the expression $2^k - 1$.

This example illustrates a general property that sequences from a factorable generator polynomial can be obtained by summing combinations of the sequences which are solutions to its factors.

9. Cross correlation between maximal length sequences of the same length.

If two maximal length sequences $\{u\}$ and $\{v\}$, length N, are transformed into the sequences of +1's and -1's, $\{u'\}$ and $\{v'\}$, as in section 7, the cross correlation function will be given by

$$R(\Delta) = \frac{1}{N} \sum_{0}^{N-1} u'_i v'_{i+\Delta} \qquad (A.4.31)$$

and its value for some value of Δ can be found from the difference between the number of '0's, S_Δ and the number of '1's, T_Δ in the sequence $\{u_i + v_{i+\Delta}\}$.

$$R(\Delta) = \frac{1}{N}\left[S_\Delta(+1) + T_\Delta(-1)\right]$$

$$= (S_\Delta - T_\Delta)/N \qquad (A.4.32)$$

Now $S_\Delta + T_\Delta$ is the total number of elements in the sequence $\{u_i + v_{i+\Delta}\}$. Since the sequences $\{u\}$ and $\{v\}$ both come from rth order generator polynomials, it follows that

$$S_\Delta + T_\Delta = 2^r - 1$$

This is an odd integer. Therefore $S_\Delta - T_\Delta$ is also an odd integer. Now (A.4.32) becomes

$$R(\Delta) = M_\Delta / N \qquad (A.4.33)$$

where M_Δ is an odd integer.

It follows immediately that $R(\Delta)$ cannot be zero for any Δ.

It is of interest to discover what the spread of $R(\Delta)$ is for all values of Δ. One indication of this is the sum of the values

$$\sum_{\Delta=0}^{N-1} R(\Delta) = \frac{1}{N} \sum_{\Delta=0}^{N-1} (S_\Delta - T_\Delta) \qquad (A.4.34)$$

This will now be determined.

The sequence $\{u_i + v_{i+\Delta}\}$ is a linear combination of the sequences $\{u\}$ and $\{v\}$.

It was stated in section 8 that if the maximal length solutions to two polynomials order r and s are added, the resulting sequences are those which can be obtained from the generator polynomial, order r + s, which is the product of the original polynomials. These sequences account for all possible $2^{r+s}-1$ solutions, and accordingly the total number of '1's and '0's occurring in these sequences taken together will be $2^{r+s}/2$ and $(2^{r+s}/2 - 1)$ respectively. This is analagous to a single maximal length sequence, period 2^k-1 which contains all 2^k-1 solutions itself, section 6. In the case of two polynomials, both of order r, the number of '0's will be $(2^{2r-1}-1)$ and the number of '1's will be 2^{2r-1}

The sequences associated with the polynomial of order 2r are all those which can be obtained by adding together shifted versions of both maximal length sequences, together with the maximal length sequences themselves. The numbers of '0's and '1's stated above relate to the grand total over all these sequences. However, the maximal length sequences do not occur in the set of cross correlation sequences $\{u_i + v_{i+\Delta}\}$, and to find the number of '0's and '1's in the cross correlation set, the sub-totals in each maximal length sequence must be subtracted from the total for all the sequences.

$$\sum_{\Delta=0}^{N-1} S_\Delta = (2^{2r-1}-1) - 2(2^r-1) \qquad \text{(A.4.37)}$$

and

$$\sum_{\Delta=0}^{N-1} T_\Delta = 2^{2r}-1 - 2.2^{r-1} \qquad \text{(A.4.38)}$$

From (A.4.34) (A.4.37) and (A.4.38),

$$\sum_{\Delta=0}^{N-1} R(\Delta) = \frac{1}{N}\sum_{0}^{N-1}(S_\Delta - T_\Delta)$$

$$\sum_{\Delta=0}^{N-1} R(\Delta) = \frac{1}{N}\left[2^{2r-1} - 1 - 2^r + 2 - 2^{2r-1} - 2^r \right]$$

$$= \frac{1}{N} \qquad \text{(A.4.37)}$$

This establishes that $R(\Delta)$ cannot be constant over all Δ. Any number of -1's, say, must be balanced by approximately the same number of +1's to satisfy (A.4.37). The greater the number of -1's, the higher any positive peak will be (for example, the shape of the autocorrelation function of a maximal length sequence).

A.5.1. CROSS CORRELATION BETWEEN SEQUENCES OF THE SAME LENGTH

A computer program has been written in Atlas Autocode to calculate the discrete interval cross correlation between sequences of the same length. This program is given in Table A.5.1

The results of a study on sequences of length 15, 31, 63, 127 are given in Tables A.5.2 and A.5.3. These tables list the total number of occurrences of each value of the correlation function in any one period.

Table A.5.2 shows the results for all shift register sequences of length 31, and demonstrates that there is a certain consistency of structure in the correlation functions. The principal observations are

(1) There are no all-zero correlation functions.

(2) The average value of every correlation function is 1/N.

(3) The different values of each correlation function fall into a simple set of 'quantum levels', which are all odd integers. The set includes -1, and successive levels are separated by multiples of 4. The different sets can all be produced by correlating any one sequence with all the others. This fact is established by Pierce [44] and is used to condense the results for other sequence lengths in table A. 5.3.

```
begin
integer r,n,N                          |  r is the number of sequences
1: read(r) ; stop if r=-1              |  n is the shift register length
read(n)                                |  N is 2↑n-1
N=2↑n-1
2: begin
integer p,q,u
integer array A(1:2*N),B(1:N),X(1:r,1:N)
routine spec nextcode
routine spec copy
routine spec correlate

cycle p=1,1,r                          |  this section assembles routines
nextcode
copy
cycle q=1,1,p
cycle u=1,1,N
B(u)=X(q,u)
repeat
correlate
cycle u=1,1,N
B(N+1-u)=X(q,u)
repeat
correlate
repeat
newline
repeat
->4

routine nextcode                       |  generates shift register sequence
integer i,j,k,s                        |  according to feedback connections w
integer array w(1:n)                   |  and puts two complete cycles into A
newline
caption (
print(n,1,0)
k=0
3: k=k+1
read(w(k))
print(w(k),1,0)                        |  prints feedback connections for current
->3 if w(k)≠0                          |   equence
caption ß)
A(1)=1
cycle i=2,1,N
A(i)=0
repeat
cycle i=1,1,N-n
s=0
cycle j=1,1,k
s=s+A(i+w(j))
repeat
A(i+n)=1 if parity(s)<0
repeat
cycle i=1,1,N                          |  Table A.5.1
A(N+i)=A(i)
repeat                                 |  Program to compute cross correlation
end                                    |  between sequences of the same length.
```

```
routine copy                          | copies one cycle of sequence into X
integer i
newline
cycle i=1,1,N
X(p,i)=A(i)
repeat
end

routine correlate                     | cross correlates current sequence with
integer i,j,c,d                       | all others already stored in X
integer array H(-N:N)
newline
d=0
cycle i=-N,1,N
H(i)=0
repeat
cycle i=0,1,N-1
c=0
cycle j=1,1,N
c=c+parity(A(i+j)+B(j))
repeat
d=d+c
H(c)=H(c)+1
repeat
j=0
cycle i=-N,2,N
->5 if H(i)=0
j=j+1
->6 unless j=9
newline
j=0
6: print(H(i),3,0)                    | output is list of correlation functions
caption (                             | followed by the number of occurences of
print(i,3,0)                          | each level
caption ) ß ,
5: repeat
newline
caption SUM ß =
print(d,3,0)
newline
end
4: end
newline
->1

end of program

9  7 1 0                              | number of sequences listed followed by
     3 0                             | list of feedback connections
     3 2 1 0
     5 2 1 0
     4 3 2 0
     5 3 1 0
     6 3 1 0
     6 5 4 3 2 0
     6 5 4 2 1 0
-1
```

Table A.5.1 (continued)

Sequence A	Sequence B	Number of occurrences of indicated level in cross correlation between A and B						
		-9	-5	-1	3	7	9	11
5,4,2,1	5,2	6		15		10		
	5,3	6		15		10		
	5,3,2,1	6		15		10		
	5,4,3,2	6		15		10		
	5,4,3,1	5	5	5	10	5		1
5,3,2,1	5,2	6		15		10		
	5,3	6		15		10		
	5,4,3,2	5	5	5	10	5		1
5,2,0	5,3	5	5	5	10	5		1
	5,2	6		15		10		
	5,3	5	5	5	10	5		1
	5,3,2,1	6		15		10		
	5,4,3,2	5	5	5	10	5		1
	5,4,2,1	6		15		10		
	5,4,3,1	5	5	5	10	5		1

Table A.5.2 Levels present in cross correlation between sequences A and B, and the frequency of their occurrence. The sequences are described by the stages on the shift register from which feedback is taken.

Sequence A	Sequence B	Occurrence of levels in correlation between A and B												
		-41	-21	-17	-13	-9	-5	-1	3	7	11	15	19	23
4,1	4,3						4	5	4	2				
6,4,3,1	6,1			6				47				10		
	6,5					18		27		12		4		2
	6,5,2,1,					18		27		12		4		2
	6,5,4,1			6				47				10		
	6,5,3,2				6	7	12	12	6	9	8	3		
7,6,5,4,2,1	7,1			28				63				36		
	7,6	1		14		28		35		28		14		7
	7,3	1		14		28		35		28		14		7
	7,4			28				63				36		
	7,3,2,1	1		14		28		35		28		14		7
	7,4,5,6			28				63				36		
	7,5,2,1	1		14		28		35		28		14		7
	7,2,5,6			28				63				36		
	7,4,3,2	1		14		28		35		28		14		7
	7,3,4,5			28				63				36		
	7,5,3,1			28				63				36		
	7,2,4,6	1		14		28		35		28		14		7
	7,6,3,1			28				63				36		
	7,1,4,6			28				63				36		
	7,6,5,4,3,2			28				63				36		
	7,1,2,3,4,5			28				63				36		
	7,1,2,3,5,6		7	7	8	21	7	14	21	7	14	14	7	

Table A 5 3 Levels present in cross correlation between sequences of the same length N when N = 4, 63, 127.

The maximum number of different levels are occupied when a sequence is correlated with that from the reverse shift register connection. This maximum is compared in table A. 5. 4. with the upper bound on the number of levels published by Pierce [44].

N	Upper bound	Actual number
15	5	4
31	7	6
63	13	8
127	19	11

Table A. 5. 4 Comparison of maximum number of different levels in a correlation function with the theoretical upper bound.

Some of the correlation functions for a given length, N, have smaller peak values than others. The observed smallest peak for each N is compared in table A. 5. 5 with the lower bound predicted by Stalder and Cahn [35].

N	$\sqrt{\frac{1}{N} - \frac{1}{N^2}}$	M_c/N
15	.25	.47
31	.177	.29
63	.125	.24
127	.089	.134

Table A. 5. 5 Smallest peak of cross correlation function

A.5.2 MODIFIED SEQUENCES

The method for obtaining these sequences is illustrated in figure A.5.1.

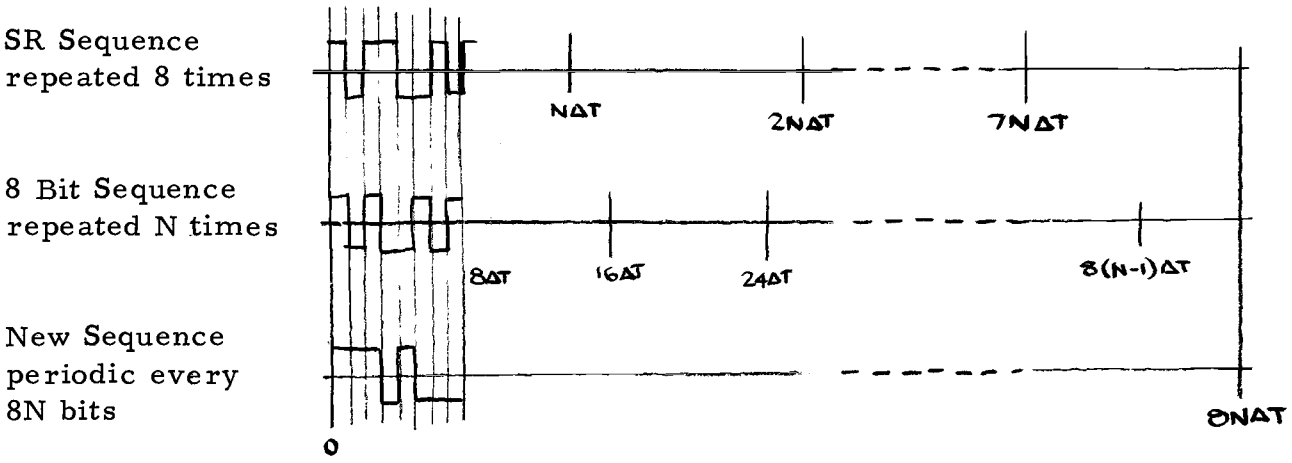

Figure A.5.1 Generating a modified sequence.

The original sequence is copied down 8 times, and compared bit by bit with N cycles of the 8 bit sequence. The new sequence is formed by the product of these individual elements if the sequences are all ± 1' s, (As indicated in appendix A.4.1, the corresponding operation when the sequences are '0's and '1's is modulo 2 addition).

The new sequences formed in this way are mutually uncorrelated, and uncorrelated with the original sequence, when the average is taken over $8N\Delta T$.

The autocorrelation functions of these sequences have been calculated and are illustrated in figure A.5.2. The main features are,

1) There are subsidiary spikes which can appear at multiples of the original length, N. These mean that to determine an impulse response with no processing other than cross correlation, this response must still be shorter than $N\Delta T$.

2) There is a ripple component on the autocorrelation function. It can be seen that the fundamental frequency of the ripple is $1/2\Delta T$, $1/4\Delta T$, or $1/8\Delta T$ and the

usefulness of the sequences will depend on the extent to which this frequency falls within the desired passband.

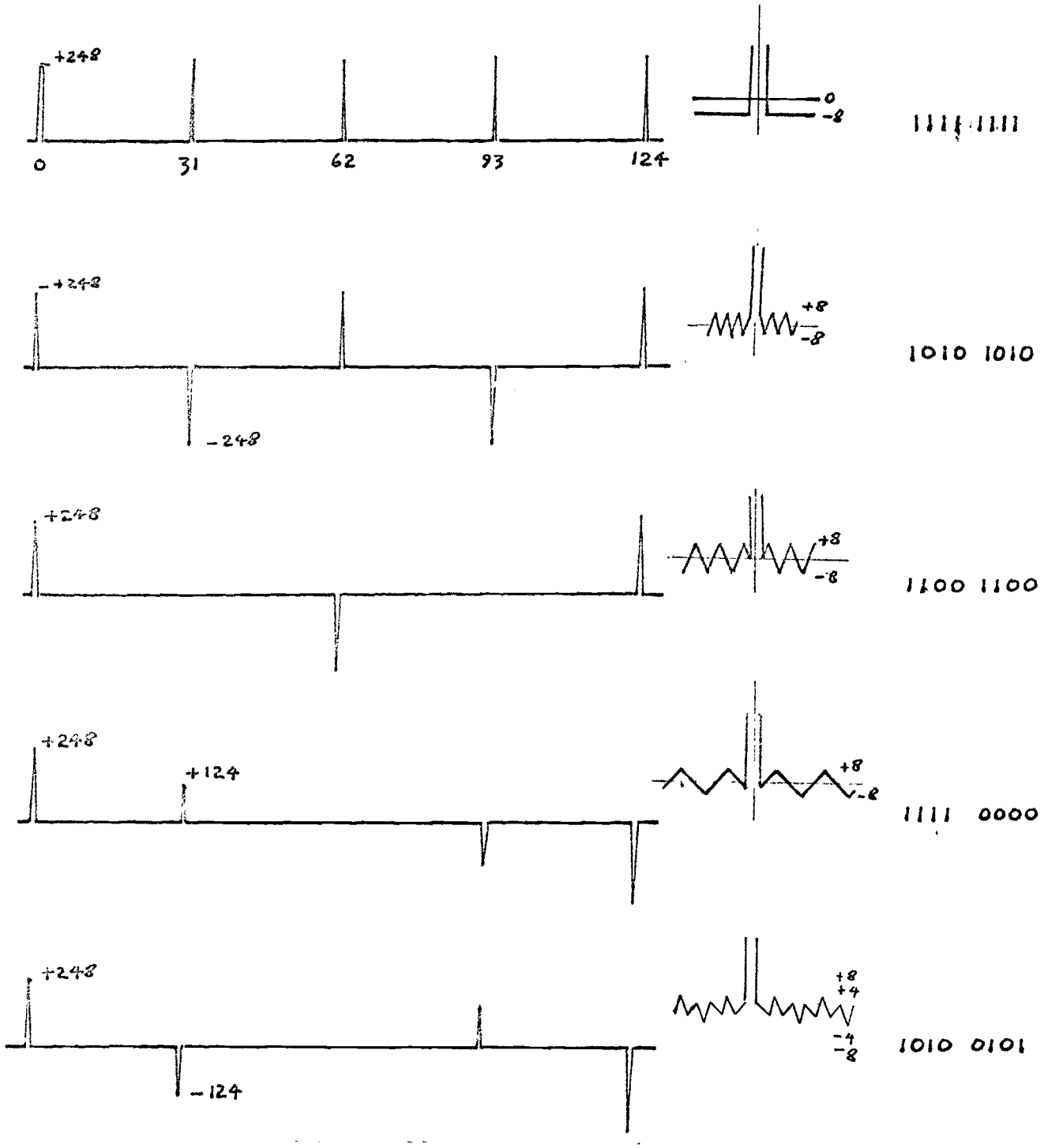

Figure A.5.2. Autocorrelation functions of modified binary sequences. Each pattern repeats after 248 bits, and is symmetrical about the 124 point. Also shown is the ripple pattern at zero delay, and the appropriate modifying 8 bit sequence.

A. 5. 3 CLOCK MODIFIED SEQUENCES

Inverting a maximal length sequence every second half clock period, figure A. 5. 3 results in a new sequence, uncorrelated with the first, which has a different form of autocorrelation function. This is illustrated in figure A. 5. 4.

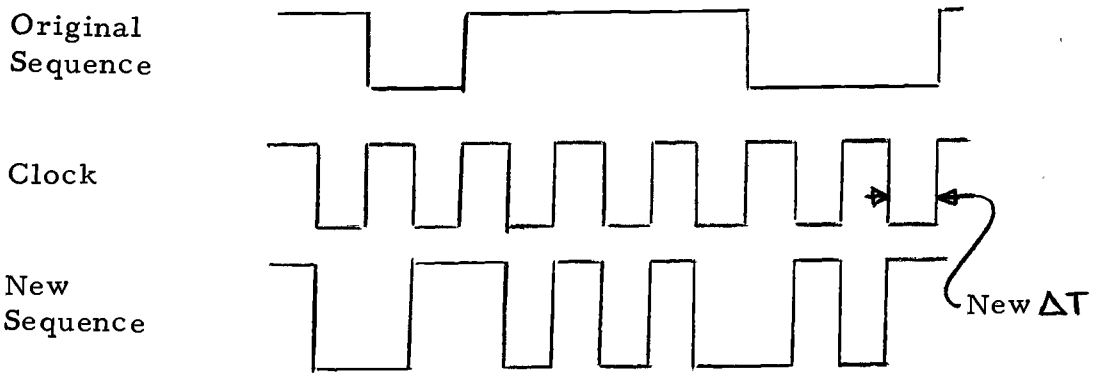

Figure A. 5. 3 Clock modified sequence

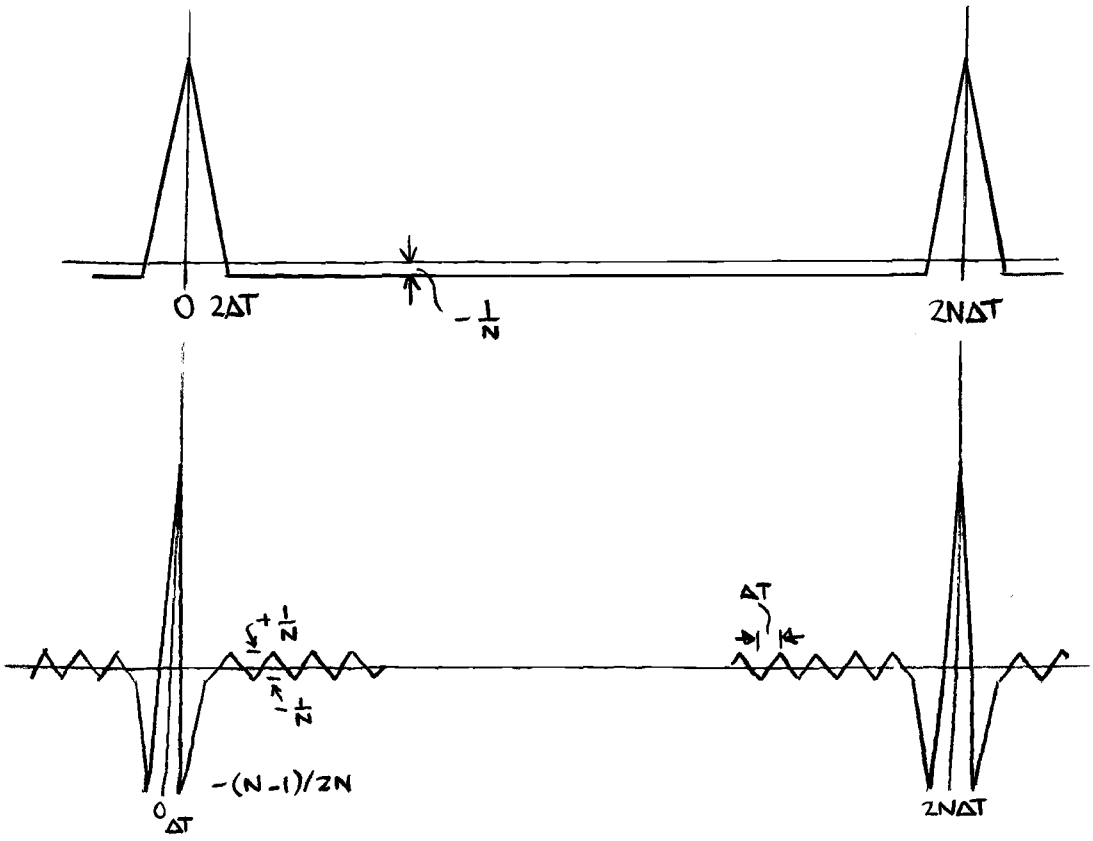

Figure A. 5. 4. Autocorrelation function of a clock modified sequence (bottom) compared with autocorrelation function of original (top)

The correlation function can be divided into two separate components $R_1(\tau)$ and $R_2(\tau)$ as in figure A. 5. 5.

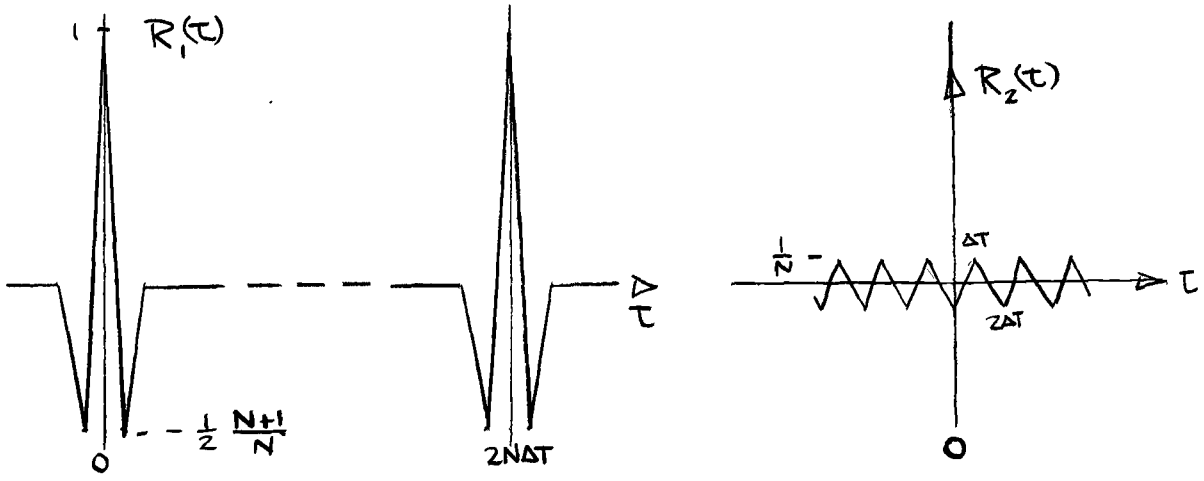

Figure A. 5. 5 Main (a) and ripple (b) components of sequence autocorrelation function

The envelope of the spectrum for a clock modified sequence will be developed from figure A. 5. 5 (a) and (b). For simplicity, assume that N is large so that $R_2(\tau)$ can be neglected, and $(N + 1)/N \simeq 1$. Then, $R_1(\tau)$ is the Fourier series

$$R_1(\tau) = \sum_1^\infty G(n) \cos \frac{2\pi}{\Delta T} \frac{n}{2N} \qquad \text{(A. 5. 1)}$$

The envelope of the spectrum G(n) will be [3]

$$G(n) = \frac{1}{N\Delta T} \int_{-N\Delta T}^{N\Delta T} R(\tau) \cos \frac{\pi}{\Delta T} \frac{n}{N} \tau \, d\tau \qquad \text{(A. 5. 2)}$$

$$= \frac{2}{N\Delta T} \int_0^{\Delta T} \left(1 - \tfrac{3}{2\Delta T}\tau\right) \cos \alpha\tau \, d\tau + \frac{2}{N\Delta T} \int_{\Delta T}^{2\Delta T} \left(-1 + \tau/2\Delta T\right) \cos \alpha\tau \, d\tau \qquad \text{(A. 5. 3)}$$

where

$$\alpha = \frac{\pi}{\Delta T} \cdot \frac{n}{N}$$

$$\frac{N\Delta T}{2} G(n) = \int_0^{\Delta T} \cos\alpha\tau \, d\tau - \int_{\Delta T}^{2\Delta T} \cos\alpha\tau \, d\tau - \frac{3}{2\Delta T}\int_0^{\Delta T} \tau \cos\alpha\tau \, d\tau$$

$$+ \frac{1}{2\Delta T}\int_{\Delta T}^{2\Delta T} \tau \cos\alpha\tau \, d\tau \qquad \text{(A.5.4)}$$

$$= -\frac{2}{\alpha^2\Delta T}\cos\alpha\Delta T + \frac{1}{2\alpha^2\Delta T}\left(2\cos^2\alpha\Delta T - 1\right) + \frac{3}{2\alpha^2\Delta T} \qquad \text{(A.5.5)}$$

From A.5.5

$$\alpha^2 N(\Delta T)^2 G(n) = -4\cos\alpha\Delta T + 2\cos^2\alpha\Delta T + 2 \qquad \text{(A.5.5)}$$

$$\left(\frac{\pi}{\Delta T}\frac{n}{N}\right)^2 N(\Delta T)^2 G(n) = 2\cos^2\frac{n}{N}\pi - 4\cos\frac{n}{N}\pi + 2$$

$$= 2\left(\cos\left(\frac{n}{N}\pi\right) - 1\right)^2$$

$$= 8\sin^4\left(\frac{n}{N}\frac{\pi}{2}\right) \qquad \text{(A.5.6)}$$

Finally,

$$G(n) = \frac{2}{N}\frac{\sin^4\left(\frac{n}{N}\cdot\frac{\pi}{2}\right)}{\left(\frac{n}{N}\cdot\frac{\pi}{2}\right)^2} \qquad \text{(A.5.7)}$$

The envelope of this spectrum is illustrated in figure A.5.6. The slope at low frequencies is 20dB/decade.

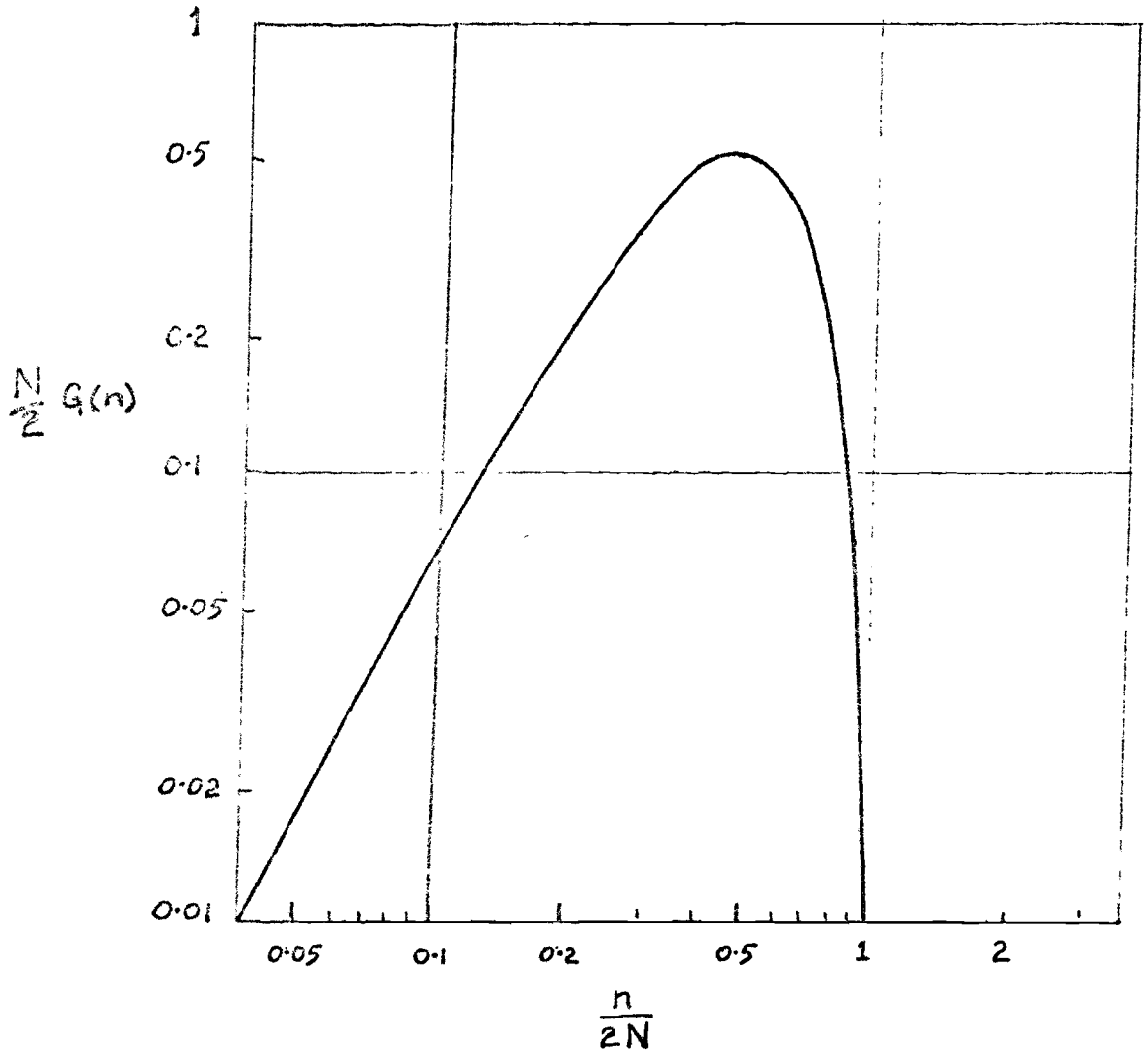

Figure A. 5. 6 Envelope of spectrum for a clock modified sequence